Technical Report Documentation Page

1. Report No.	2. Government Accession No.	3. Recipient's Catalog No.
FHWA/TX-97/1360-1		

4. Title and Subtitle	5. Report Date
EVALUATION OF REPAIR PROCEDURES FOR WEB GAP FATIGUE DAMAGE	September 1996
	6. Performing Organization Code

7. Author(s)	8. Performing Organization Report No.
Peter B. Keating, Scott D. Wilson, and Terry L. Kohutek	Research Report 1360-1

9. Performing Organization Name and Address	10. Work Unit No. (TRAIS)
Texas Transportation Institute The Texas A&M University System College Station, Texas 77843-3135	
	11. Contract or Grant No. Study No. 0-1360

12. Sponsoring Agency Name and Address	13. Type of Report and Period Covered
Texas Department of Transportation Research and Technology Transfer Office P. O. Box 5080 Austin, Texas 78763-5080	Final: September 1992 - August 1994
	14. Sponsoring Agency Code

15. Supplementary Notes

Research performed in cooperation with the Texas Department of Transportation and the U.S. Department of Transportation, Federal Highway Administration.
Research Study Title: Repair Procedures for Fatigue Damage in Steel Highway Bridges

16. Abstract

Connection plates cross frame diaphragms not rigidly attached to tension flanges can develop fatigue cracking in the unstiffened web gap due to the out-of-plane distortion. This report investigates repair procedures for fatigue damage in the web gap of steel highway bridges. The procedures investigated include drilling holes at crack tips, flame-cutting holes to remove extensively cracked regions, and gouging and re-welding. In addition, rigid attachment retrofits of tight-fit and cut-short connection plate details are examined. The evaluation of these repairs are made by monitoring their implementation on an in-service bridge, laboratory fatigue testing of simulated repairs, and finite element analysis.

All three crack repair procedures were found to be viable. However, procedures outlined must be followed to achieve the quality in the repair that will insure continued safe use of the bridge throughout its remaining life. The results indicate that the degree of finish given to the repair is as important as satisfying the prescribed repair criteria.

17. Key Words	18. Distribution Statement
Fatigue, Diaphragms, Web Gap, Cracking, Repair, Welding	No restrictions. This document is available to the public through NTIS: National Technical Information Service 5285 Port Royal Road Springfield, Virginia 22161

19. Security Classif.(of this report)	20. Security Classif.(of this page)	21. No. of Pages	22. Price
Unclassified	Unclassified	166	

Form DOT F 1700.7 (8-72) Reproduction of completed page authorized

EVALUATION OF REPAIR PROCEDURES FOR WEB GAP FATIGUE DAMAGE

by

Peter B. Keating, Ph.D.
Engineering Research Associate
Texas Transportation Institute

Scott D. Wilson
Graduate Research Assistant
Texas Transportation Institute

and

Terry L. Kohutek, Ph.D.
Engineering Research Associate
Texas Transportation Institute

Research Report 1360-1
Research Study Number 0-1360
Research Study Title: Repair Procedures for Fatigue Damage in Steel Highway Bridges

Sponsored by the
Texas Department of Transportation
In Cooperation with
U.S. Department of Transportation
Federal Highway Administration

September 1996

TEXAS TRANSPORTATION INSTITUTE
The Texas A&M University System
College Station, Texas 77843-3136

IMPLEMENTATION STATEMENT

This study provides competent recommendations to Structural Engineers for the repair of web-gap fatigue cracking. This type of fatigue cracking is common to steel highway bridges where there is no rigid attachment of the diaphragm connection plate to the tension flange. Repair options outlined include; hole drilling at the crack tips, flame-cutting holes to remove extensive cracking patterns, and gouging and re-welding of the cracks. By permanently removing the driving source of the web-gap out-of-plane distortion (by cross frame removal or rigid attachment of the connection plate), these repairs will result in an acceptable performance of the bridge when combined with continued inspection and sound engineering judgement.

DISCLAIMER

The contents of this report reflect the views of the authors who are responsible for the facts and the accuracy of the data presented herein. The contents do not necessarily reflect the official views or policies of the Texas Department of Transportation or the Federal Highway Administration. This report does not constitute a standard, specification, or regulation. It is not intended for construction, bidding, or permit purpose.

ACKNOWLEDGMENTS

The repair procedures for web-gap cracking described herein are the results of TxDOT Research Project 1360 titled *Repair Procedures for Fatigue Damage in Steel Highway Girders.* The research was preformed by the Texas Transportation Institute, Texas A&M University System in cooperation with the Texas Department of Transportation and the U.S. Department of Transportation, Federal Highway Administration The research project was coordinated for TxDOT by Gregg Freeby, P.E. under the supervision of Mark Bloschock, P.E.

Special thanks are extended to "Little" Bill Kohutek, Welding Inspector, for TxDOT. He supervised the Midland County bridge repair contract and performed the repairs evaluated in the laboratory fatigue testing phase of the project. His unending cooperation and thorough knowledge of welding and weld repairs contributed significantly to the overall success of the project.

TABLE OF CONTENTS

Chapter		Page
LIST OF FIGURES		xi
LIST OF TABLES		xv
LIST OF ABBREVIATIONS AND SYMBOLS		xvii
ACKNOWLEDGMENTS		xix
SUMMARY		xxi
One	INTRODUCTION	1
Two	SUMMARY OF REPAIRS	5
2.1	Background	5
2.2	Accurate Crack Locations	6
2.3	Arresting of Web-to-Flange Web Crack	6
2.4	Fatigue Crack Repair Procedures	9
2.5	Welded Connection Plate Attachments	23
Three	EXPERIMENTAL EVALUATION OF WEB-GAP REPAIR PROCEDURES	25
3.1	Test Program	25
3.2	Pre-Cracking of Girder 2	30
3.3	Simulated Repairs to Test Girders	38
3.4	Instrumentation	48
3.5	Static Load Test	49
3.6	Fatigue Testing of Girders	53
3.7	Analysis of Fatigue Test Results	55
3.8	Fracture Toughness Evaluation	57
Four	ANALYTICAL EVALUATION OF REPAIR PROCEDURES	59
4.1	Simple Plate Model with Crack	59
4.2	Stress Concentration as a Function of θ	62
4.3	Stress Concentration as a Function of s	66
4.4	Alternatives to the Drilled Hole Technique	67
4.5	General Repair Guidelines for Drilled Holes	73
4.6	Flame-Cut Hole Model	75
4.7	Criteria Development For Flame-Cut Holes	82
4.8	Comparison of Multiple Drilled Holes to Flame-Cut Holes	85
4.9	Web-to-Flange Crack Study	89
4.10	Model with Web-to-Flange Crack Arrested by Two Holes	93

TABLE OF CONTENTS (continued)

Five RECOMMENDATIONS AND CONCLUSIONS 97

5.1 Drilling Holes at Crack Tips 97
5.2 Flame-Cut Holes 104
5.3 Gouging and Re-Welding 109
5.4 Welded Attachment of Existing Tight-Fit Connection Plate 110
5.5 Welded Attachment of Connection Plate with Clip 111
5.6 Recommendations for Additional Research 112

REFERENCES 113

APPENDICES

A Pre-Cracking Test Log (Girder 2) 115
B Static Load Test Data 119
C Test Log, Girder 1 125
D Test Log, Girder 2 133
E Test Log, Girder 3 141

LIST OF FIGURES

Figure		Page
1-1	View of IH-20 Midland County bridge.	1
1-2	Fatigue crack at end of unstiffened web gap of diaphragm connection plate.	2
1-3	View of typical cross frame diaphragm at outer bay.	3
1-4	Fatigue cracking in tight-fit detail.	4
1-5	Fatigue cracking in web-gap detail.	4
2-1	Crack in web-to-flange fillet weld	7
2-2	Web plate after removal of connection plate end by air-arc gouging.	8
2-3	Grinding to remove remaining web material and connection plate	9
2-4	Backside detail of Type 1 repair	11
2-5	Frontside (stiffener side) detail of Type 1 repair	11
2-6	Examples of U-shaped and V-shaped bevels.	12
2-7	Frontside detail of Type 2 repair	13
2-8	Backside detail of Type 2 repair	14
2-9	Location and marking of the cracked area.	14
2-10	Removal of cracked material with cutting torch	15
2-11	Grinding of hole to a smooth surface.	15
2-12	Web after initial repairs.	16
2-13	Dye penetrant test showing remaining cracks	16
2-14	Removal of remaining cracks with grinder	17
2-15	Frontside (stiffener side) detail for Type 3 repair	18
2-16	Backside (stiffener side) detail for Type 3 repair	18
2-17	Drilling at crack tip ends.	19
2-18	Drilling to arrest all finger crack lines.	19
2-19	Overlapping holes slotted to remove cutting edges	20
2-20	Repaired web section after hole-slotting.	20
2-21	View of completed Type I repair procedure	21
2-22	View of completed Type II repair procedure.	22
2-23	View of completed Type III repair procedure.	22
2-24	View of replacement cross-frame diaphragm with welded connection plate	23
3-1	Test Girder 2 and cross section.	26
3-2	Test Girder 1 and cross section.	27
3-3	Plan of Test Girder 3 and cross section.	27
3-4	Plan view of test apparatus.	28
3-5	Profile view of test apparatus.	29
3-6	View of girder and fatigue test apparatus.	29
3-7	Pre-cracking load frame.	30
3-8	Pre-cracking of Girder 2.	31

LIST OF FIGURES (continued)

Figure		Page
3-9	Pre-cracking in web plate of Girder 2 behind Stiffener 1.	32
3-10	Examination of crack using dye penetrant.	32
3-11	Pre-cracking in web plate of Girder 2 at weld toe of Stiffener 1.	33
3-12	Examination of crack using dye penetrant.	33
3-13	Pre-cracking in web plate of Girder 2 behind Stiffener 2.	34
3-14	Examination of crack using dye penetrant.	34
3-15	Pre-cracking in web plate of Girder 2 at weld toe of Stiffener 2.	35
3-16	Examination of crack using dye penetrant.	35
3-17	Pre-cracking in web plate of Girder 2 behind Stiffener 3.	36
3-18	Examination of crack using dye penetrant.	36
3-19	Pre-cracking in web plate of Girder 2 at weld toe of Stiffener 3.	37
3-20	Examination of crack using dye penetrant.	37
3-21	Shortening of stiffeners by flame-cutting.	39
3-22	Shortening of Stiffener 1-1.	39
3-23	Shortening of Stiffener 1-2.	40
3-24	Shortening of Stiffener 1-3.	40
3-25	Removal of "cracked" material by flame-cutting.	41
3-26	Flame-cut hole in web plate at Stiffener 1-1.	41
3-27	Flame-cut hole in web plate at Stiffener 1-2.	42
3-28	Flame-cut hole in web plate at Stiffener 1-3.	42
3-29	Shortening of stiffeners of Girder 2.	43
3-30	View of back gouged fatigue crack lines.	44
3-31	View of re-welded fatigue crack lines.	44
3-32	Tight-fit retrofit details.	46
3-33	Tight-fit welded detail.	46
3-34	Tight-fit retrofit using welded clips.	47
3-35	Strain gage locations in areas between stiffeners (common for all girders).	48
3-36	Additional strain gage locations for Girder 1 (at stiffener locations).	49
3-37	Stress distribution at Stiffener 1-1 derived from strain gage data.	50
3-38	Stress distribution at Stiffener 1-2 derived from strain gage data.	51
3-39	Stress distribution at Stiffener 1-3 derived from strain gage data.	52
3-40	Crack propagating from surface flaw near Stiffener 1-1.	54
3-41	S-N plot of fatigue data for Girder 1 with AASHTO curves.	56
3-42	Growth of web-to-flange cracking Test Girder 2.	57
4-1	Variables in simple plate proximity study.	60
4-2	Finite Element mesh and boundary conditions for trial model.	61
4-3	Comparison of theoretical and finite element stress plots.	61
4-4	Simulated crack with drilled holes in simple plate model.	62

LIST OF FIGURES (continued)

Figure		Page
4-5	FEM stress contour plot for simulated crack with drilled holes	63
4-6	Labeling Scheme for drilled holes.	64
4-7	Plot of stress concentration vs. θ for simple plate with crack (s = 38 mm (1-1/2 in.)).	65
4-8	Crack initiation due to stress concentrations at drilled holes.	67
4-9	Large circular hole repair method.	68
4-10	Slotted hole repair technique.	69
4-11	Finite element mesh for a slotted hole model: $\theta = 45°$.	70
4-12	FEM stress contour plot for a slotted hole model ($\theta = 45°$).	71
4-13	Comparison of maximum stress concentrations for drilled hole and slotted hole models.	72
4-14	Repair guidelines for cracks with lower values of θ.	73
4-15	Minimizing separation of drilled holes arresting the same crack.	74
4-16	Propagation of crack tip not contained by drilled hole.	75
4-17	Finite element model for web holes.	76
4-18	Loading and boundary conditions for web holes.	77
4-19	Comparison of stress plot to experimental data for Stiffener 1.	78
4-20	Comparison of stress plot to experimental data for Stiffener 2.	79
4-21	Comparison of stress plot to experimental data for Stiffener 3.	80
4-22	Flame-cut hole after repair of fatigue crack	82
4-23	Elliptical hole in plate girder model.	83
4-24	Comparison of section loss between drilled and flame-cut holes.	86
4-25	FEM stress contours for flame-cut hole model.	87
4-26	FEM stress contours for multiple drilled hole model.	88
4-27	FEM mesh for a partial plate girder section with a crack at the web-to-flange connection.	91
4-28	FEM stress contours in the x-direction for a partial plate girder section with a crack at the web-to-flange connection.	92
4-29	FEM stress contours for web plate.	94
4-30	FEM stress contours for tension flange.	95
4-31	FEM stress contours for fillet weld.	96
5-1	Possible drilled hole locations relative to crack tip.	99
5-2	Marked hole centers at crack tips.	100
5-3	Hole drilled to final diameter, note 6 mm (1/4 in.) pilot holes	100
5-4	View of slotted holes	101
5-5	Alignment of holes to minimize web section loss	101
5-6	View of irregular web-to-flange fillet weld toe	102
5-7	Removal of web-to-flange fillet weld crack	103
5-8	Large hole repair technique for web crack	104

LIST OF FIGURES (continued)

Figure		Page
5-9	Guidelines for the used of flame-cut holes	106
5-10	View of outlined hole for flame-cutting	106
5-11	Removal of missed crack tips by grinding	107
5-12	View of die grinder used to finish holes	108
5-13	Example of undesirable curvature near web-to-flange weld.	108

LIST OF TABLES

Table		Page
2-1	Repair procedure designation and description	6
2-2	Summary of necessary labor and equipment for repair procedures.	10
3-1	CVN test data from Girder 2 gouge and re-weld repair	58
4-1	Summary of stress concentrations for varying θ.	64
4-2	Stress concentration verses s for simple plate with crack $\theta = 90°$	66
4-3	Comparison of finite element analysis point stresses to strain gage data for Stiffener 1	79
4-4	Comparison of finite element analysis point stresses to strain gage data for Stiffener 2	80
4-5	Comparison of finite element analysis point stresses to strain gage data for Stiffener 2	81
4-6	Stresses at toe of stiffener and top edge of hole versus toe-to-toe hole spacing	84

LIST OF ABBREVIATIONS AND SYMBOLS

δ	Forced displacement for finite element models, mm (in.)
θ	Angular orientation of adjacent drilled holes, degrees
σ	In-plane web plate bending stress, MPa (ksi)
ϕ	Specified hole diameter for crack tips, mm (in.)
d	Depth of plate girder, mm (in.)
E	Modulus of elasticity of steel, MPa (ksi)
F_y	Yield strength of web plate, MPa (ksi)
i	Half-length of finite element model for forced displacement, mm (in.)
L	Total length of drilled crack, mm (in.)
s	Center-to-center spacing of adjacent drilled holes, mm (in.)
S_r	Maximum expected nominal stress range at drilled hole location, MPa (ksi)

SUMMARY

Failure to provide rigid attachment of a diaphragm connection to the tension flange of a steel girder bridge and the resulting out-of-plane distortion can lead to web-gap fatigue cracking. Repair procedures for the fatigue cracking were evaluated through field investigation of repairs made to an in-service bridge, laboratory fatigue testing of simulated repairs of large-scale specimens, and by finite element analyses. The repair procedures investigated include:

- drilled holes at the crack tips;
- flame-cut holes to remove entire region of cracking; and
- gouging and re-welding of cracks.

All three methods were found to be viable options. However, the procedures outlined must be followed to achieve the quality in the repairs that will insure continued safe use of the bridge throughout its remaining life. The drill hole option requires the least amount of skill but may not be as practical a repair for extensively cracked web gaps as the flame-cut hole option. Gouging and re-welding restores the web plate to its original uncracked state but requires a high degree of skill and inspection. The results of this study show that the degree of finish given to the repair (e.g., smoothness of a hole perimeter) is as important as satisfying the prescribed repair criteria.

Chapter One
INTRODUCTION

An inspection of the IH-20 Midland County (Texas) bridge performed in 1989 found that the structure was experiencing fatigue related problems caused by the unintended interaction between the longitudinal girders and the cross-frame diaphragms (Diaz and Andrews 1990, Keating and Crozier 1992). The original construction of the bridge did not specify a rigid attachment between the ends of the connection plate and the flanges. Figure 1-1 provides a view of the twin structure.

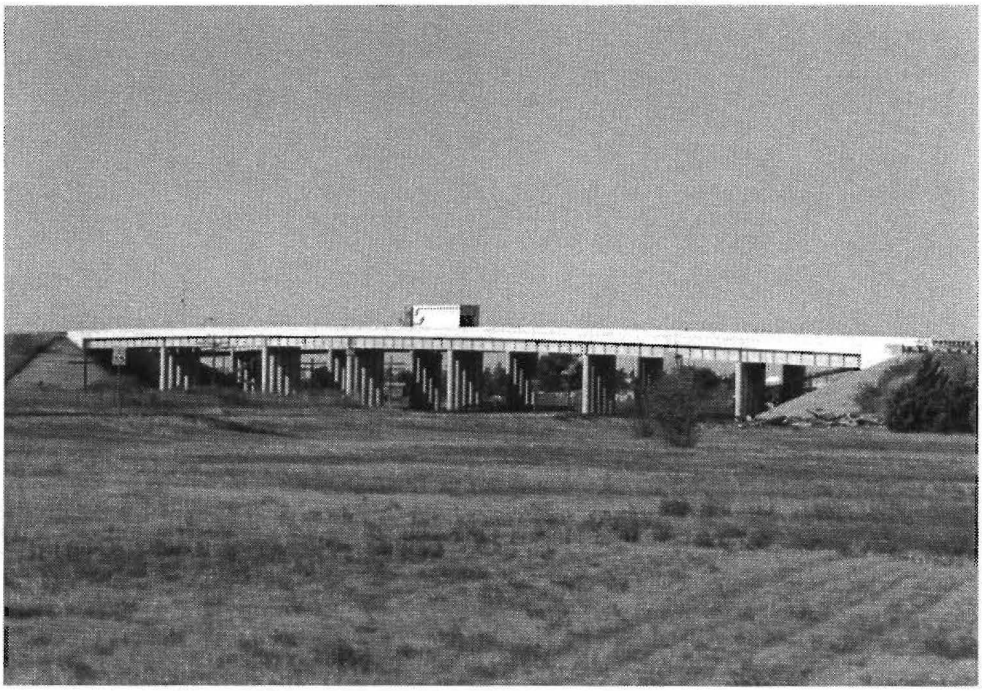

Figure 1-1: View of IH-20 Midland County bridge.

Current AASHTO bridge design specifications require a rigid attachment between the ends of the connection plate and the flanges of the girder (AASHTO 1992, AASHTO-1994). The attachment can be in the form of either a welded or bolted connection. A welded connection for this detail is preferred for new construction since the weld quality can be controlled easily in

a fabrication shop setting. Bolted connections for new construction are generally found to be more costly and are, therefore, to be avoided. Past experience with welded retrofits has not always been successful (i.e., resulting in fatigue crack development in the repair weld) and welded retrofits have been avoided by many state highway departments.

Due to the lack of rigid connection plate attachments, fatigue cracks developed in the unstiffened web gaps at the ends of diaphragm connection plates, shown in Fig. 1-2. Fatigue cracks developed along the upper toe of the web-to-flange fillet weld, as well as from the end termination of the connection plate fillet weld. The vertical weld toe crack is particularly critical since it is driven not only by the out-of-plane distortion stresses but also by the in-plane bending stress.

Figure 1-2: Fatigue crack at end of unstiffened web gap of diaphragm connection plate.

A partial solution to the fatigue cracking was to remove the source of the distortion by either permanently removing diaphragms or using a connection plate welded to the flanges.

While these methods prevented further fatigue crack growth, it was still necessary to remove or arrest the existing fatigue cracks since they could propagate when subjected to the primary stresses. The present study focuses on the evaluation of the methods used to remove or arrest the existing fatigue crack. In addition, the retrofit of field welding the connection plate to the tension flange was also investigated.

Two types of connection plate termination details were used on the bridge. On the original construction, a 25 mm (one-inch) web gap was used to terminate the connection plate short of the tension flange. When a shoulder lane was later added to the bridge, the additional girder used a tight-fit detail. The tight-fit termination normally bears against the flange, but is not welded. The cracking was observed at both details. The type of cracking to be repaired was found at or near the web gap in positive moment regions. Therefore, the cracking occurred near the bottom flange. Figure 1-3 provides a view of a typical cross frame in the outer bay with both types of connection plate details.

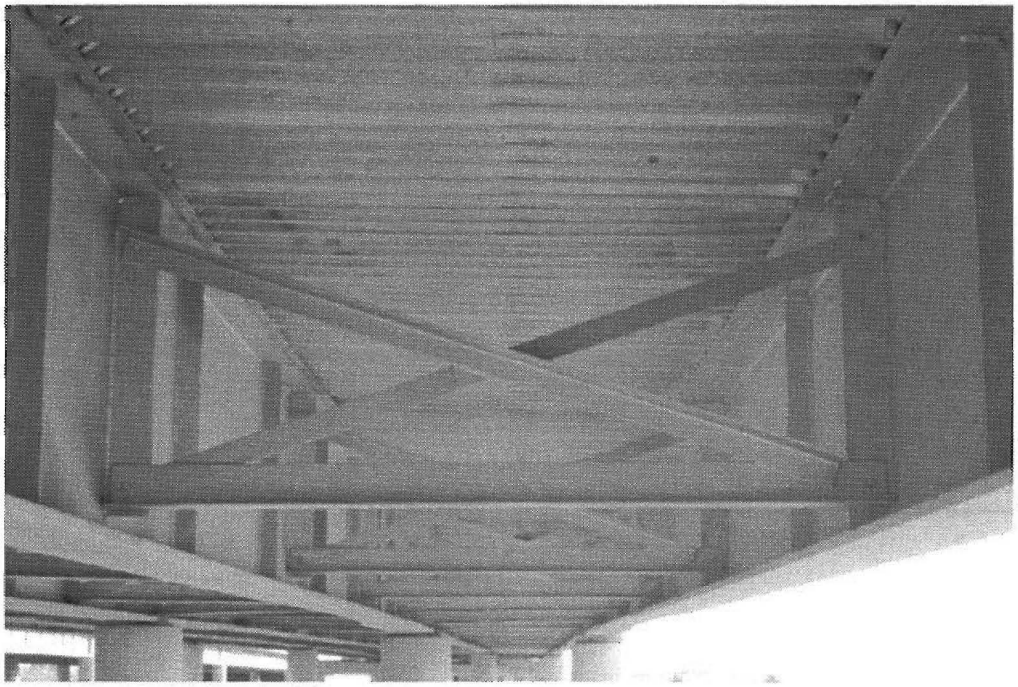

Figure 1-3: View of typical cross frame diaphragm at outer bay.

Illustrative examples of the cracking are given in Figs. 1-4 and 1-5 for the tight-fit and 25 mm (one-inch) web-gap detail respectively. Note that the cracking can occur at one or both boundaries of the web gap. A fatigue crack can develop along the web-to-flange fillet weld, running parallel with the primary bending stress. Fatigue cracks also develop vertically along the toe of the fillet weld, between the connection plate and the web plate. As this crack increases in length, there is a tendency for it to turn perpendicular to the weld axis.

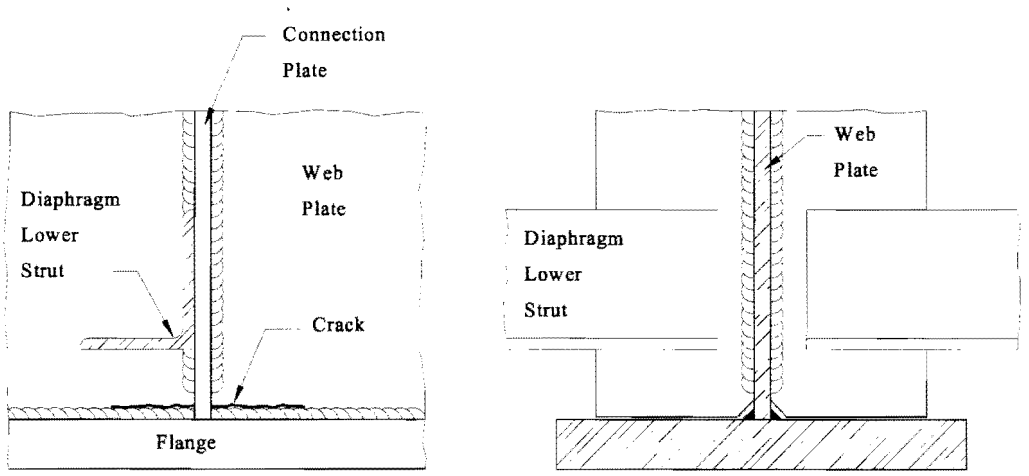

Figure 1-4: Fatigue cracking in tight-fit detail.

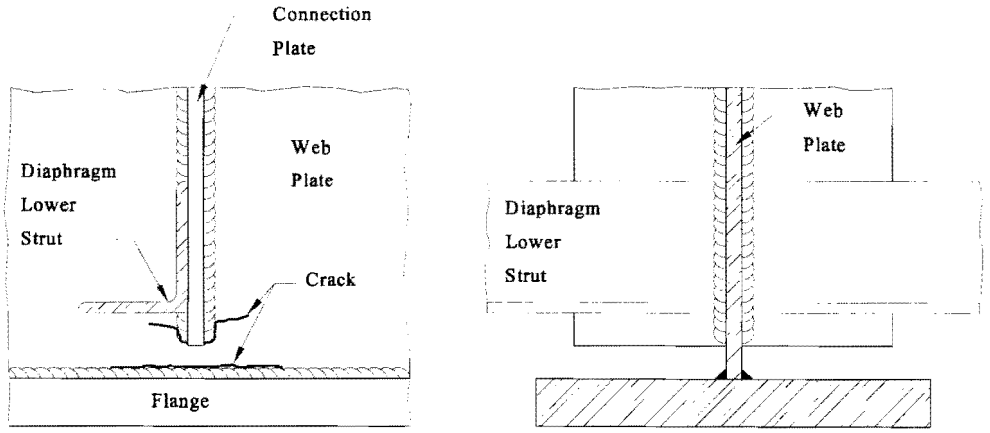

Figure 1-5: Fatigue cracking in web-gap detail.

Chapter Two
SUMMARY OF REPAIRS

2.1 BACKGROUND

During the Fall of 1992, repairs to the Midland County bridges were performed. As part of the repair contract, researchers investigated several different methods for the repair of the fatigue damage due to web gap distortion, enabling the researchers to evaluate each method with regard to its suitability and ease of repair. The repairs were performed by the contractor's personnel and equipment. Inspection of the repairs was performed by TxDOT personnel.

The web gaps suffering the most extensive fatigue damage were chosen for these repairs. The web gaps were located on the 129.5 m (425 ft.) structures between Bents 1 and 2 in Girders 4 and 5, where an assumed fabrication error resulted in the adjacent diaphragms between girder bays being offset by approximately 100 m (4 in.). It was determined that no location had enough extensive fatigue cracking to warrant a bolted splice of the web plate.

The three different procedures developed by TxDOT's Bridge Division to repair the fatigue-damaged web gaps at selected locations are summarized in Table 2-1. The extent of the fatigue cracking at the detail location determined the repair procedure used. Type 2 was used when a high level of distortion resulted in extensive cracking. TxDOT's Bridge Division determined that cutting out the entire cracked region of the web plate would be easier than drilling holes at each crack tip (Type 3 repair). Type 1 involved gouging out the crack and re-welding. This repair type results in no loss of the cross section. However, extensive re-welding in a localized region can result in undesirable heat effect with a reduction in the fracture toughness of the web plate.

Designation	Description
Type 1	Gouge and re-weld
Type 2	Web plate flame-cutting
Type 3	Holes at crack tips

Table 2-1: Repair procedure designation and description.

2.2 ACCURATE CRACK LOCATIONS

Accurate location of all crack tips was necessary to determine which type of repair method to use. Determining the exact location of the crack tips is essential in evaluating the extent of fatigue damage. Also, all crack tips must be found prior to repair to ensure that every tip is removed from the web plate and arrested from further propagation.

The first step in crack tip identification is blast-cleaning the surrounding area to remove all paint and foreign matter. Crack growth may be more extensive than previously revealed through the paint film. Grinding to remove the paint should be limited, since it plastically deforms the surface of the plate and may prevent properly locating the crack tip. Dye penetrant should then be used and the crack tip clearly identified as the person performing the inspection may not be performing the drilling operation.

2.3 ARRESTING OF WEB-TO-FLANGE WEB CRACK

At every location where fatigue cracks developed at and around the end of the diaphragm connection plate, a crack also developed along the toe of the web-to-flange fillet weld (see Fig. 2-1). Regardless of which of the three repair procedures were used to arrest the web plate crack, this crack was repaired in the same manner (i.e., no gouging and re-welding).

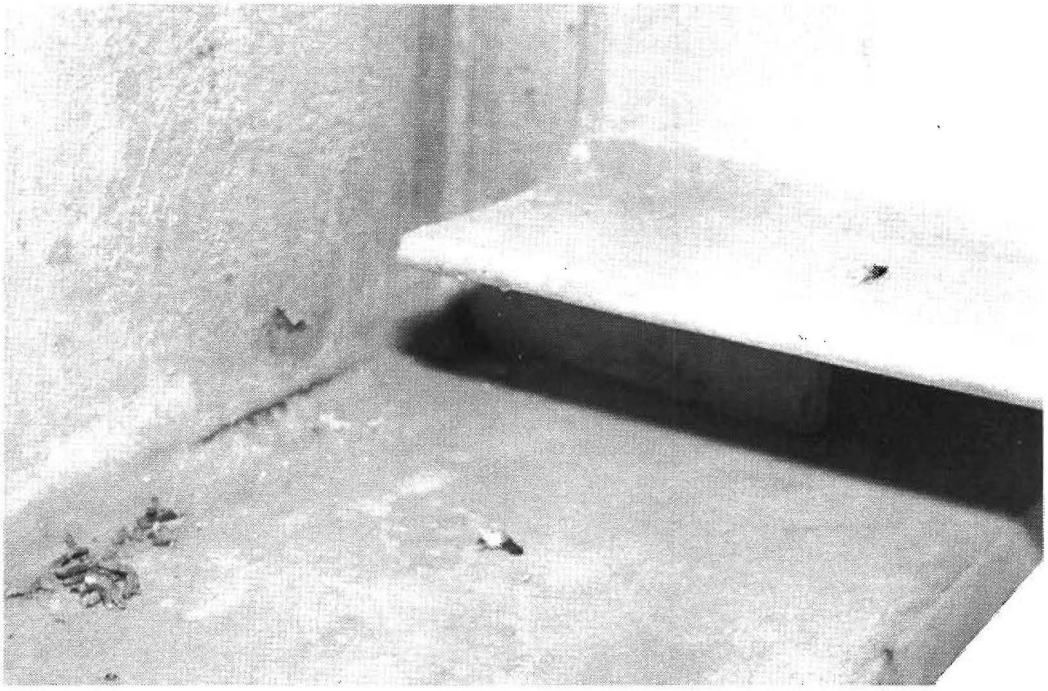

Figure 2-1: Crack in web-to-flange fillet weld.

If the source of the web-gap distortion is removed (either by removing the diaphragm or by providing a rigid attachment), the web-to-flange crack need not be retrofitted. Since the stresses driving the crack no longer exist, continued crack propagation is not possible. The crack is oriented parallel with the in-plane bending stress and will not propagate. However, common practice is to drill holes at the crack tips to prevent any possible crack extension from unforeseen sources.

Prior to hole drilling, the end of the connection plate was removed to provide better access to the region. Approximately 150 mm (6 in.) of the connection plate was removed by air-arc gouging. Care was taken to avoided gouging the web plate as the melted metal was washed from the cut. These gouges, if not repaired, could become initiation sites for additional fatigue cracking. The welders performing this portion of the repair were instructed to cut no closer than 3 mm (1/8 in.) from the web-plate to prevent web plate gouging. Figure 2-2 shows a connection plate with the end removed by air-arc gouging. Note that a portion of the connection plate fillet weld (and connection plate edge) still remains on the web plate.

Figure 2-2: Web plate after removal of connection plate end by air-arc gouging.

The remaining 3 mm (1/8 in.) of connection plate and weld was then removed by grinding. Typically, a rotary grinder was used for this operation, as shown in Fig. 2-3. This operation also prepared the web plate for the next step in the repair procedure by providing a smooth surface.

Figure 2-3: Grinding to remove remaining web material and connection plate.

2.4 FATIGUE CRACK REPAIR PROCEDURES

TxDOT developed three different procedures to provide field evaluation of repair procedures for fatigue-damaged web gaps. The intent of the repair procedures was to remove the fatigue-damaged web plate material from the structure. It is important to note that these procedure were not developed to prevent further damage from the distortion at the cross-frame diaphragm locations. As previously mentioned, the out-of-plane distortion was eliminated by either the permanent removal of the diaphragms or a rigid (welded) attachment of the connection plate end to the flange. Table 2-2 summarizes the labor and equipment used in each of the three repair procedures evaluated.

Procedure	Labor	Equipment
Type 1	Certified Welder (C-6 TxDOT Papers)	200 amp welder Torch and accessories: Air compressor Arc-air gouger Grinder and tools (welder's items) Approved welding electrodes (per D-9 Matls. and Test Div. Cert.) Air or electric die or straight grinder
Type 2	Welder (does not have to be certified) or Laborer with knowledge of welding and use of torch	Torch and accessories Grinder and tools Air or electric die or straight grinder
Type 3	Common laborer	Magnetic base drill press Annular cutters -- steel twist drill bits 25 mm, 22 mm, 19 mm (1 in., 7/8 in., 3/4 in.) Grinder and tools Air or electric die or straight grinder

Table 2-2: Summary of necessary labor and equipment for repair procedures.

Each procedure was evaluated on the basis of ease of performing the repairs and its success in adequately removing the fatigue-damaged web plate material. A detailed description and discussion of the procedures follows.

2.4.1 Type 1 Repair Procedure

The Type 1 repair procedure involves arc-gouging the fatigue cracks and rewelding. This method of repair was selected, since web plate section loss is avoided. The backside and frontside repairs are shown schematically in Fig. 2-4 and 2-5, respectively.

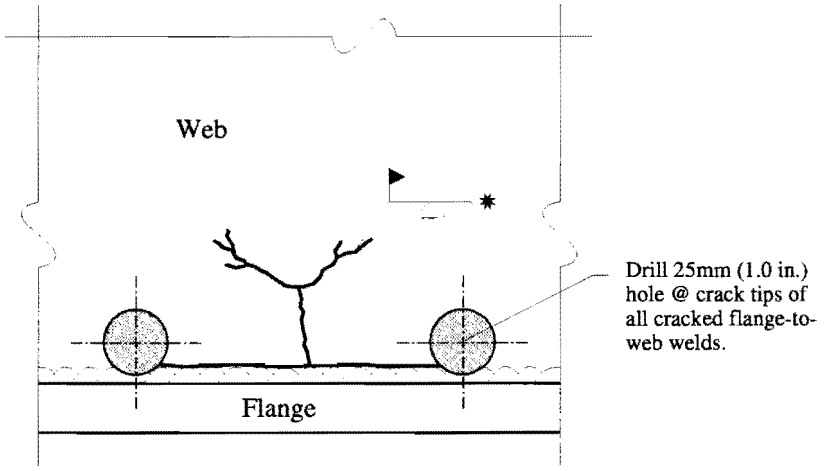

Figure 2-4: Backside detail of Type 1 repair.

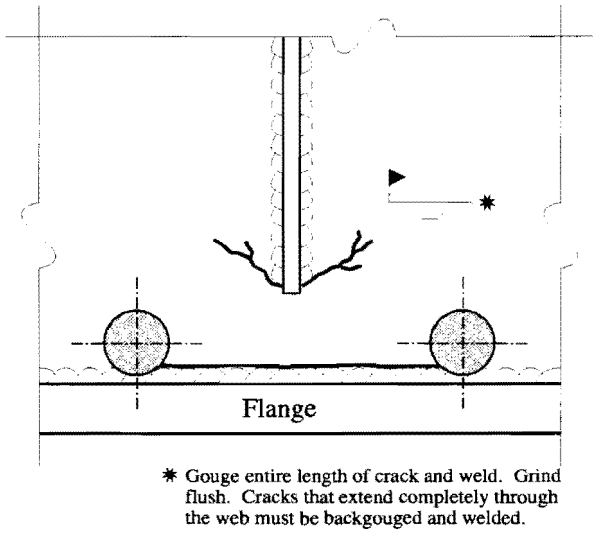

Figure 2-5: Frontside (stiffener side) detail of Type 1 repair.

After TxDOT personnel properly identified and marked all crack tips, each crack was removed beginning 12 mm (1/2 in.) beyond the crack tip and progressing toward the origin of the crack. A 6 mm (1/4 in.) copper coated rod was used in conjunction with a pressurized air supply to gouge out the cracks. Care was taken not to make a U-shaped bevel, but a V-shaped bevel, to

prevent the entrapment of slag during the re-weld operation. A U-shaped bevel has the tendency to trap slag when re-welding because there is no room to oscillate the welding rod to tie the sides together. A V-shaped bevel, on the other hand, allows the welder room to move the rod back and forth and minimizes the accumulation of slag. Figure 2-6 shows examples of U-shaped and V-shaped bevels.

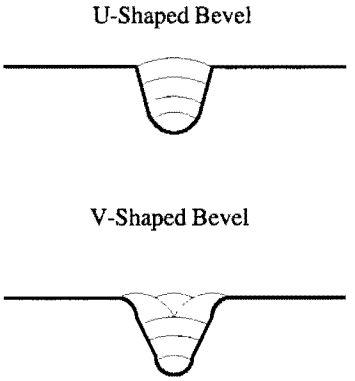

Figure 2-6: Examples of U-shaped and V-shaped bevels.

After the gouges on one side of the web plate were filled and completed, the welder moved to the other side of the web or flange and gouged out the remainder of the crack line. The gouge line was taken beyond the crack tip to a distance of a little greater than half the thickness of the material, ensuring that all of the crack was removed from the stressed area back to the solid weld material that had been placed on the other side earlier.

The gouged out areas were filled to a level 3 mm (1/8 in.) above the level of the present plate material. The surface of the welds were then ground smooth and flush with the original surface. Finally, dye penetrant tests were performed to check the repaired surfaces.

The Type 1 repair procedure is adequate, but costly. There is a tendency to miss following a crack line to the end of its crack-stress plane. Doing an X-ray inspection of the repaired area is the only way of insuring a thorough repair job. Also, if the stress in the area of

the crack or cracks is not eliminated, it is locked into the area again, and cracks will probably re-appear.

2.4.2 Type 2 Repair Procedure

Repair Procedure Type 2 was used if cracks were clustered and if three or more finger cracks extended from one crack line. Figures 2-7 and 2-8 show excerpts from the actual repair drawings, detailing the process. First, the ends of the cracks were located visually by the dye penetrant method and marked approximately 6 mm (1/4 in.) to 10 mm (3/8 in.) beyond the end of each tip (Fig. 2-9). A cutting torch was then used to cut out the cracked material in the web along the marks made (Figure 2-10). The holes were kept as small as possible. They could be egg-shaped, oblong, or tapered, but they had to have smooth transition radii on the cut lines and no sharp 45° or 90° corners. The flame out lines were then ground to a smoothness of 0.050 mm (2000 μin.) or less (see ANSI/AASHTO/AWS D1.5 (Sec. 3.2.2)), leaving smooth radii and finishes to the repaired areas (Figures 2-11 and 2-12). Finally, the holes were checked again with dye penetrant to ensure a proper repair (Figures 2-13 and 2-14). Any remaining cracks were ground out and smoothed to the required finish.

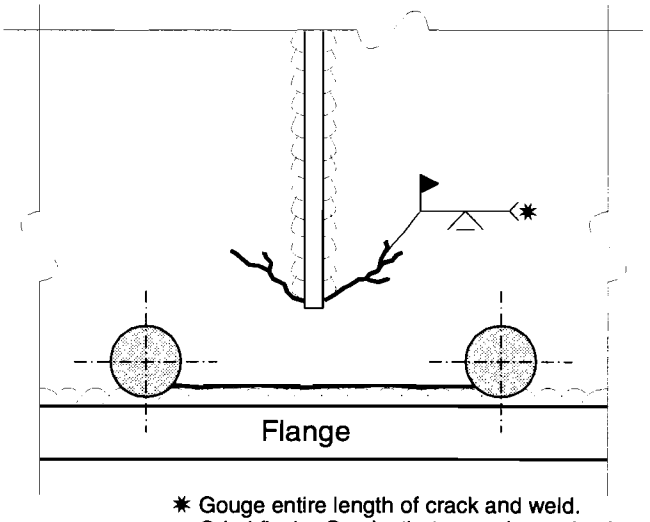

Figure 2-7: Frontside detail of Type 2 repair.

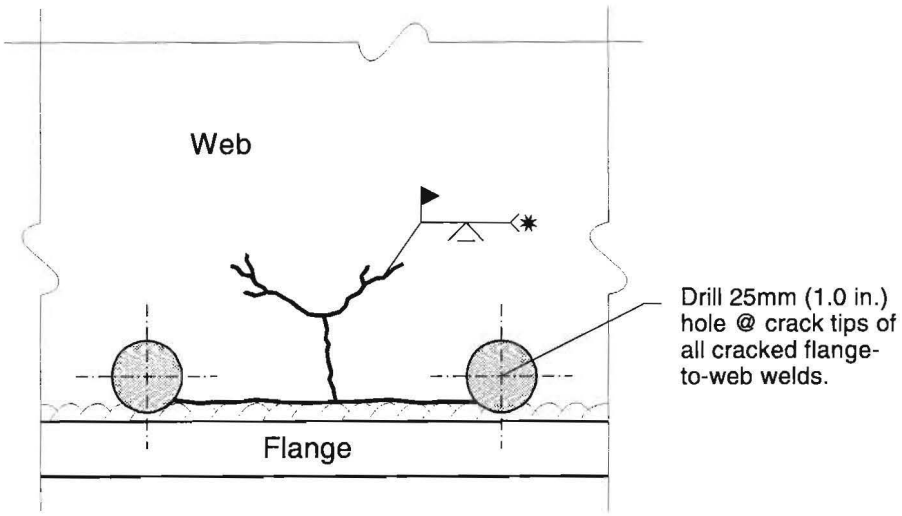

Figure 2-8: Backside detail of Type 2 repair.

Figure 2-9: Location and marking of the cracked area.

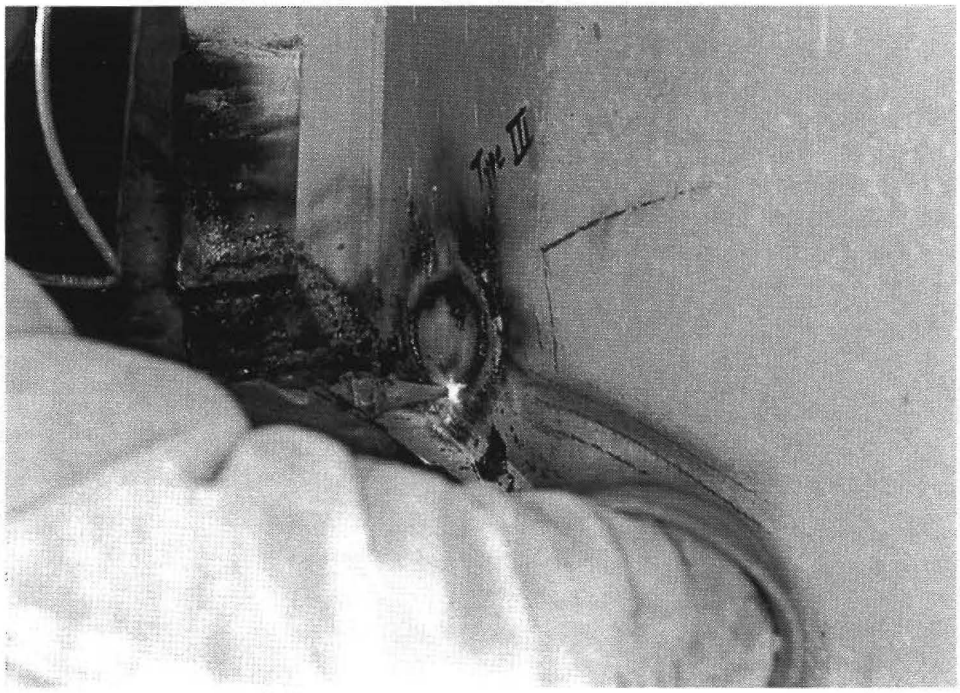

Figure 2-10: Removal of cracked material with cutting torch.

Figure 2-11: Grinding of hole to a smooth surface.

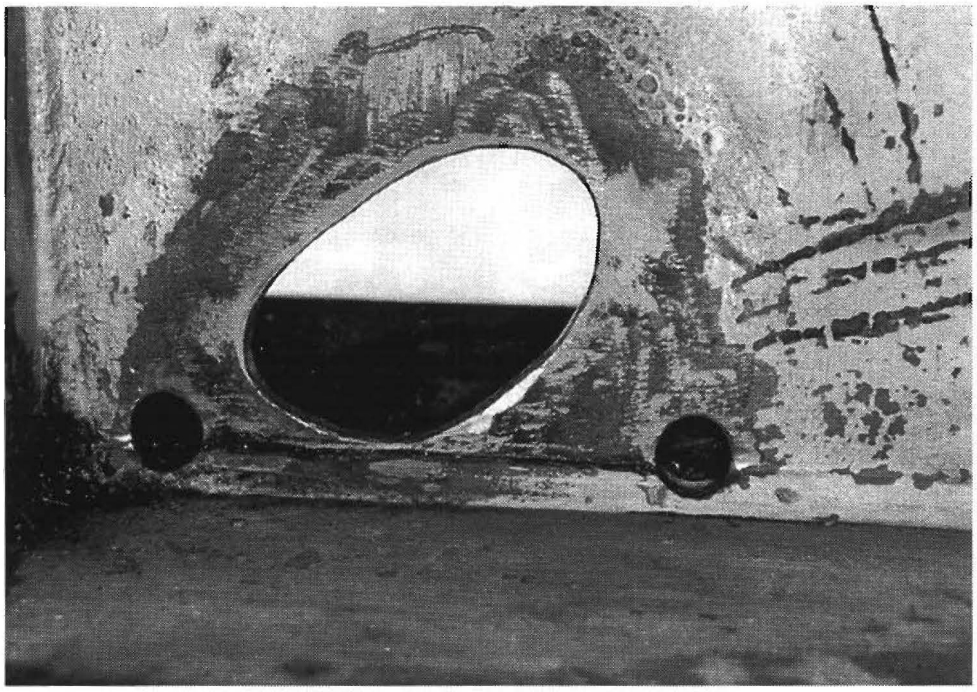

Figure 2-12: Web after initial repairs.

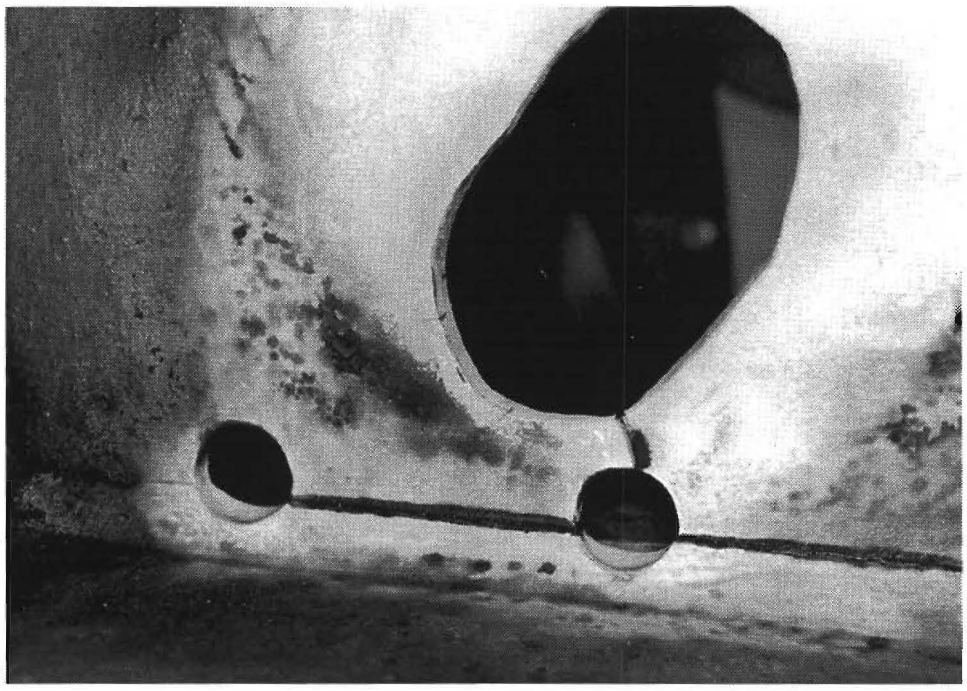

Figure 2-13: Dye penetrant test showing remaining cracks.

Figure 2-14: Removal of remaining cracks with grinder.

The Type 2 repair procedure is adequate and less expensive than the Type 1 procedure. Most of the time, an entire group of stress cracks and finger cracks may be completely removed in one repair section. The torch operator, however, must be able to cut a smooth hole with a minimum of flame-cut lines. Flame-cut lines require grinding, and too often slow down the progress of the repairs. In addition, large holes are left in the web section. Again, it is important that the high stress area around the cracks be relieved to ensure that the cracks will not spread from the coped out area in the web.

2.4.3 Type 3 Repair Procedure

Figures 2-15 and 2-16 show repair drawings for the Type 3 repair procedure. For this repair procedure, the ends of cracks were visually located by the dye penetrant method. Holes were drilled, or cored, approximately 6 mm to 10 mm (1/4 in. to 3/8 in.) onto the crack tip ends. After drilling the holes, visual inspections were performed to make sure that the crack was

arrested and did not protrude through the hole to the other side. If a crack line had several finger crack lines coming off of it, holes were drilled to arrest all crack tips (Figures 2-17 and 2-18). If the holes overlapped each other, the sides of the slots were ground smooth to an ANSI 500 finish (Figures 2-19 and 2-20), removing any drill-through cutting edges. The areas were checked with dye penetrant to make sure that the crack tip was removed.

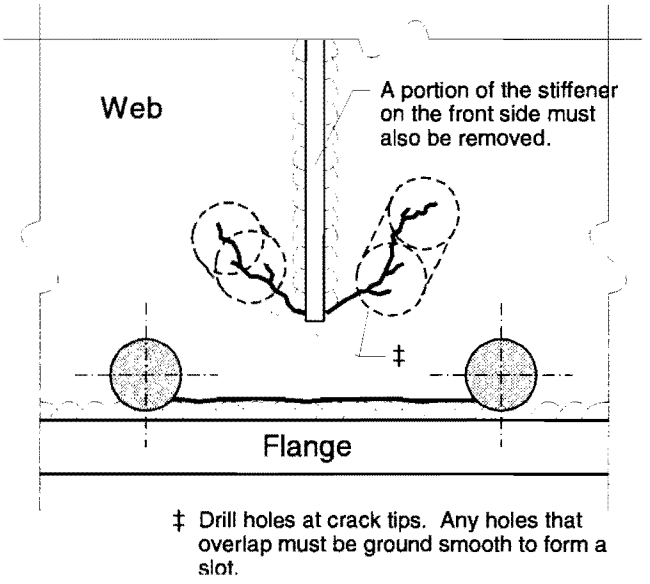

Figure 2-16: Frontside (stiffener side) detail for Type 3 repair.

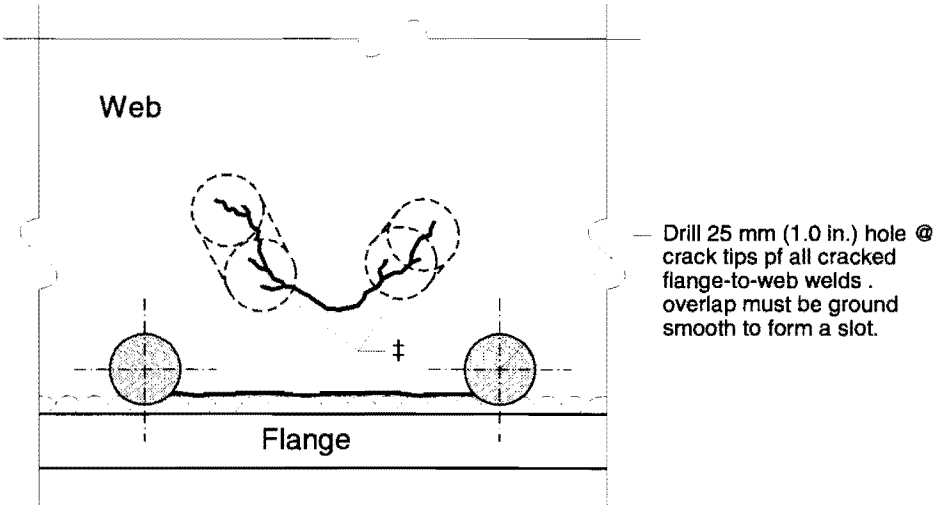

Figure 2-15: Front side (stiffener side) detail for Type 3 detail.

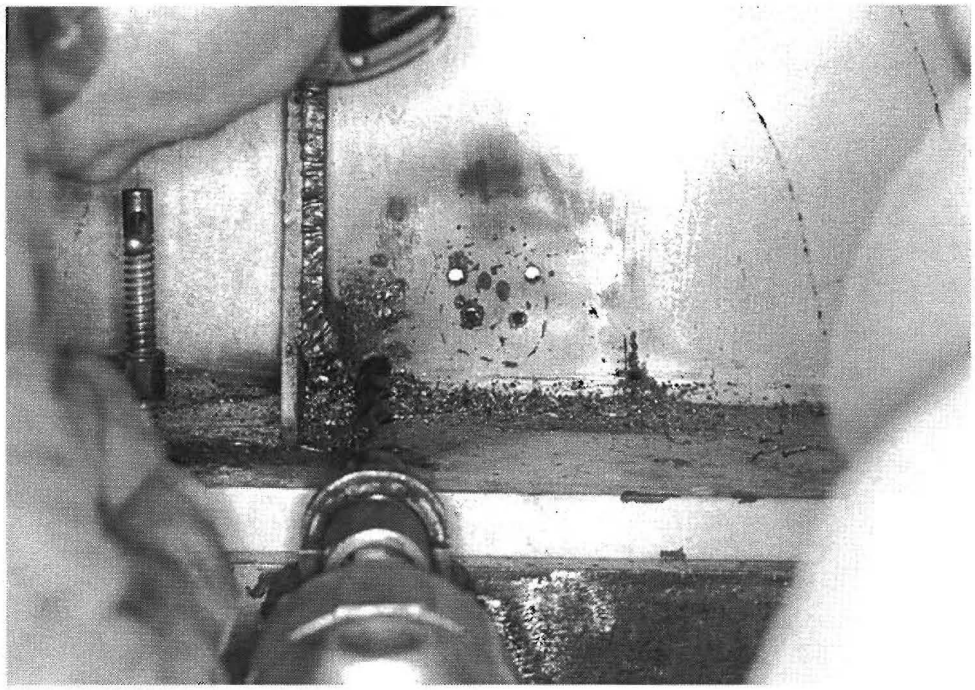

Figure 2-17: Drilling at crack tip ends.

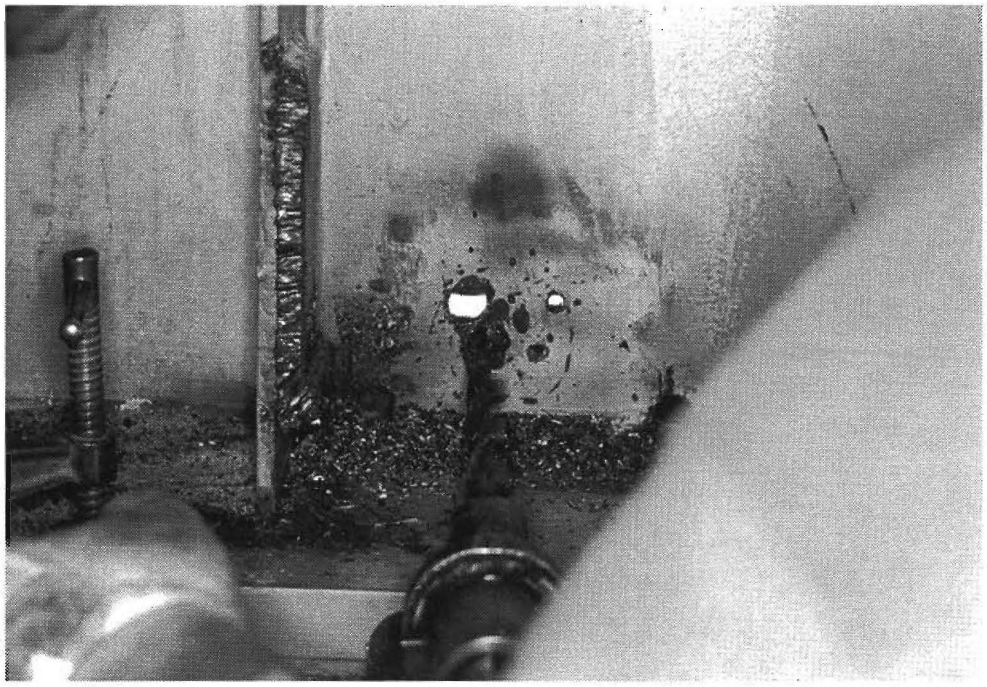

Figure 2-18: Drilling to arrest all finger crack lines.

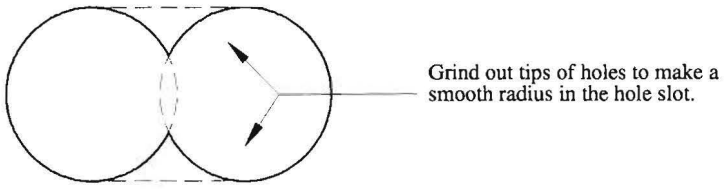

Figure 2-19: Overlapping holes slotted to remove cutting edges.

Figure 2-20: Repaired web section after hole-slotting.

The Type 3 repair procedure is the least expensive of the three repair procedures, as labor and equipment costs are low if the contractor has the equipment available to him. It is probably the easiest method to check visually when making sure that the crack tip has been removed. No weld metal or heat is applied to the web plate. No large holes are drilled into the web section and no paint is burned off, making it a fairly clean repair procedure. Again, the high stress areas must be relieved in order to stop any cracks from forwarding through the drilled or cored holes. The Type 3 procedure is fairly quick, and is useful in stopping cracks in emergency situations.

It is important to note that, regardless of which procedure is used, all known fatigue cracks must be arrested to prevent continued propagation. If not, these cracks could propagate to failure due to the primary or in-plane bending stresses, even though the distortion stresses may have been eliminated by the removal of the bracing. A view of each completed repair type is given in Fig. 2-21 through 2-23.

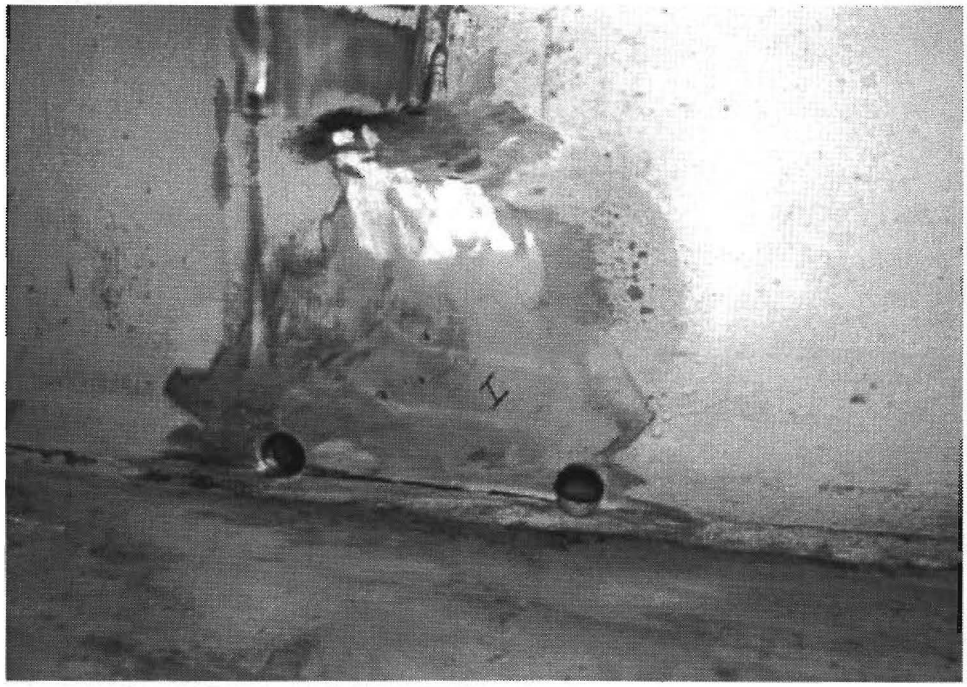

Figure 2-21: View of completed Type I repair procedure.

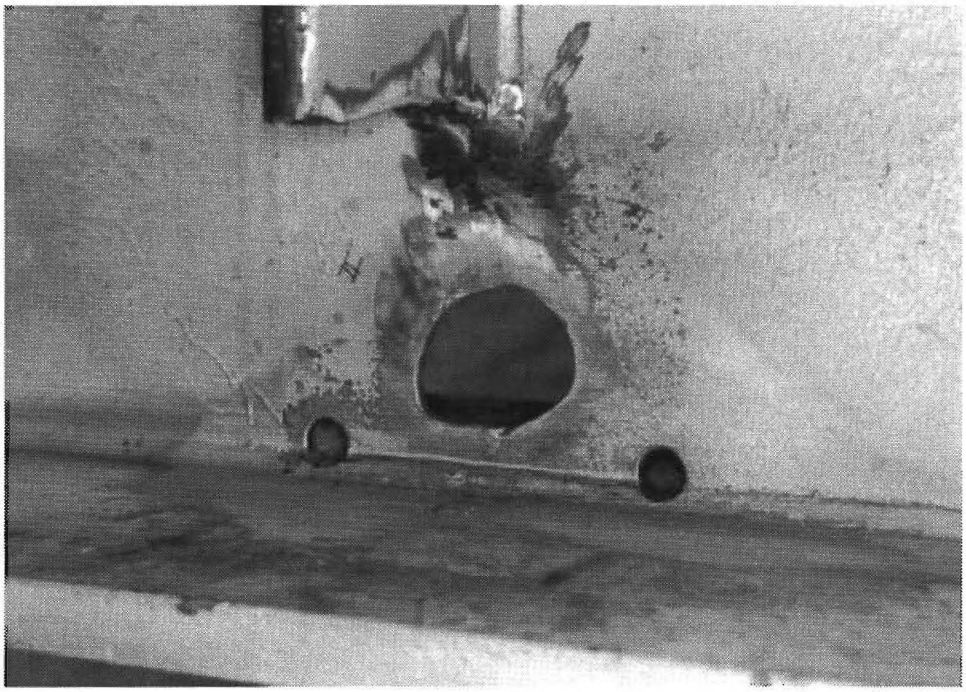

Figure 2-22: View of completed Type II repair procedure.

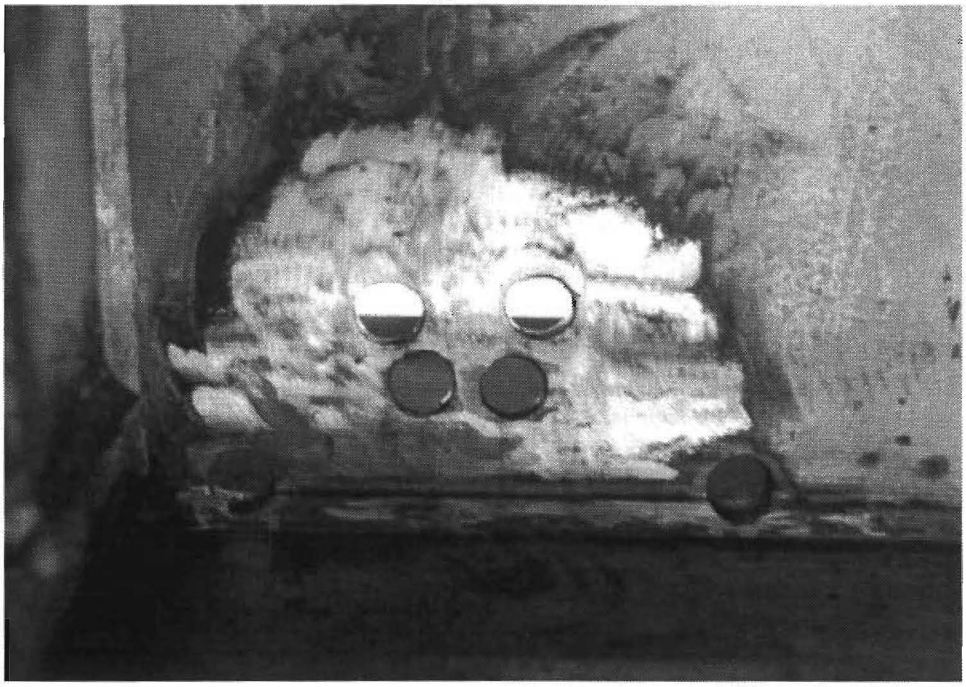

Figure 2-23: View of completed Type III repair procedure.

2.5 WELDED CONNECTION PLATE ATTACHMENTS

In addition to the web-gap fatigue crack repairs, additional repair methods were used during the contract that could influence the fatigue life of the structure. This involved the field welding of the existing connection plates to the flange. This operation was performed at locations where new cross-frame diaphragms were re-installed. Figure 2-24 shows a replacement cross frame and connection plate. Again, concern is with the quality of the field welding. Since the connection plate was not originally attached to avoid a tension flange weldment, welding it now would result in a fatigue-sensitive detail. If the connection plate end termination was a tight-fit detail, it would not be possible to thoroughly clean the gap between the end of the connection and the flange surface. Any impurity could affect weld metal quality. If the connection plate end was a cut-short detail, some type of plate extension will be required to make the rigid attachment. While adequate cleaning could be performed prior to welding, concern again is with the field welding.

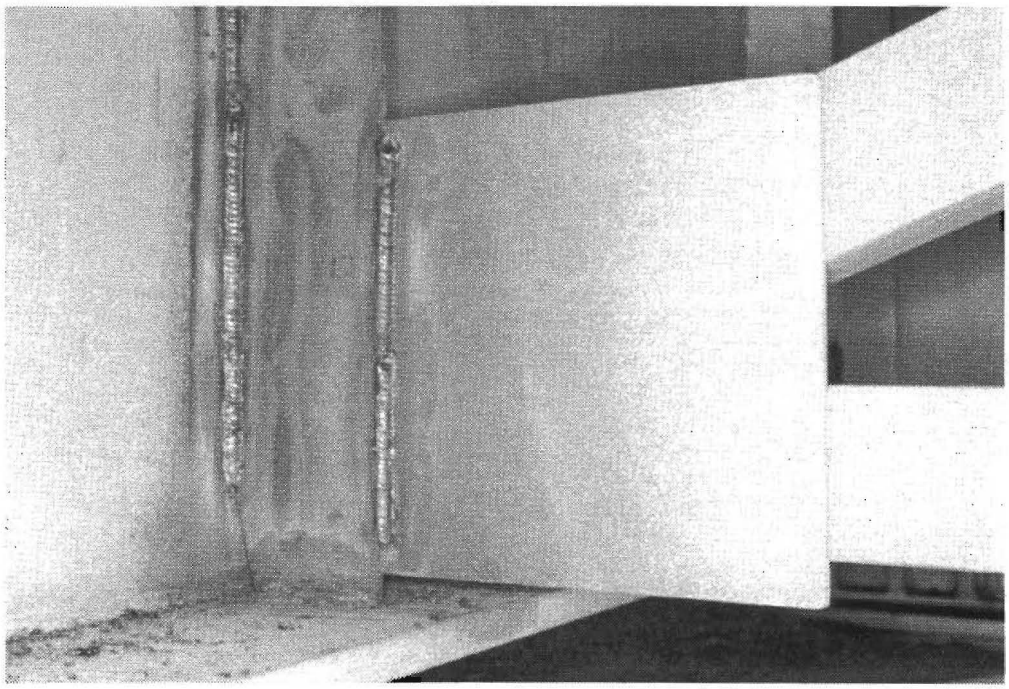

Figure 2-24: View of replacement cross-frame diaphragm with welded connection plate.

Chapter Three

EXPERIMENTAL EVALUATION OF WEB-GAP REPAIR PROCEDURES

Laboratory tests were conducted on large-scale plate girder specimens to determine the effectiveness of the fatigue repair procedures used on the Midland County bridges, as discussed in Chapter Two. The fatigue repair procedures investigated included:

- gouge and re-weld;
- web plate flame cut;
- drilled holes at the crack tips;
- welded attachment of tight-fit connection plate detail; and
- tight-fit retrofit with welded clips.

The tests were performed at the Materials and Structures Laboratory in the Wisenbaker Engineering Research Center on the campus of Texas A&M University in the summer and fall of 1993.

Trinity Industries, Inc. of Houston, Texas fabricated each test specimen and all necessary test apparatus members. Trinity Industries was chosen based on its experience in fabricating highway bridge members to TxDOT standards. Fabrication techniques, consistent with the standards employed by TxDOT, were used in the fabrication of the test specimens.

3.1 TEST PROGRAM

The plate girder specimens consisted of three different designs. Each girder had a total depth of 760 mm (30 in.) and flange width and thickness dimensions of 305 mm (12 in.) and 25 mm (1.0 in.) respectively. All web-to-flange connections were made using 8 mm (5/16 in.) fillet

welds with E70XX electrodes. The stiffeners were attached to the girder web plates with 6 mm (1/4 in.) fillet welds. Girder 1, the least stiff of the three, had a web plate thickness of 8 mm (5/16 in.), while Girders 2 and 3 had 10 mm (3/8 in.) thick web plates. Girders 1 and 2 had stiffeners attached to one side of the web plate with a 38 mm (1-1/2 in.) web gap (see Fig. 3-1). The stiffeners on Girder 3 were placed on both sides of the web with a tight-fit detail between the stiffeners and the bottom flange. Figures 3-1 through 3-3 show design drawings used in the fabrication of the test girders.

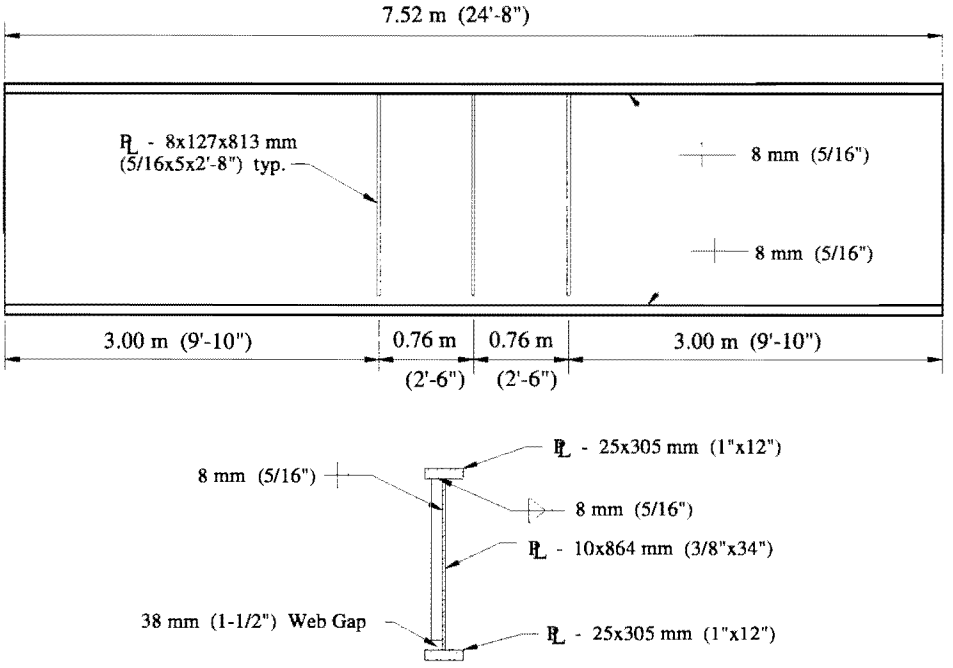

Figure 3-1: Test Girder 2 and cross section.

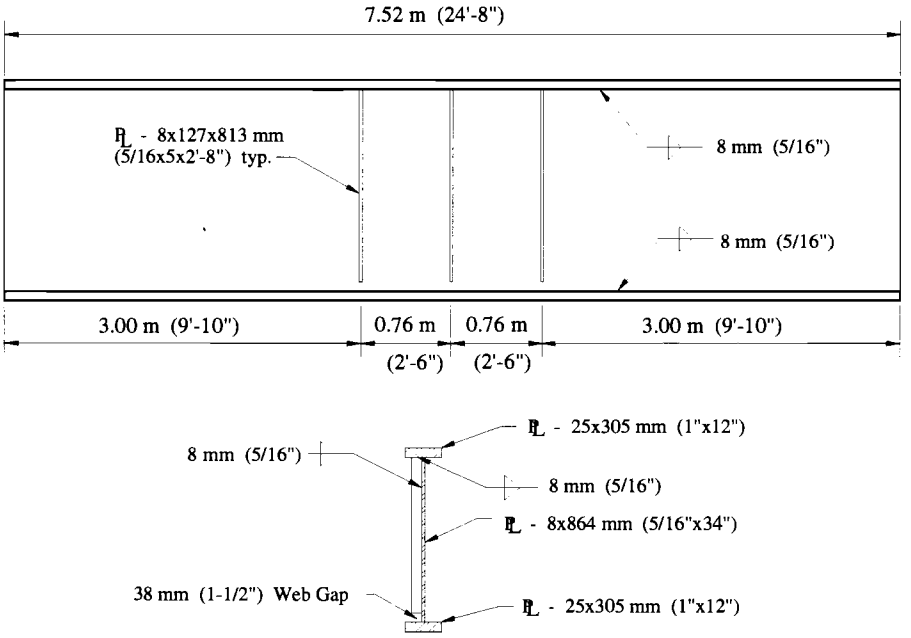

Figure 3-2: Plan of Test Girder 3 and cross section.

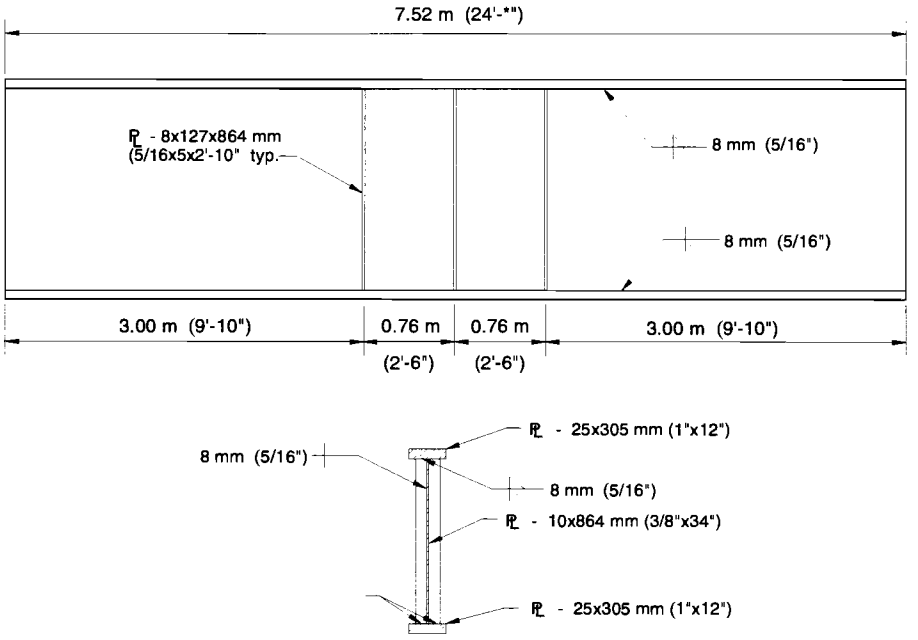

Figure 3-3: Test Girder 1 and cross section.

Plan and profile views of the test assembly are given in Figs. 3-4 and 3-5. Two pairs of columns and header beams were used to support two 490 kN (110 kip) actuators in the proper loading positions over the girders. The girders were supported by a fixed rocker bearing at one end and a rocker bearing that allowed horizontal movement at the other end. The Materials and Structures Lab has a 610 mm (24 in.) thick concrete strong-floor that allowed the columns and rocker bearing assemblies to be bolted tightly in place. The load frames were lashed to the strong floor with 13 mm (1/2 in.) steel cables to increase the stiffness of the structure and prevent sideways movement due to unintended eccentricity of load during the fatigue testing. This is shown in Fig. 3-5. A view of a girder in the test apparatus is shown in Fig. 3-6.

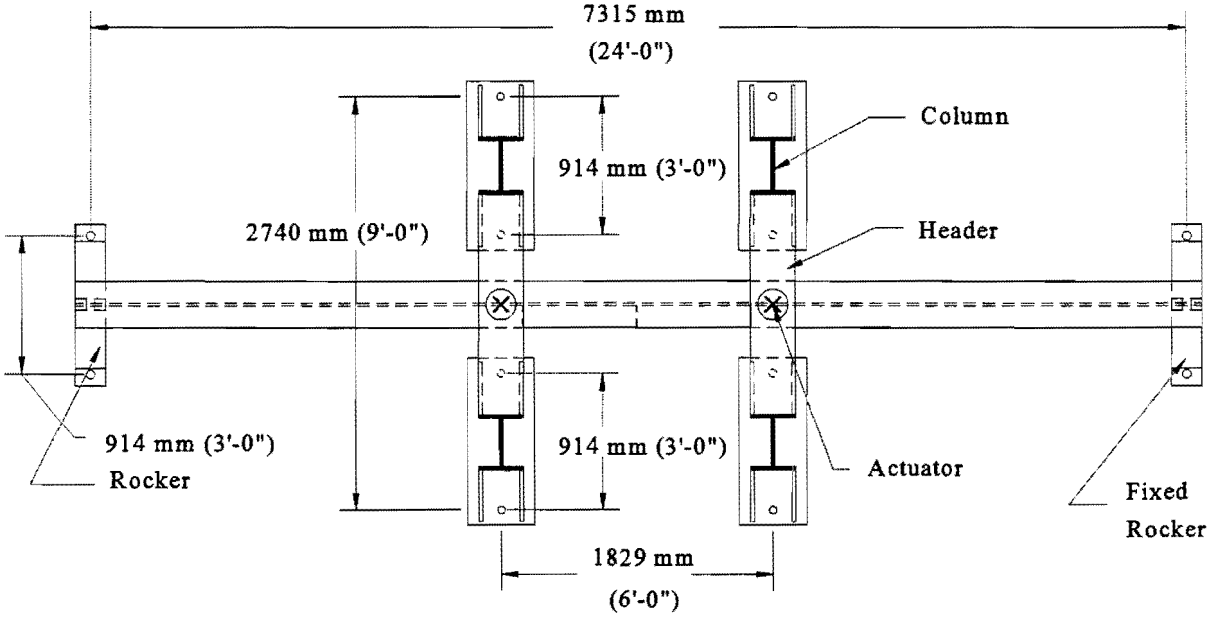

Figure 3-4: Plan view of test apparatus.

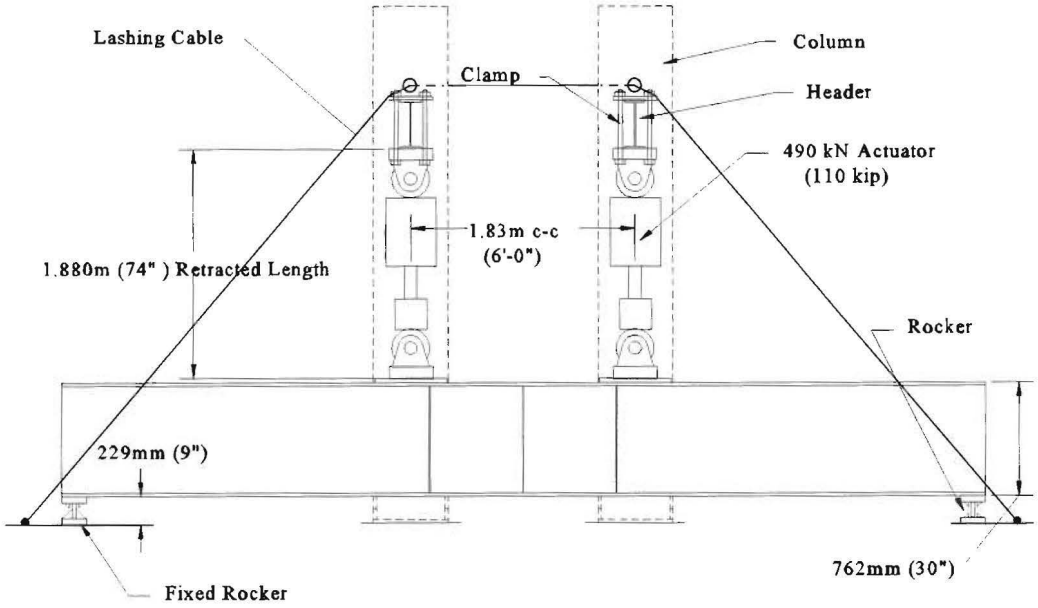

Figure 3-5: Profile view of test apparatus.

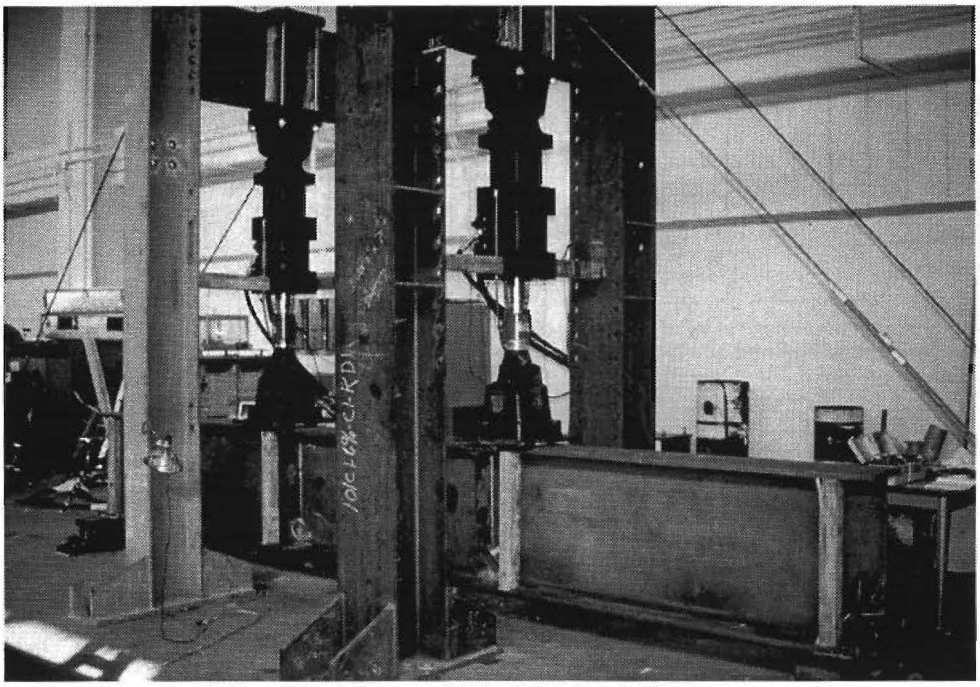

Figure 3-6: View of girder and fatigue test apparatus.

3.2 PRE-CRACKING OF GIRDER 2

Girder 2 was selected for the pre-cracking phase of the experiment. The purpose of pre-cracking was to simulate the out-of-plane distortion and fatigue crack damage caused by unstiffened web gaps and improperly designed connection plates. The girder was placed on its side underneath the load frame shown in Figure 3-7. A 220 kN (50 kip) actuator was used to apply cyclic loads through the edges of each of the three stiffeners. The actuator was attached to the edge of the stiffeners with a clevice (shown in Figure 3-8). The test log in Appendix A shows the magnitude, direction, and frequency of the loads applied to the girder. Larger actuator compressive cycles initiated cracking on the bottom side of the web plate, and smaller actuator tensile forces propagated the crack through the plate

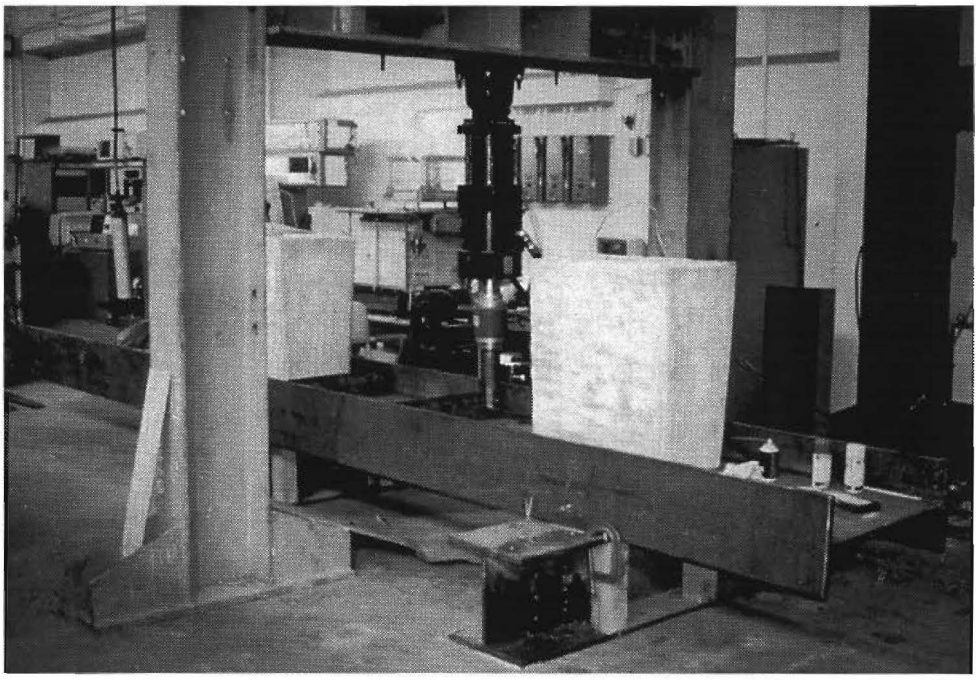

Figure 3-7: Pre-cracking load frame.

Figure 3-8: Pre-cracking of Girder 2.

Figures 3-9 through 3-20 show the fatigue cracking in the web plate around each stiffener. Each pair of figures (Figs. 3-9 and 3-10 for example) provides a schematic drawing of the mapped cracking pattern for one side of the web plate and the corresponding view photographed after dye penetrant inspection was performed. The crack patterns that developed were similar to those commonly found on in-service highway bridges suffering from distortion induced fatigue. Fatigue cracks developed in the toe of the web-to-flange fillet weld, as well as around the end of the connection plate.

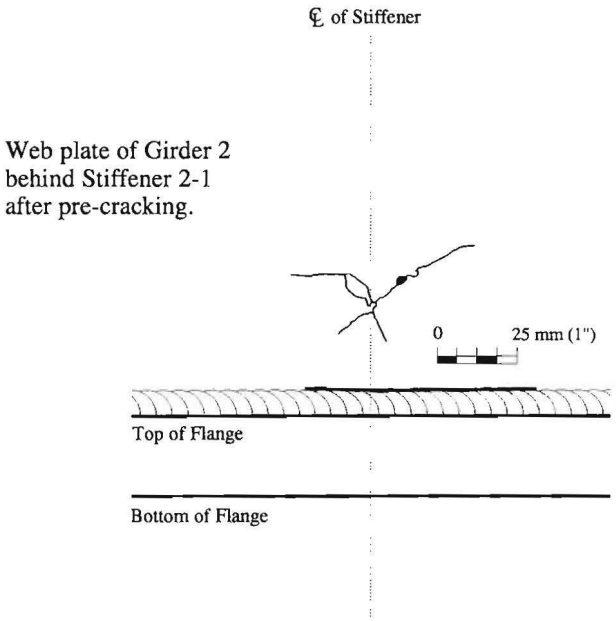

Figure 3-9: Pre-cracking in web plate of Girder 2 behind Stiffener 1.

Figure 3-10: Examination of crack using dye penetrant.

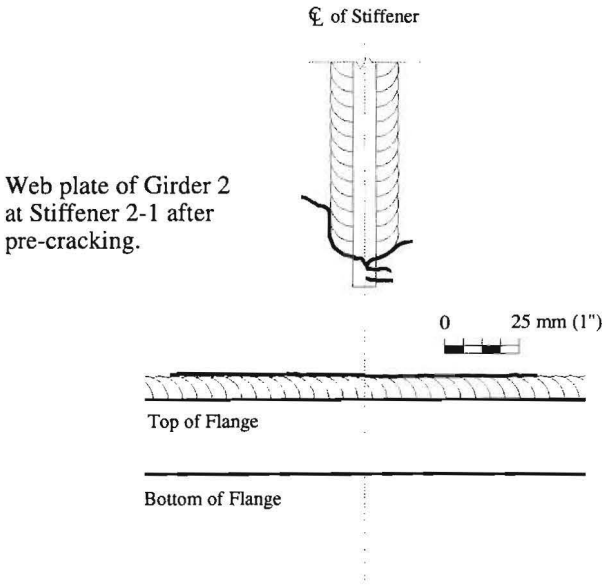

Figure 3-11: Pre-cracking in web plate of Girder 2 at weld toe of Stiffener 1.

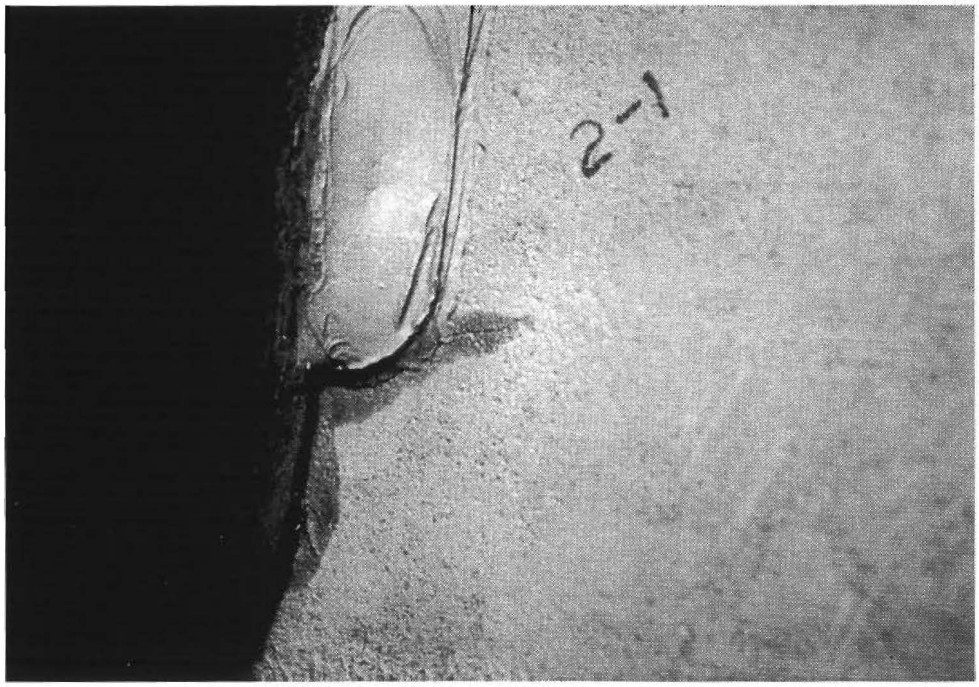

Figure 3-12: Examination of crack using dye penetrant.

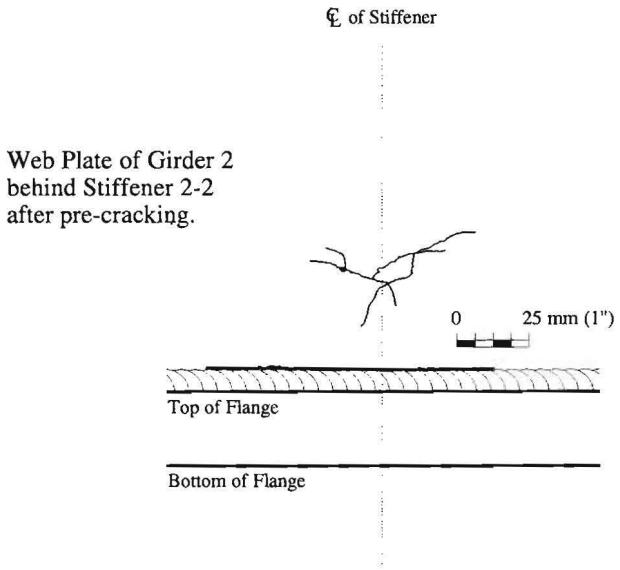

Figure 3-13: Pre-cracking in web plate of Girder 2 behind Stiffener 2.

Figure 3-14: Examination of crack using dye penetrant.

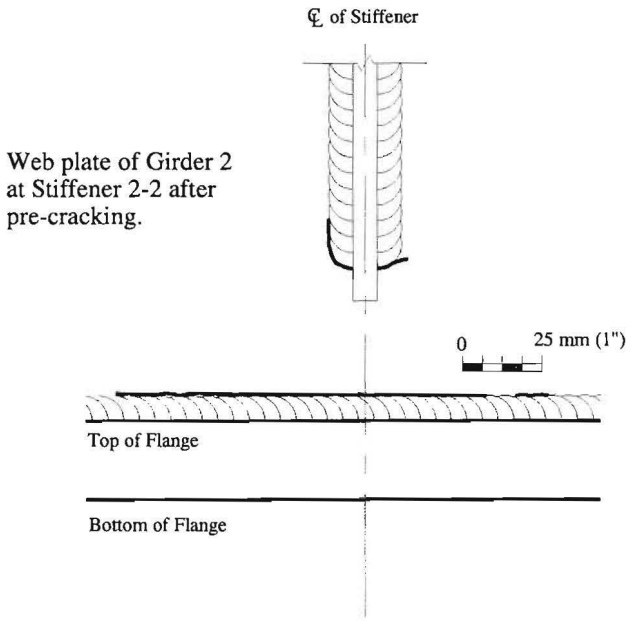

Figure 3-15: Pre-cracking in web plate of Girder 2 at weld toe of Stiffener 2.

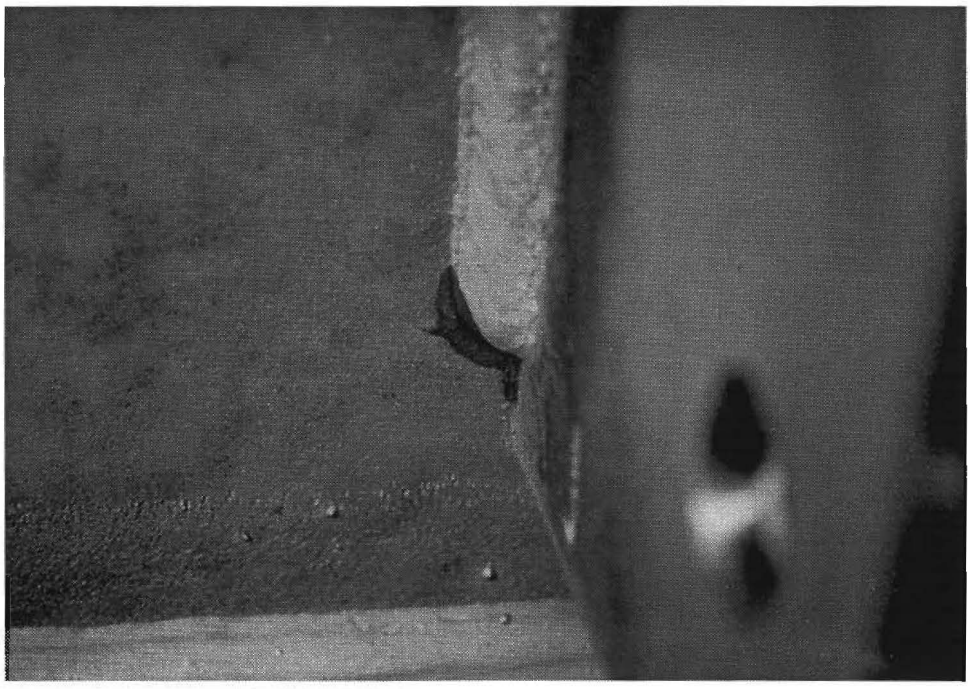

Figure 3-16: Examination of crack using dye penetrant.

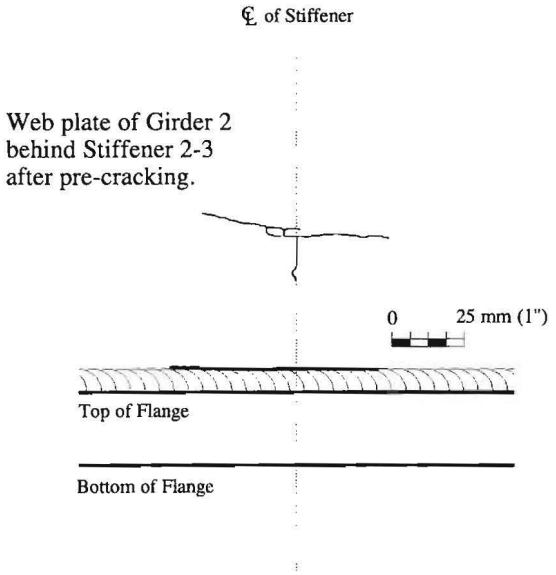

Figure 3-17: Pre-cracking in web plate of Girder 2 behind Stiffener 3.

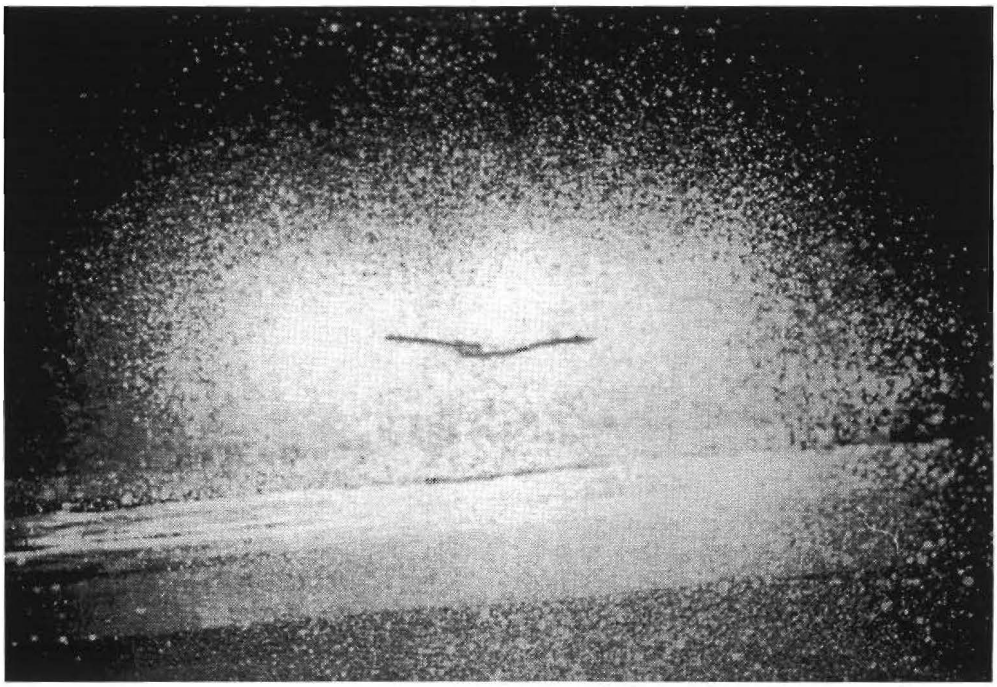

Figure 3-18: Examination of crack using dye penetrant.

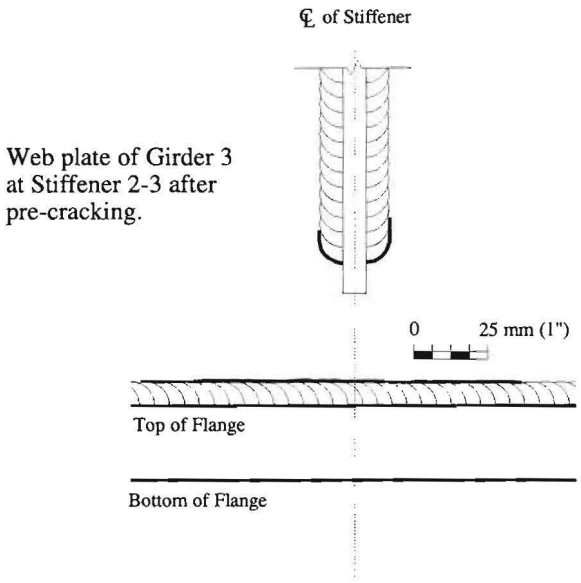

Figure 3-19: Pre-cracking in web plate of Girder 2 at weld toe of Stiffener 3.

Figure 3-20: Examination of crack using dye penetrant.

3.3 SIMULATED REPAIRS TO TEST GIRDERS

Repairs simulating those used by TxDOT were performed on all three test girders. The repairs made on Girders 1 and 2 closely modeled the web cracking repair procedures used on the Midland County bridges. The welded attachment retrofit was used on Girder 3. Both the welding of the tight-fit detail and the welded clip were examined. A welding inspector for TxDOT made all of the repairs. This welding inspector was the same inspector who monitored the repairs for the Midland County bridges. His knowledge of TxDOT standards for welding and repair ensured that the repairs were performed consistent with those performed in the field.

Girder 1: Drilling holes at the tip of a crack is the most common means of arresting a crack's growth. In some cases, however, crack density is so severe that drilling holes to arrest all of the cracks is not feasible. As a result, complete removal of the cracked material may be necessary. The repairs to Girder 1 simulate this type of repair. Since this repair involved complete removal of cracked material, pre-cracking was not necessary. First, the stiffeners were shortened to provide access to the "cracked" web area. This was done with a cutting torch, as shown in Figure 3-21. Three different cutting details, shown in Figures 3-22 through 3-24, were used to determine if this had any effect on the fatigue behavior of the repair. Again, a torch was used to remove the "cracked" material near the toe of each stiffener.

Figures 3-25 through 3-27 show the size and shape of each torched hole. The holes at Stiffeners 1-1 and 1-2 are very similar to those used on the Midland County bridges. In the case of the hole near Stiffener 1-2, notches were ground into the edges of the hole to simulate removal of any crack tips that may remain after flame-cutting, and to determine if the notches would have any adverse effects on the fatigue life of the girder. Finally, all torched surfaces on the stiffeners and around the holes were ground to a smoothness of 0.050 mm (2000 μin.) or less. As will be discussed later, it is extremely important to obtain this finish to eliminate any surface discontinuities which might be a site of additional crack initiation and propagation.

Figure 3-21: Shortening of stiffeners by flame-cutting.

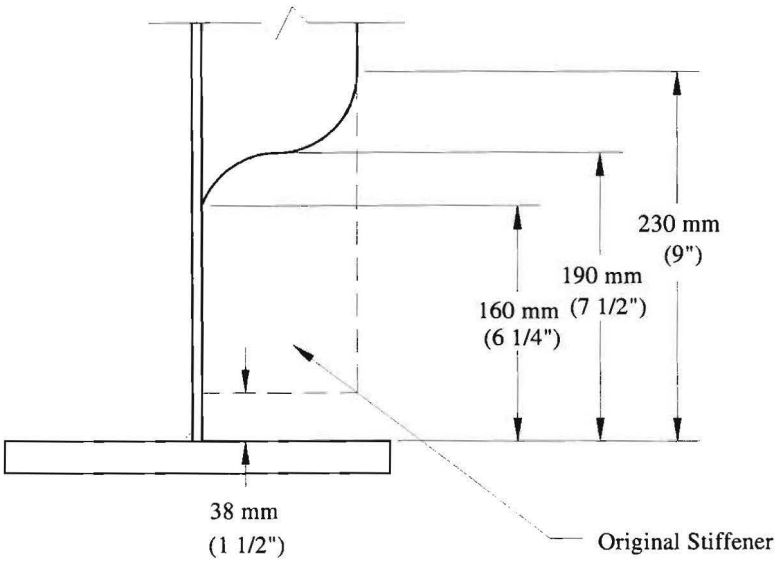

Figure 3-22: Shortening of Stiffener 1-1.

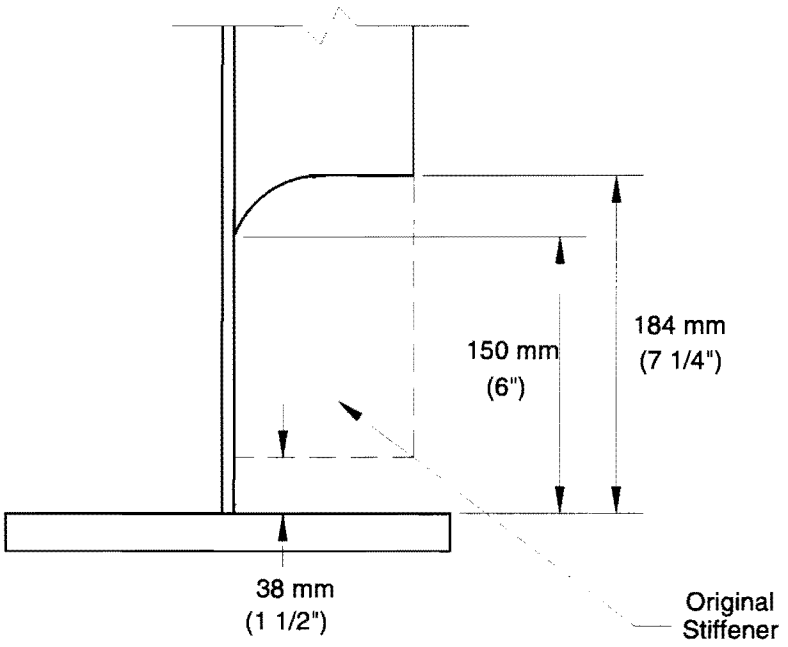

Figure 3-23: Shortening of Stiffener 1-2.

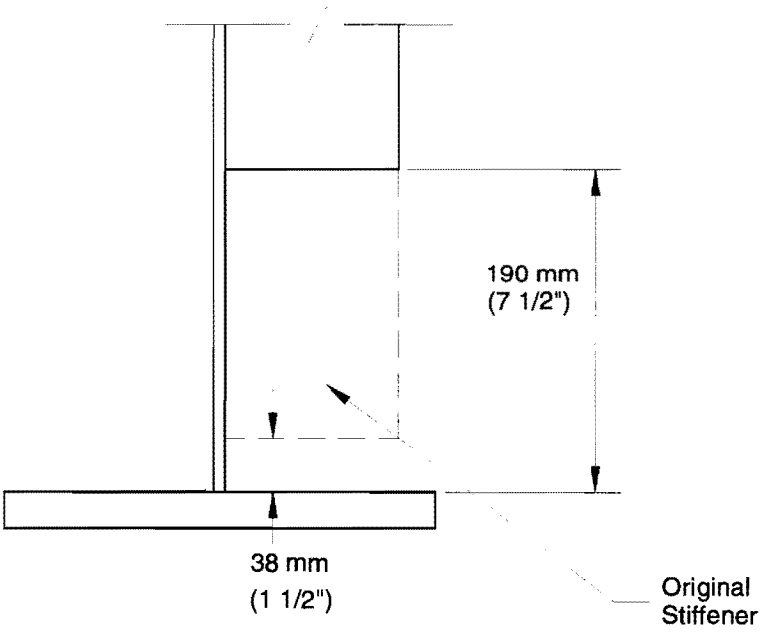

Figure 3-24: Shortening of Stiffener 1-3.

Figure 3-25: Removal of "cracked" material by flame-cutting.

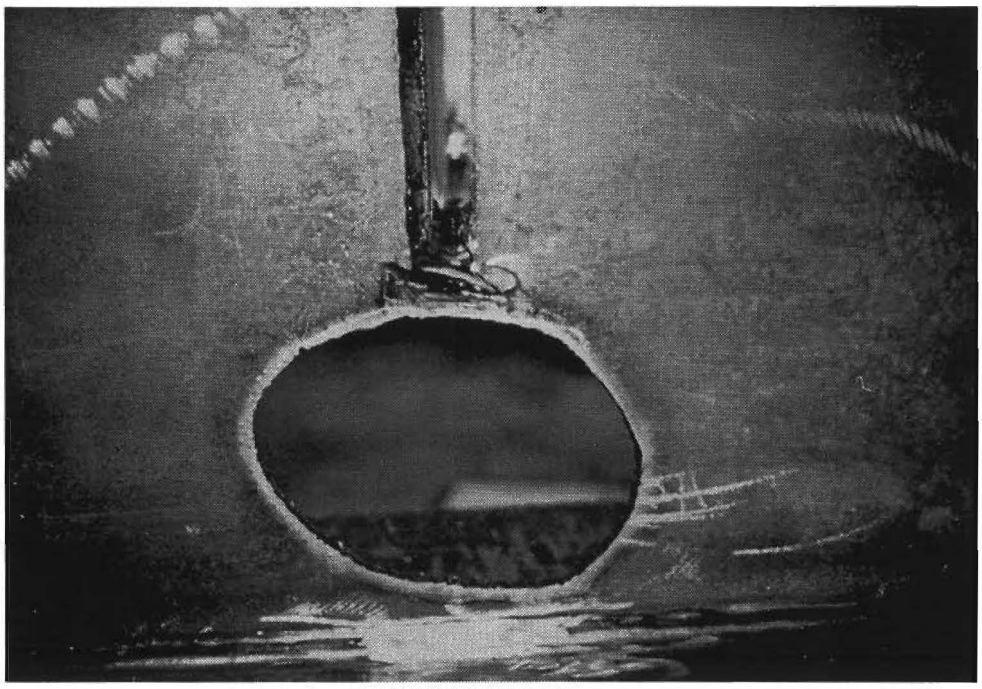

Figure 3-26: Flame-cut hole in web plate at Stiffener 1-1.

Figure 3-27: Flame-cut hole in web plate at Stiffener 1-2.

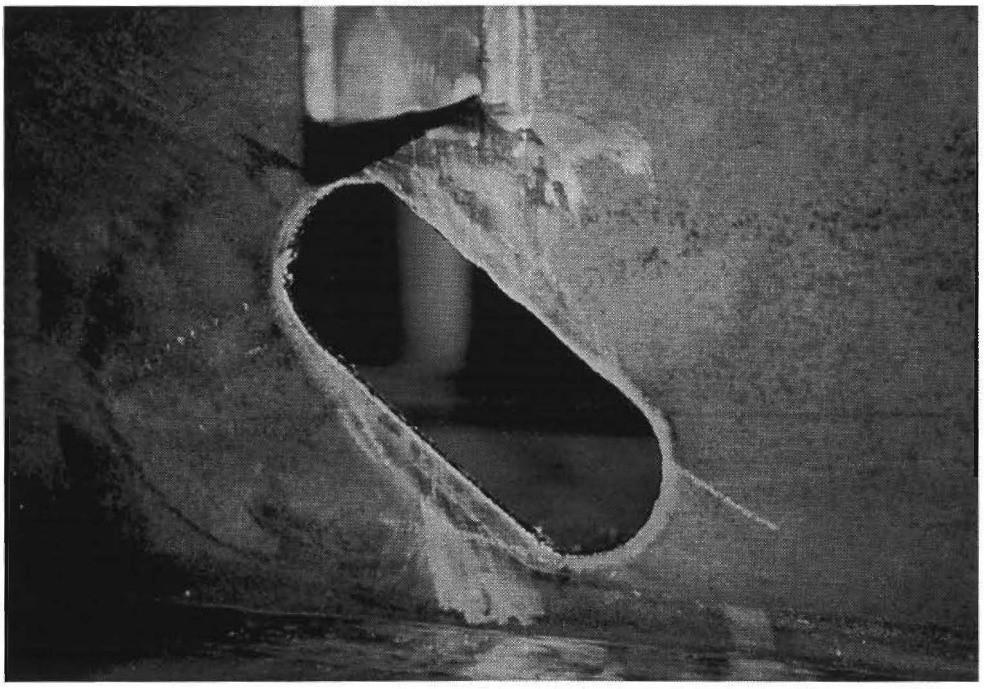

Figure 3-28: Flame-cut hole in web plate at Stiffener 1-3.

Girder 2: The "back-gouge and re-weld" technique was used to repair the cracking at all three stiffeners in Girder 2. First, the fatigue damaged areas on both sides of the web were sand-blasted clean. The stiffeners were then shortened with a cutting torch, creating a gap of approximately 100 mm (4 in.) between the end of the stiffener and top of the flange plate, as shown in Fig. 3-29. An air gouger was then used to remove the material on one side of the web plate along the crack lines (see Fig. 3-30). The depth of the gouge was a little more than one-half of the web plate thickness. Care was taken to avoid burning all the way through the plate. A burn- or blow-through of the web plate would increase the subsequent re-welding difficulty. The removed material was then replaced by arc welding using the shielded metal (SMAW) process with E70XX electrodes (see Fig. 3-31). The same procedure was then performed on all crack lines on the other side of the web. After the newly placed weld metal cooled, it was ground smooth using a standard hand-held grinder to an ANSI finish of 500.

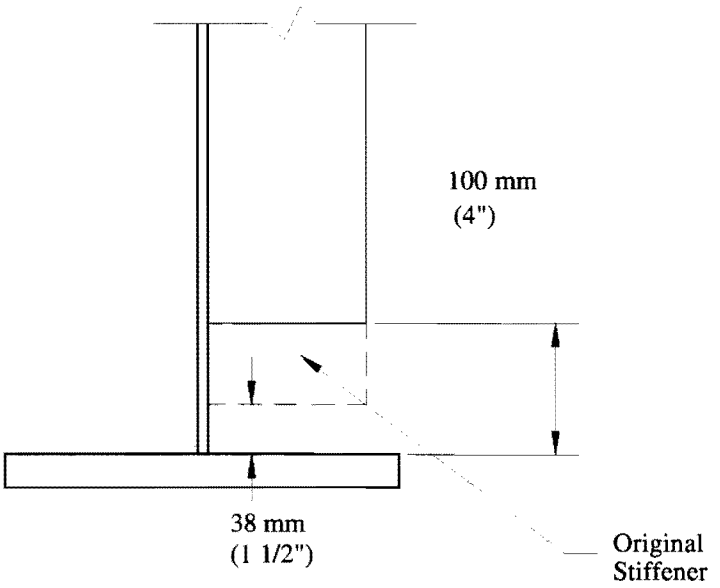

Figure 3-29: Shortening of stiffeners of Girder 2.

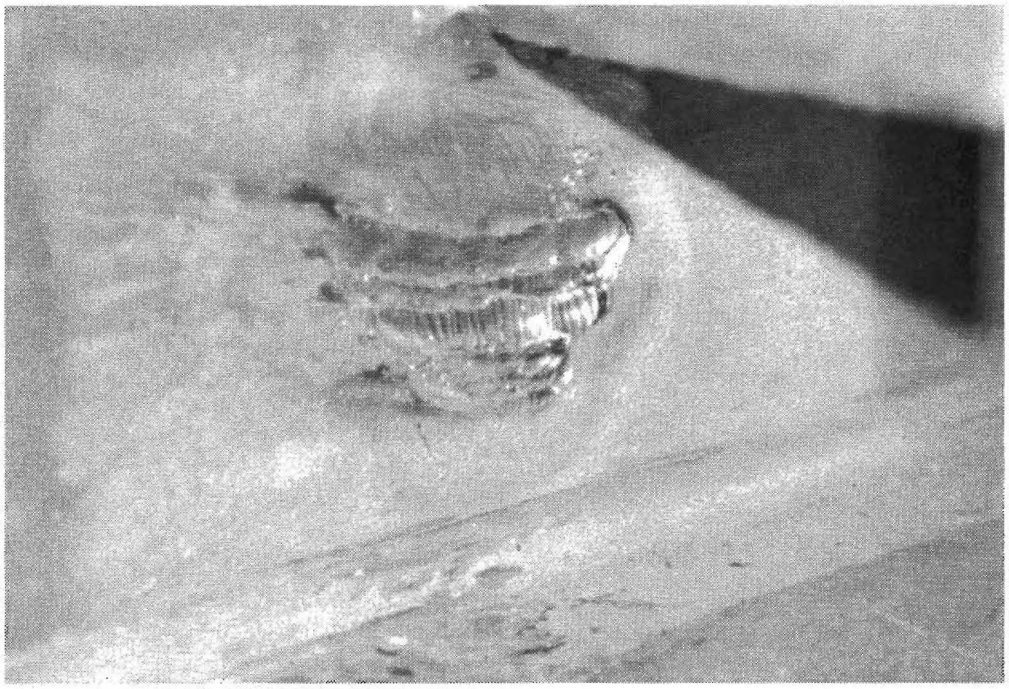

Figure 3-30: View of back gouged fatigue crack lines.

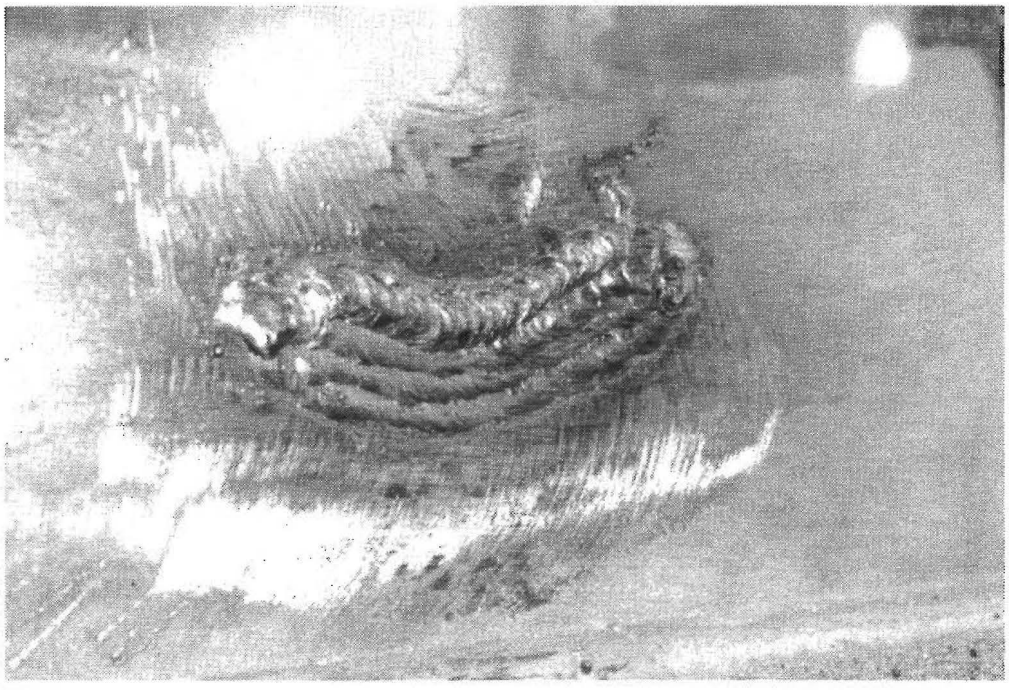

Figure 3-31: View of re-welded fatigue crack lines.

Two significant events occurred during the repair of Girder 2. At Stiffener 2-2, the web was inadvertently burned through during the air gouging process. The welder (inspector) was able to replace the material with weld metal. However, this requires a highly skilled welder and greatly increases the time and cost of the repair. At Stiffener 2-3, the repair was completed on one side of the web. During the gouging process on the other side of the web, the remaining crack propagated back into the newly-repaired region. Consequently, the repair had to be repeated in the area of the new crack. After the gouging and re-welding was completed, all repaired web surfaces were ground smooth using a disc grinder. Additional dye penetrant tests were performed to ensure that no other heat-driven cracks had propagated.

The longitudinal cracks in the web-to-flange plate fillet weld were not repaired. Since these cracks were oriented in the direction of bending stress, it was assumed that these cracks would not propagate further under cyclic loading. As will be discussed later in this chapter, these cracks did propagate under cyclic loading but did not effect the final results of the test.

Girder 3: No pre-cracking was performed on Girder 3. Instead, two different retrofit procedures were used on the tight-fit stiffener details as shown in Fig. 3-32. On one side of the girder, the paint around the stiffener-to-flange weld areas was sand-blasted clean. The ends of the stiffeners were then welded directly to the flange (see Fig, 3-33). The paint underneath the stiffener usually cannot be completely removed, therefore, it is likely that a lack-of-fusion plane will develop at this site. As a result, the stiffener-to-flange weld was monitored closely during fatigue testing.

On the other side of the girder, in order to eliminate any lack-of-fusion planes due to paint, each stiffener was shortened with a cutting torch to create 100 mm (4 in.) web gaps. This repair also simulated the condition where web-gap cracking had to be repaired prior to welding the connection plate to the flange. The torched surfaces of the web were ground smooth using a standard hand-held grinder. One hundred two mm x 203 mm (4 in. x 8 in.) clips were then fillet welded to the stiffeners and flange as shown in Fig. 3-34.

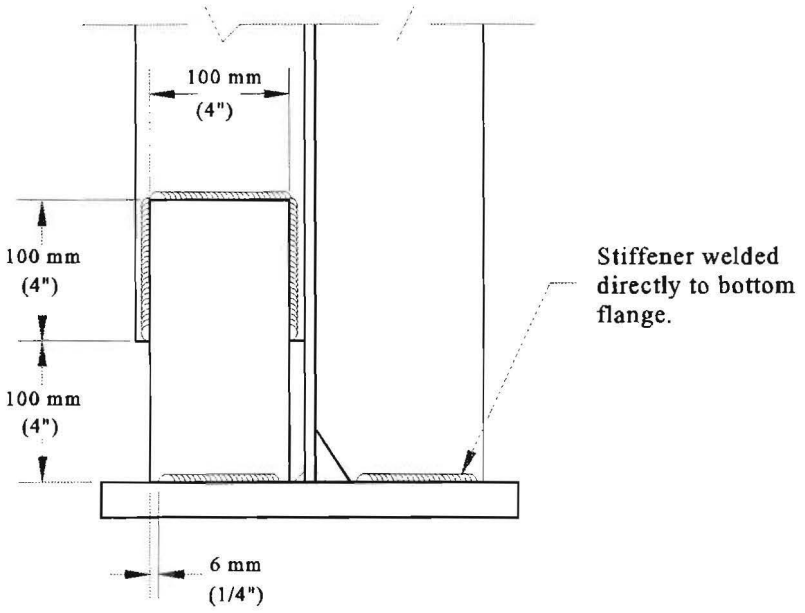

Figure 3-32: Tight-fit retrofit details.

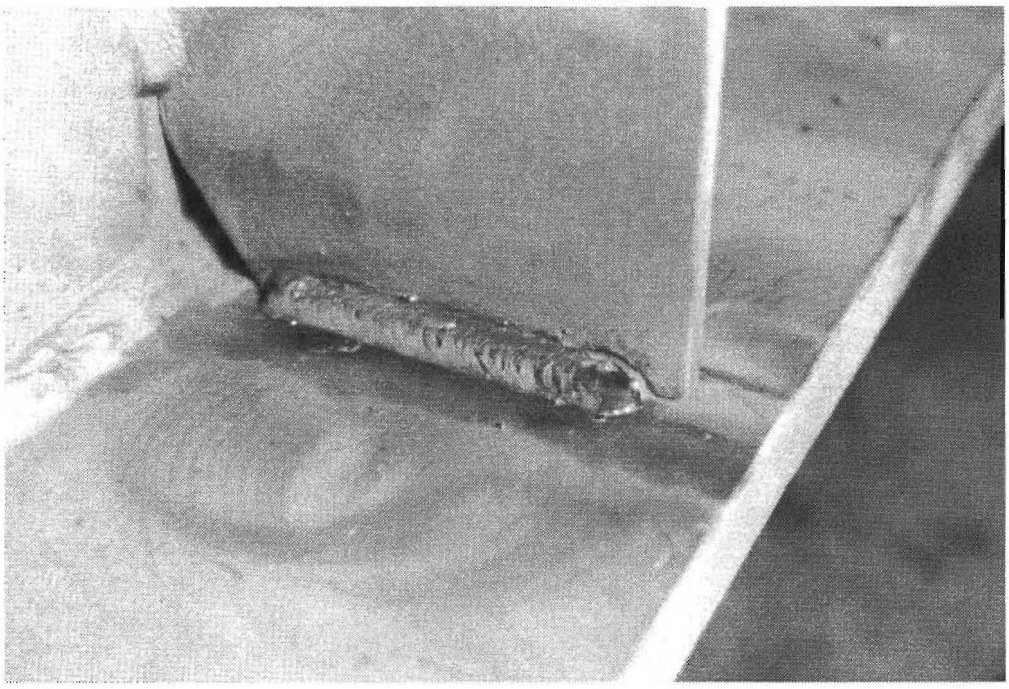

Figure 3-33: Tight-fit welded detail.

Figure 3-34: Tight-fit retrofit using welded clips.

3.4 INSTRUMENTATION

Strain gages were mounted on each of the three girders and centered at 380 mm (1 ft.- 3 in.) between stiffeners. The location and numbering system used for all girders is shown in Figure 3-35. Girder 1 contained additional gages around the three weld repair regions, as shown in Figure 3-36, so that the stress distribution in these areas could be measured.

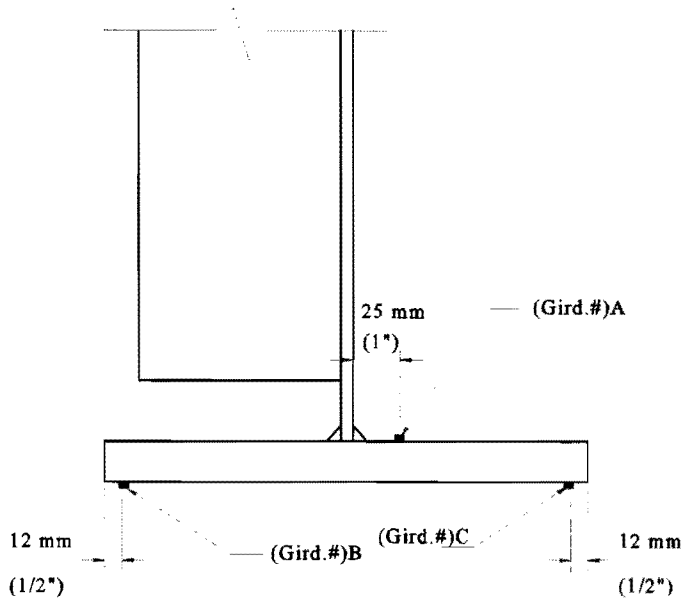

Figure 3-35: Strain gage locations in areas between stiffeners (common for all girders).

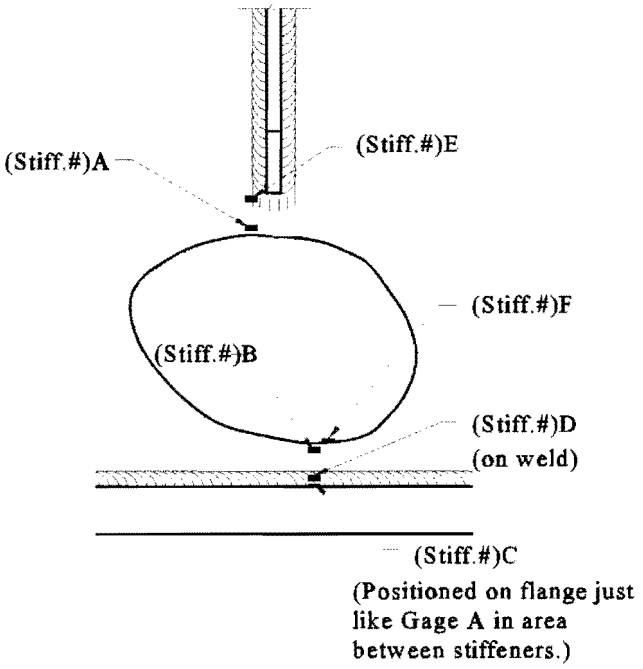

Figure 3-36: Additional strain gage locations for Girder 1 (at stiffener locations).

3.5 STATIC LOAD TEST

Static load tests were performed on all girders to determine the load required to produce the desired stress range, 82.7 MPa (12 ksi), in the extreme fibers of the tension flange in the constant moment region. Additional static tests were conducted on Girder 1 so that the stress distribution around the weld repair areas could be measured. Appendix B contains the data from all static load tests.

Figures 3-37 through 3-39 show the measured stresses from Static Tests 1 and 2 on Girder 1. As can be seen in these figures, the weld repairs produced significant stress concentrations. These measured stresses are consistent with the analytical results presented in Chapter Five.

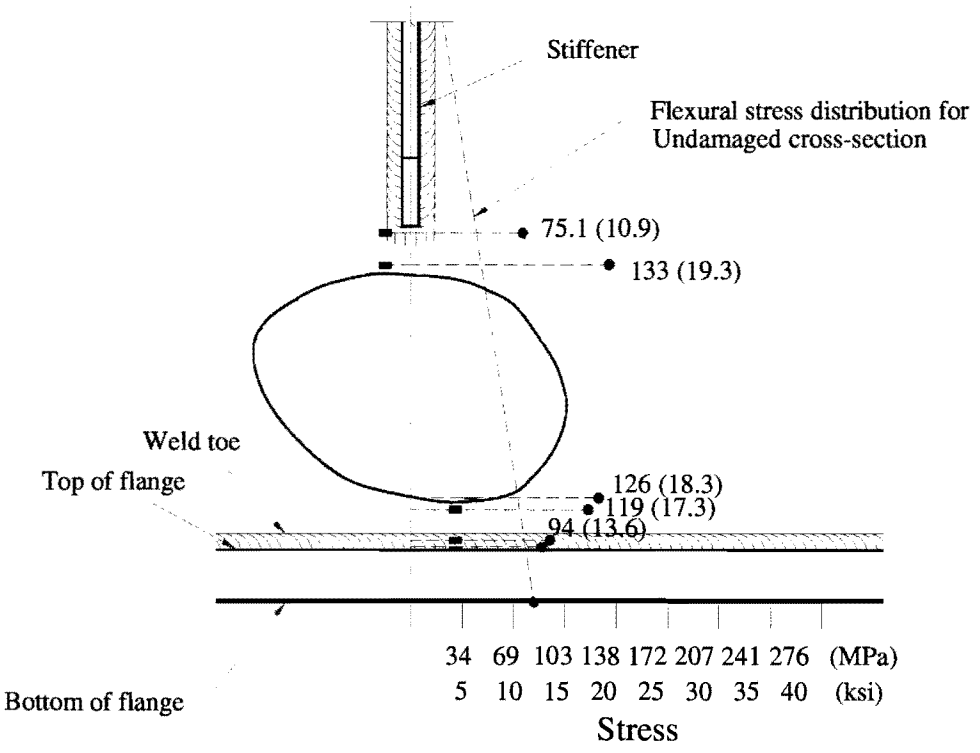

Figure 3-37: Stress distribution at Stiffener 1-1 derived from strain gage data.

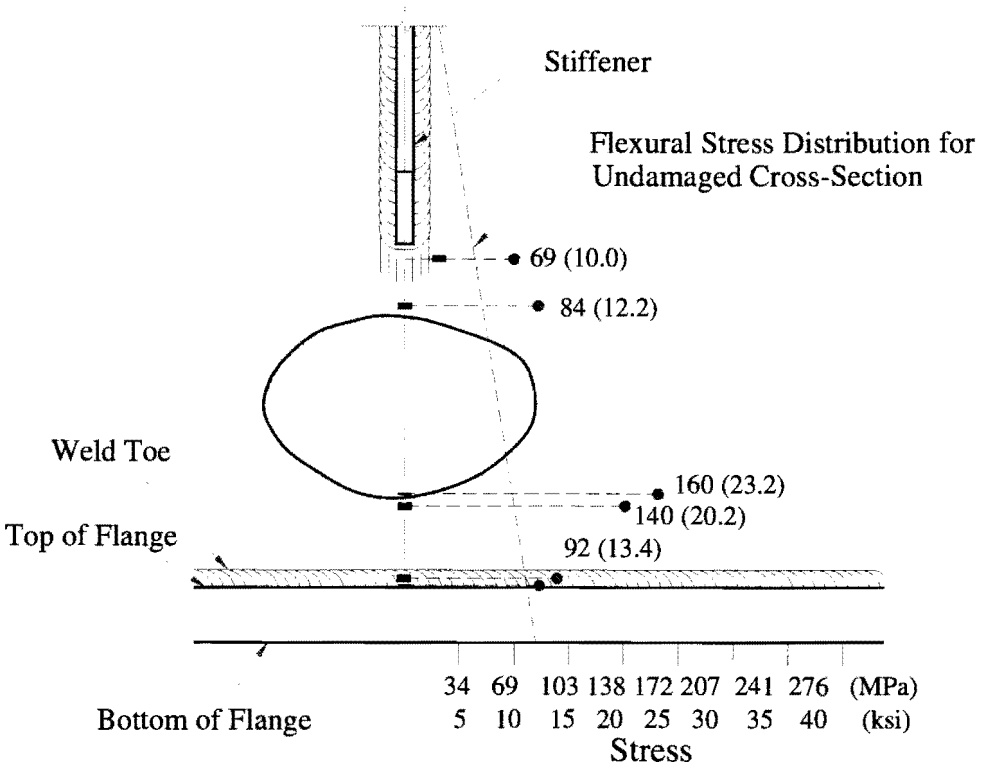

Figure 3-38: Stress distribution at Stiffener 1-2 derived from strain gage data.

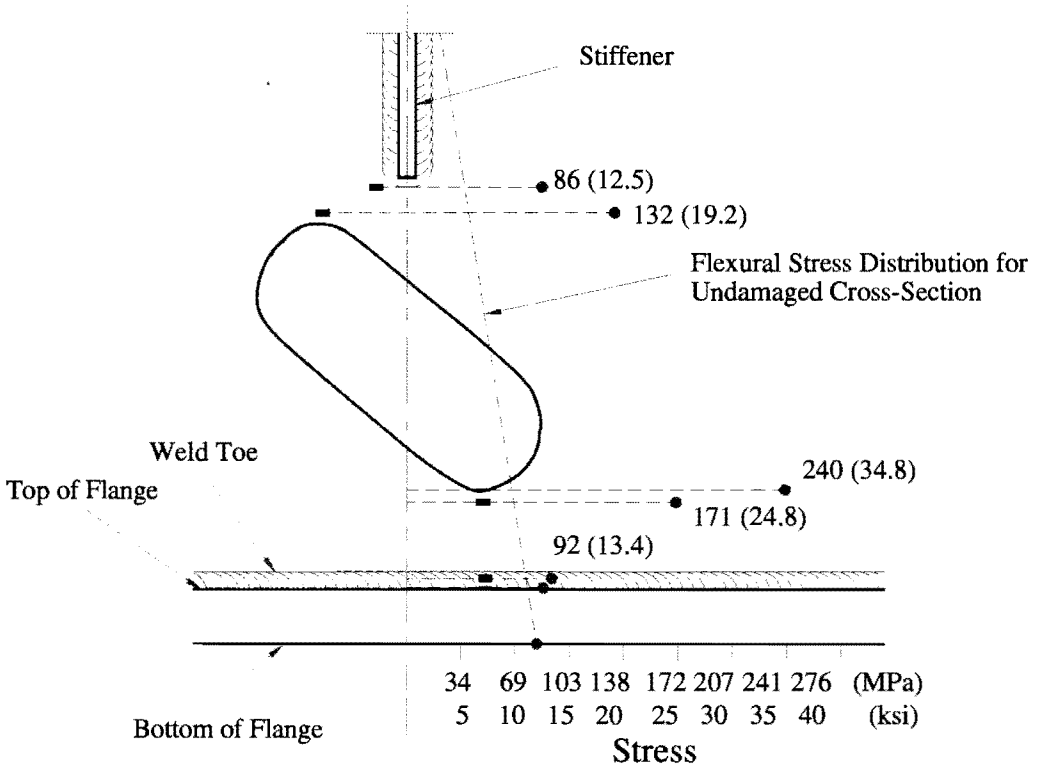

Figure 3-39: Stress distribution at Stiffener 1-3 derived from strain gage data.

3.6 FATIGUE TESTING OF GIRDERS

Each of the three girders was loaded at a frequency of approximately 2 Hz to produce an 83 MPa (12 ksi) stress range in the extreme tension fiber along the constant moment region. Appendices C, D, and E contain detailed test logs for Girders 1, 2, and 3, respectively.

Girder 1: The data from Static Test 1 indicated that a load range of 298 kN (67 kips) at each actuator was necessary to produce a stress of 83 MPa (12 ksi) in the extreme fibers of the tension flange along the constant moment region. The area around each weld repair area was closely monitored visually, and periodically inspected using dye penetrant.

At approximately 1.8 million cycles, a crack developed in the top of the flame-cut hole near Stiffener 1-1. Even though the area above the hole was in a relatively low-stress region, the crack originated from a surface flaw on the upper surface of the hole. The crack extended upward from the flaw, propagating to a length of 9 mm (0.35 in.) on the side of the web without stiffeners and to 11 mm (0.45 in.) on the side of the girder with stiffeners. Figure 3-40 shows the crack and the surface flaw from which it originated. A repair of the crack was made by grinding out the cracked material and the surrounding material. Care was taken to provide smooth transitions in the "notched" region and to provide a surface finish or smoothness of 0.050 mm (2000 μin.).

Fatigue testing of Girder 1 was resumed after this repair was made and ended at approximately 2.8 million cycles when a 305 mm (12-in.) crack developed in the web plate near the bottom longitudinal fillet weld at one end of the girder. The crack was due to bending stresses caused by buckling ("oil-canning") of the web plate and was not due to any problems associated with the weld repairs.

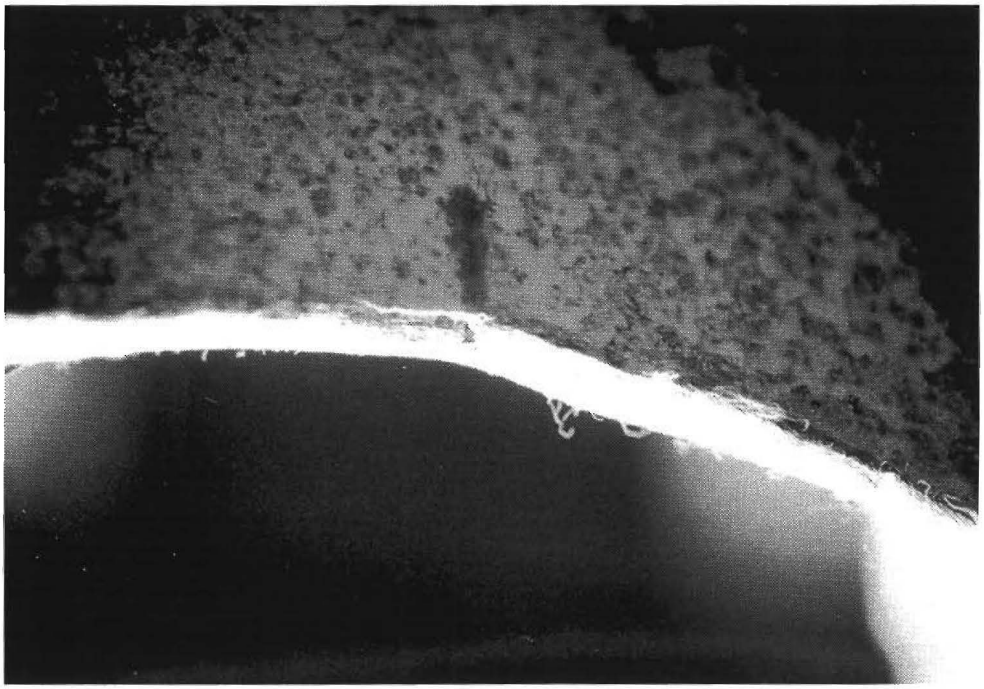

Figure 3-40: Crack propagating from surface flaw near Stiffener 1-1.

Girder 2: Static Test 5 indicated that a load range of 342 kN (77 kips) per actuator was required to produce a stress range of 83 MPa (12 ksi) in the extreme fibers of the girder. Of special interest were the pre-cracked areas that were repaired by the "air-gouge and re-weld" technique and the unrepaired longitudinal cracks in the web-to-flange plate fillet weld. These areas were closely monitored and periodically inspected using dye penetrants during fatigue testing to detect any crack reinitiation and/or propagation.

During testing of Girder 2, dynamic strain measurements were taken using an oscilloscope to verify a proper stress range during dynamic loading. The gages in the extreme fibers of the girder read exactly 83 MPa (12 ksi), thus indicating that the girder was indeed being loaded properly. Testing of Girder 2 ended at approximately 3.3 million cycles with no visibly apparent (using dye penetrant testing) cracks in any of the three weld repair areas. Subsequent ultrasonic inspection did not indicate any fatigue crack growth at the weld toe.

In addition to monitoring the gouge and re-weld repair on Girder 2, the crack growth behavior of the longitudinal web-to-flange weld toe crack was examined. None of the cracks were retrofitted (holes drilled at the crack tips) for the three connection plate locations. Prior to cyclic loading, the crack lengths were measured in reference to the center of the connection plates.

Girder 3: The purpose of testing Girder 3 was to test the fatigue performance of the welds that attach the connection plates to the tension flange of the girder. Data from Static Test 6 showed that Girder 3 was to be loaded with a force range of 302 kN (67.9 kips) per actuator to provide the proper 83 MPa (12 ksi) stress range. The weld toes at the bottom of each connection plate were carefully visually monitored using dye penetrant inspection to search for any visible crack propagation.

At about 733,000 cycles a fatigue crack in one of the header beams, having propagated from one of the drilled holes, caused the header beam to fail. The beam was removed and replaced with an identical W-shape beam from Trinity Industries, Inc. Testing of Girder 3 ended at 3 million cycles with no visible crack propagation from the weld toes of the six connection plates.

3.7 ANALYSIS OF FATIGUE TEST RESULTS

The fatigue data obtained from testing Girder 1 are plotted in Fig. 3-42 with the AASHTO Fatigue Design Categories. As indicated by the plot, the hole with the surface flaw failed at Category D. Upon completion of the testing, the inspection of the other two flame-cut holes did not indicate any fatigue cracking. Since no additional cracks formed at the edges, significant fatigue life remains. However, in the absence of further data, the flame-cut holes cannot be categorized as Category C with any certainty, and without further testing. As previously mentioned, the fatigue testing of Girder 2 was halted prematurely due to unrelated problems.

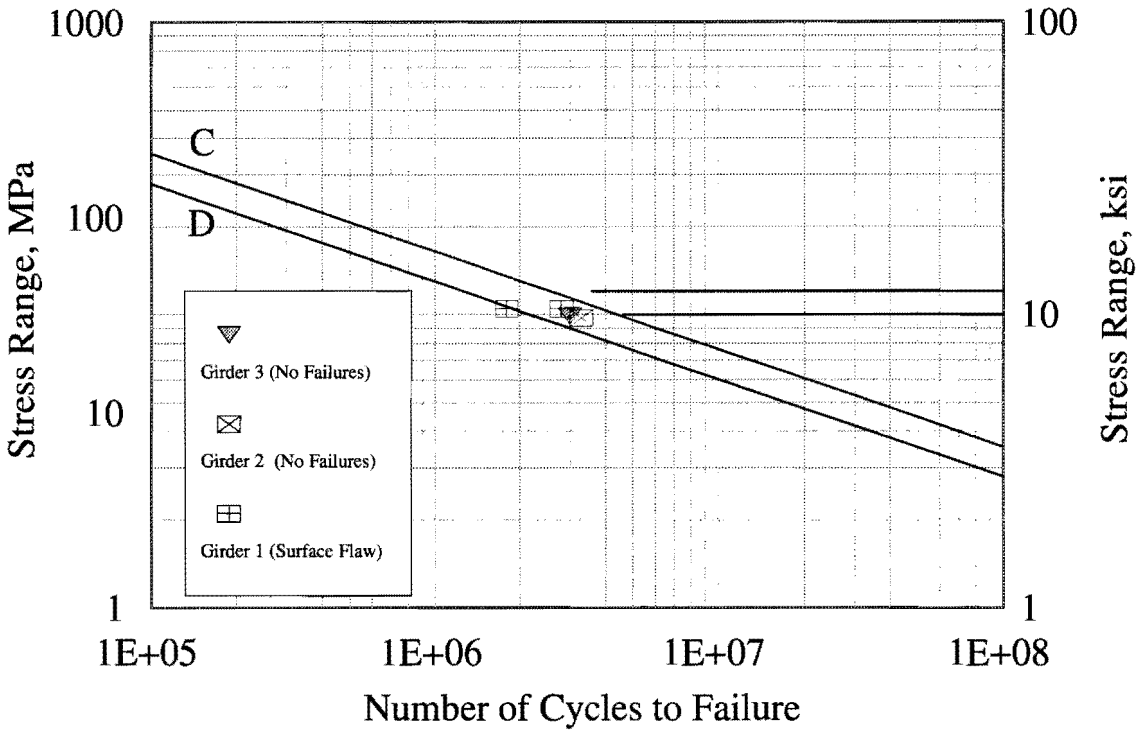

Figure 3-41: S-N plot of fatigue data for Girder 1 with AASHTO curves.

Upon completion of the fatigue testing of Girder 2 (3.3 million cycles) the crack lengths of the unretrofitted web-to-flange cracks were re-measured. As shown in Fig. 3-42, crack growth was observed at all three locations. These longitudinal cracks were located in the constant moment region of bending, so no crack extension was expected. An explanation for the crack growth is out-of-plane bending of the web plate caused by an oil can effect. A slight eccentricity in the application of the actuator loading can cause the oil canning. In addition, extensive gouging and re-welding occurred above the unrepaired cracks. The resulting heat input and shrinking would result in significant residual stresses perpendicular to the plane of the crack.

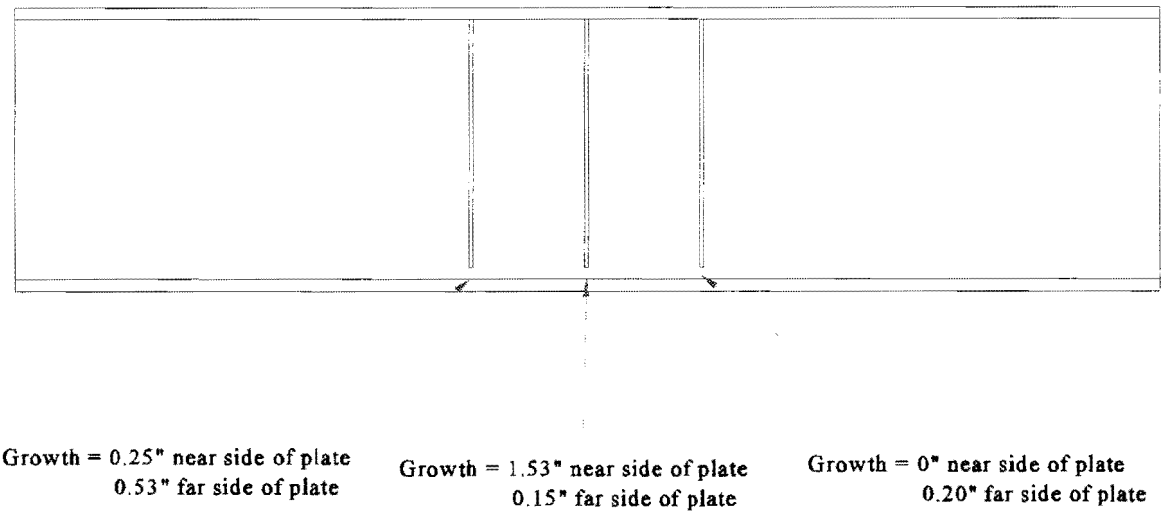

Figure 3-42: Growth of web-to-flange cracking Test Girder 2.

3.8 FRACTURE TOUGHNESS EVALUATION

One concern with the welding of steel is its effect on the fracture toughness of the base metal. A reduced fracture toughness will result in an increase in the repair's susceptibility to brittle fracture. To investigate the fracture toughness of the gouging and re-welding repair procedure, the three repaired locations on Girder 2 were cut from the web plate so that CVN test specimens could be machined. In addition, an additional section of web plate was cut out and removed from any welding, to serve as a control. The specimens were machined and tested by the Materials Testing Division of the Texas Department of Transportation according to ASTM A673.

Each of the three cut web sections had the original crack pattern mapped on it so that the notch of the specimen was located at a crack line. Three specimens were machined from each web section.

The results of the CVN tests are summarized in Table 3-1. The temperature of all specimens at testing was 21°C (70°F). The minimum CVN test result for A36 at the test temperature is given as 34 mm-kN (25 ft-lb) (AASHTO 1978, 1994). As can be seen by the test values given in the table, the fracture toughness of the repair weld metal exceeded the minimum required value. This is not unusual since the base material is produced from current steel making processes and weld metal is rich in elemental compositions that result in high fracture toughness.

Repair Detail	Specimen Number	Specimen Size	Impact Load	
			mm-kN	(ft-lb)
2-1	1	6.8x10 mm (0.269x0.395 in.)	225	166
	2	6.8x10 mm (0.269x0.395 in.)	125	92
	3	6.8x10 mm (0.269x0.395 in.)	134	99
2-2	1	6.8x10 mm (0.269x0.395 in.)	117	86
	2	6.8x10 mm (0.269x0.395 in.)	187	138
	3	6.8x10 mm (0.269x0.395 in.)	141	104
2-3	1	6.8x10 mm (0.269x0.392 in.)	No Result	
	2	6.8x10 mm (0.269x0.395 in.)	113	83
	3	6.8x10 mm (0.269x0.395 in.)	104	77
Control	1	6.8x10 mm (0.269x0.395 in.)	210	155
(RD)	2	6.8x10 mm (0.269x0.395 in.)	151	111
	3	6.8x10 mm (0.269x0.395 in.)	110	81

Table 3-1: CVN test data from Girder 2 gouge and re-weld repairs.

Examination of the fracture surface of each test specimen did not indicate the existence of any welding defects such as entrapped slag or other inclusions. These would have a deleterious effect on fracture toughness, as well as serving as initiation sites for renewed fatigue crack growth.

Chapter Four
ANALYTICAL EVALUATION OF REPAIR PROCEDURES

A series of finite element models was developed to predict the stress concentrations caused by multiple drilled holes and large flame-cut holes (Wilson 1994). The results of the analyses were compared to and combined with experimental data obtained from the laboratory testing discussed in Chapter Three. This data was used as an aid in the development of general guidelines for the use of multiple drilled holes and flame-cut holes.

Before any analyses or criteria development can take place using the finite element method, models must compare favorably to theoretical solutions and/or experimental data. All models in this study were analyzed using the finite element program, SAP90, and its model generator, SAPIN.

4.1 SIMPLE PLATE MODEL WITH CRACK

The study of drilled holes began by determining the stress distribution interaction around two drilled holes. Researchers conducted a proximity study using a model of a simple steel plate containing a crack arrested at each end by drilled holes. Various models, with different hole orientations, were developed to determine how stress concentrations at the edges of the holes change as a function of center-to-center hole spacing, s, and angular orientation with respect to one another, θ.

Figure 4-1 illustrates the variables, s and θ, involved in the simple plate model proximity study. The plate was composed primarily of four-node isoparametric plane stress elements with a thickness of 5 mm (3/16 in.). Three- and four-node plane stress elements were used to model the edges of the holes. All holes used in the analysis were 22 mm (7/8 in.) diameter, since this is a common size used in field repair of fatigue cracks. In cases where stresses exceeded the yield

strength of steel (i.e. 250 MPa (36 ksi)), elements were assumed to maintain linearly elastic behavior.

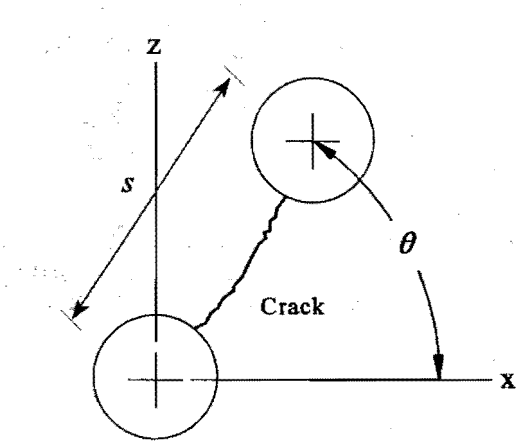

Figure 4-1: Variables in simple plate proximity study.

In order to calibrate the model, a trial model analysis was made with just a single 22 mm (7/8 in.) hole in the center of the plate. By comparing the stress concentration factor found using finite elements to the theoretical stress concentration of 3.0, from Kirsch's solution (Kirsch 1898), researchers could determine the validity of the model. A series of specified displacements corresponding to a uniaxial uniform stress distribution of 69 MPa (10 ksi) was imposed on the two ends of the plate in the x-direction. Fig. 4-2 shows the finite element mesh for the trial model and its imposed boundary conditions.

The analysis resulted in a maximum $_x$ at the edge of the hole of 185 MPa (26.8 ksi). Dividing the maximum $_x$ by the applied stress of 69 MPa (10 ksi) yielded a stress concentration factor of 2.68 and an error of 10.7 percent. Figure 4-3 shows a favorable comparison of stress plots between the finite element method (FEM) of analysis and Kirsch's theoretical stress plot. The model was calibrated by dividing the theoretical stress concentration by the finite element stress concentration. The resulting factor of 1.12 was used as a multiplier in subsequent models to help improve the accuracy of stress concentration results.

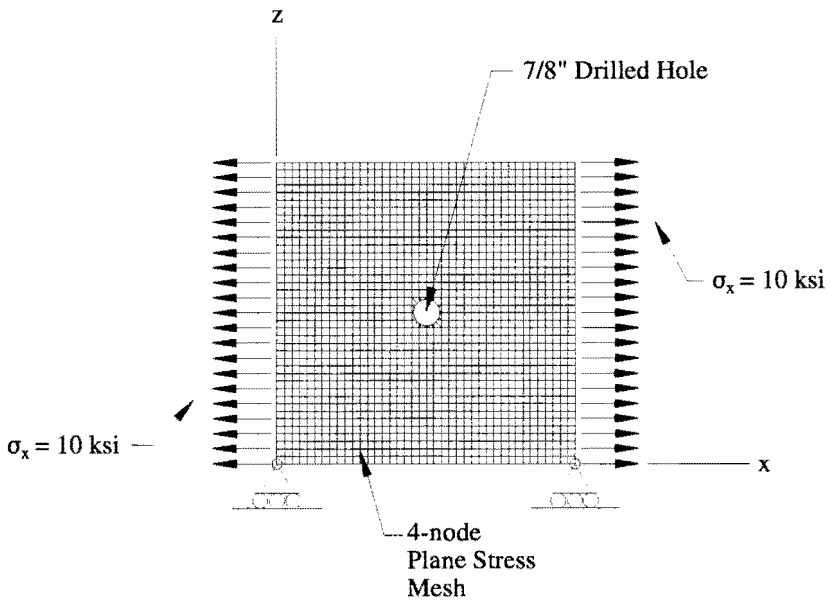

Figure 4-2: Finite Element mesh and boundary conditions for trial model.

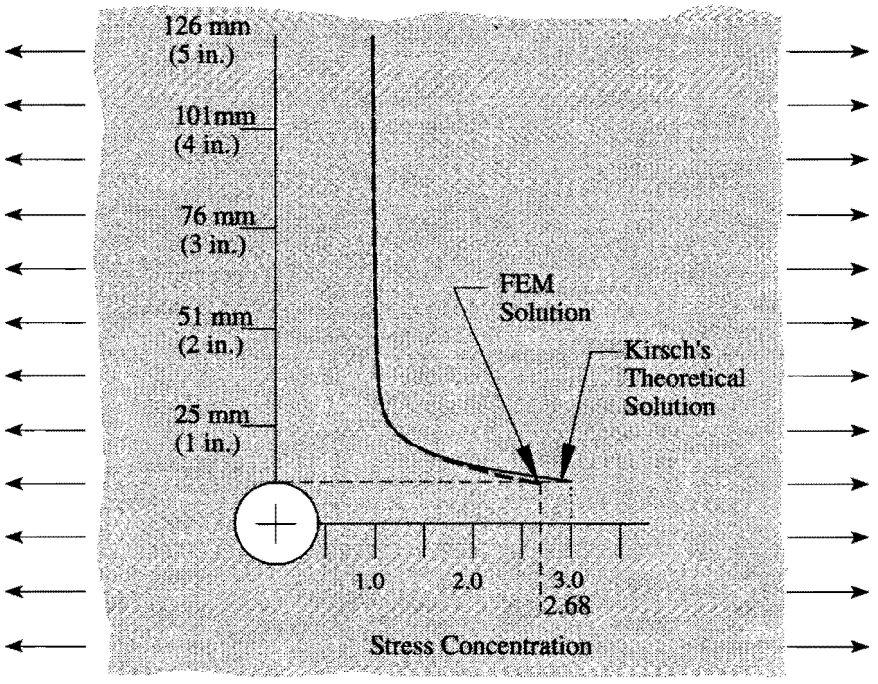

Figure 4-3: Comparison of theoretical and finite element stress plots.

4.2 STRESS CONCENTRATION AS A FUNCTION OF Θ

Once the simple plate model was calibrated, a second hole was placed at a center-to-center distance of 38 mm (1-1/2 in.) and at an angle, θ, of 90° with respect to the x-axis. In addition, a crack location was established between the two holes as shown in Fig. 4-4. The crack was modeled by placing two sets of nodes with identical coordinates along the crack. The elements on one side of the crack were then assigned to a different set of nodes than the nodes on the other side, thus eliminating the nodal connectivity between them and producing the desired effect.

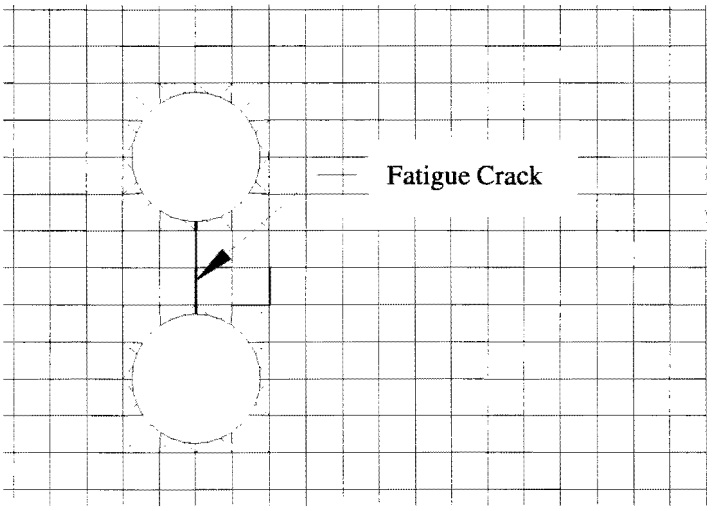

Figure 4-4: Simulated crack with drilled holes in simple plate model.

The model was analyzed, and stresses for nodes at the top and bottom edges of each hole were recorded. Figure 4-5 shows a stress contour plot for the model produced by SAP90. The four edges were labeled Edges A through D, as shown in Fig. 4-6. Stress concentrations were calculated and corrected using the multiplier, 1.12, discussed earlier. Several similar models followed. The center-to-center distance between the holes, s, remained constant at 38 mm (1-1/2 in.), while θ decreased from 90° to 0° in increments of 11.25°. For every model, the four stress concentration factors from Edges A through D were obtained and are shown in Table 6-1. The graph in Fig. 4-7 shows the plotted stress concentration values in graphical form.

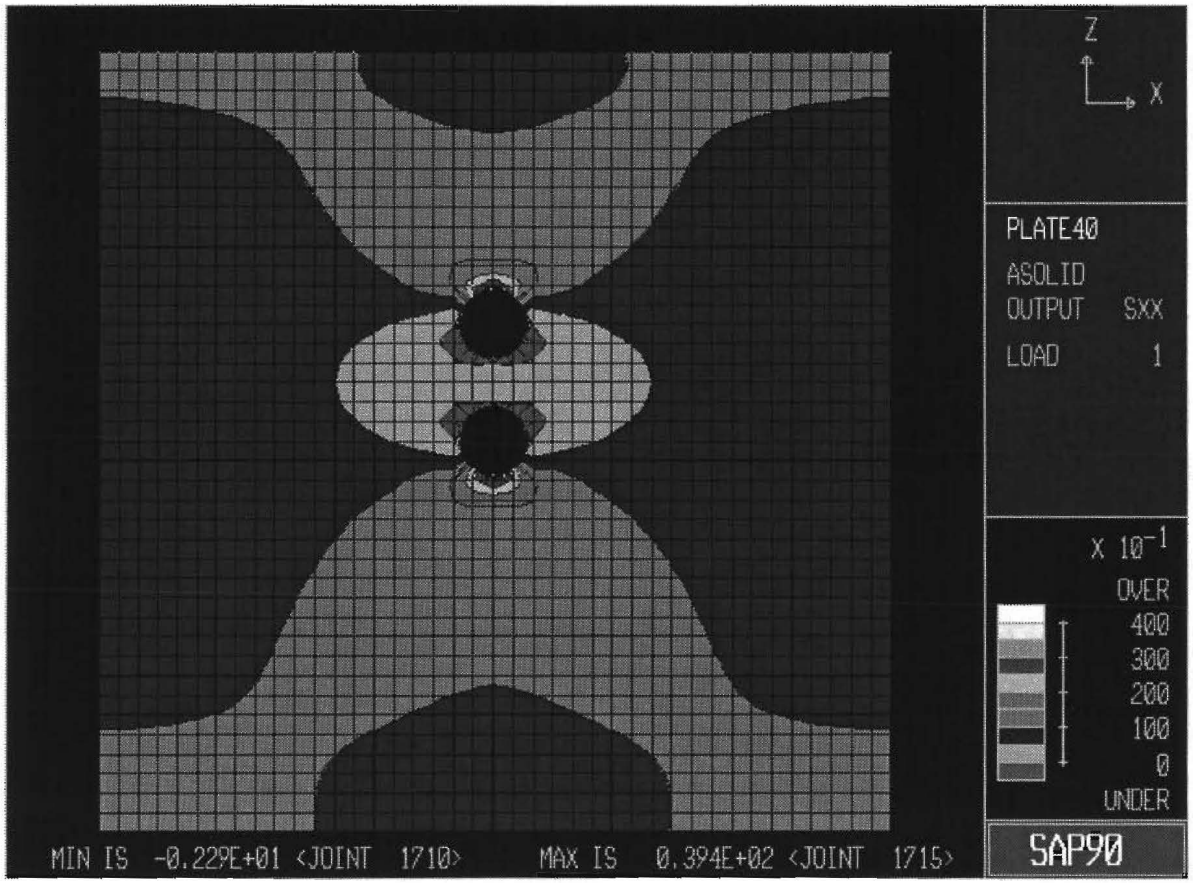

Figure 4-5: FEM stress contour plot for simulated crack with drilled holes .

θ	Stress Concentration			
	Edge A	Edge B	Edge C	Edge D
90°	-0.01	4.16	4.17	-0.01
78.75°	-0.03	4.12	4.12	-0.02
67.5°	-0.10	4.09	4.18	-0.11
56.25°	-0.17	4.02	4.01	-0.15
45°	-0.09	3.92	3.96	-0.08
33.75°	0.36	3.79	3.85	0.35
22.5°	1.09	3.57	3.59	1.07
11.25°	1.92	3.21	3.23	1.89
0°	2.64	2.64	2.63	2.63

Table 4-1: Summary of stress concentrations for varying θ.

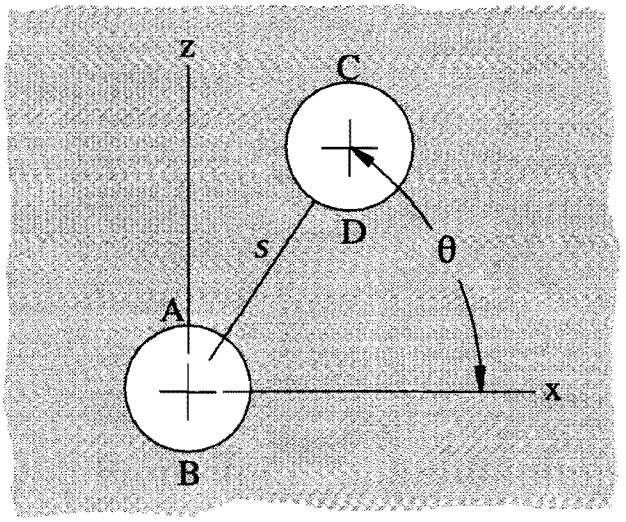

Figure 4-6: Labeling Scheme for drilled holes.

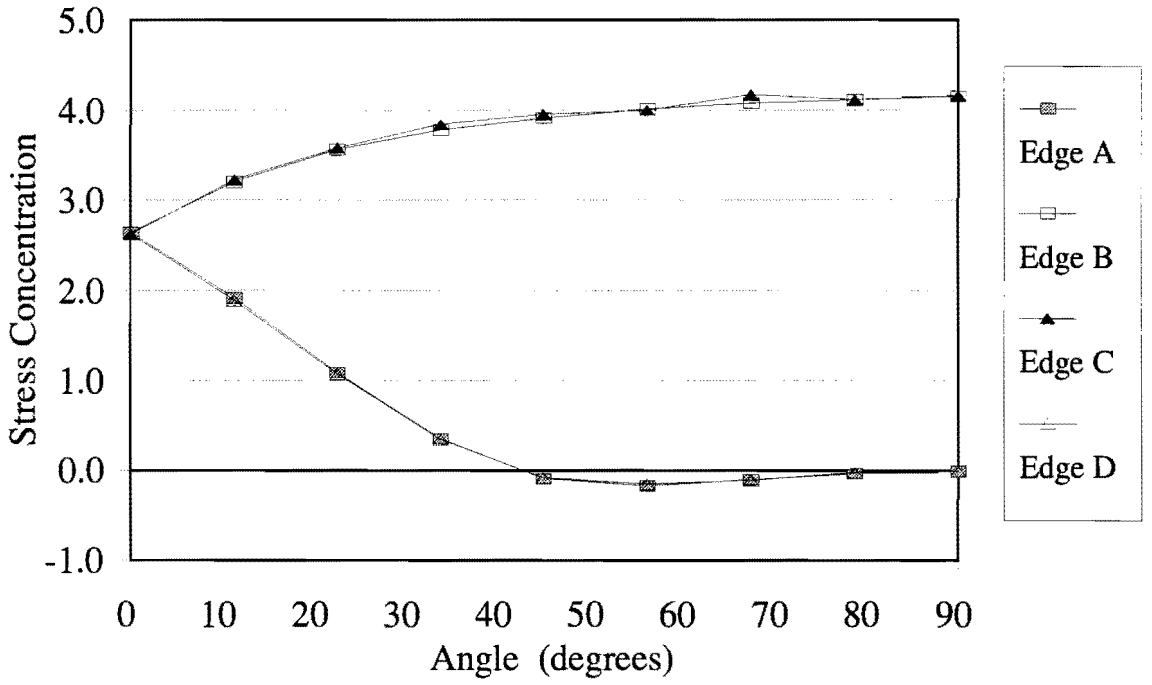

Figure 4-7: Plot of stress concentration vs. θ for simple plate with crack (s = 38 mm (1-1/2 in.)).

The results of the finite element analyses indicated that stress concentrations on Edges B and C reached a maximum of about 4 and remained fairly constant for θ greater than 45°. At higher values of θ, the applied tensile stress acted almost perpendicular to the crack, thus magnifying the stress concentrations by pulling the crack apart. At lower values of θ, the applied tensile stress acted more in the direction of the crack. The stress concentrations that did occur were caused primarily by the drilled holes used to repair the crack.

4.3 STRESS CONCENTRATION AS A FUNCTION OF *S*

The second phase of the simple plate analysis was a study of how the center-to-center hole spacing, *s*, affects stress concentration at the edges of the drilled holes. The study was conducted by varying center-to-center hole spacing, *s*, and holding hole and crack orientation, θ, constant at its most critical value, 90°. Models were developed for spacings of 25, 32, 38, and 51 mm (1, 1-1/4, 1-1/2, and 2 in.). Table 4-2 shows the stress concentrations obtained from the four models for the two outside edges, Edges B and C. The stress concentrations were corrected using the multiplier, 1.12, discussed earlier.

s		Stress Concentration	
mm	in.	Edge B	Edge C
25	1.0	3.86	3.84
32	1.25	4.02	3.99
38	1.5	4.17	4.16
51	2.0	4.41	4.35

Table 4-2: Stress concentration verses *s* for simple plate with crack θ = 90°.

The data in Table 4-2 show that longer cracks decrease the section and stiffness of the plate and significantly increase the stress concentrations on the outside edges of the drilled holes.

the drilled holes as shown in Fig. 4-8. Longer cracks and greater spacing of holes have less of an effect, however, as θ decreases.

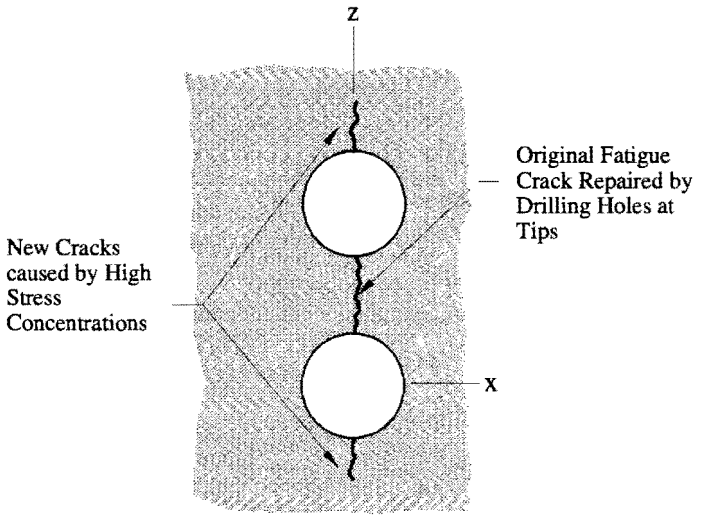

Figure 4-8: Crack initiation due to stress concentrations at drilled holes.

4.4 ALTERNATIVES TO THE DRILLED HOLE TECHNIQUE

Large Circular Hole Although drilling holes is a proven method for arresting crack growth, some multiple drilled hole patterns may provide only a temporary fix, or worse, compound the problem because of high stress concentrations. Different repair techniques may, therefore, become necessary. One such repair involves drilling or cutting one large hole to encompass the area occupied by two smaller drilled holes. Figure 4-9 illustrates the repair technique.

A large, drilled hole was modeled using finite elements and compared to the hole patterns with 38 mm (1-1/2 in.) spacing discussed earlier. The diameter of the hole was 98 mm (3-7/8

in.), equal to the center-to-center spacing, 38 mm (1-1/2 in.), plus twice the radius of a 22 mm (7/8 in.) drilled hole. As might be expected, the analysis yielded a maximum stress concentration at the edge of the hole of 2.61, quite comparable to the stress concentration of 2.68 calculated in the original test model. Kirsch's theoretical solution for maximum stress concentration in a drilled hole is a constant, and not a function of hole size. The model of the larger drilled hole, therefore, further verified Kirsch's theory.

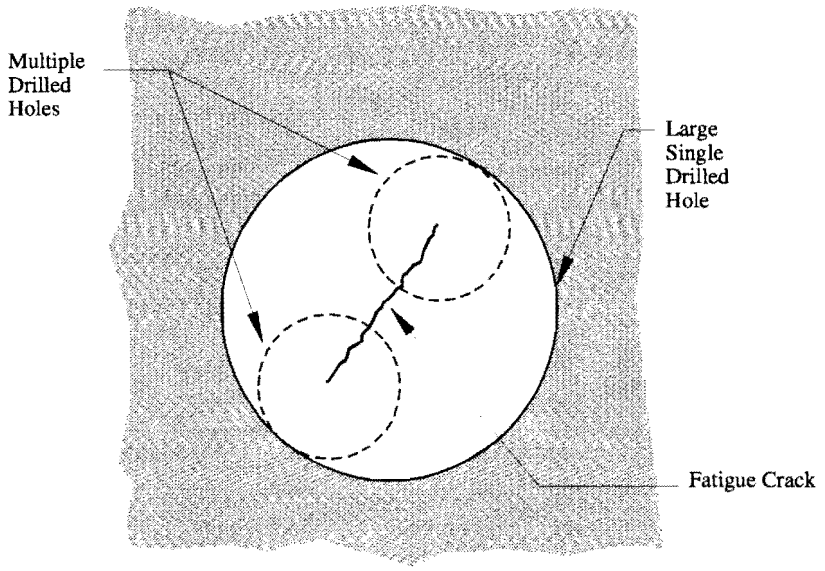

Figure 4-9: Large circular hole repair method.

Examination of Table 4-1 reveals that, for $\theta \geq 11.25°$ and $s = 38$ mm (1-1/2 in.), the maximum stress concentration factor for a crack with drilled holes at the tips exceeds 3.0, the maximum stress concentration factor for a single circular hole. Therefore, replacing two drilled holes with a single drilled hole in cracks with θ greater than $11.25°$ would definitely improve the stress concentrations in the plate and possibly provide a longer fatigue life. Such an application could reduce stress concentration factors of 4.0 or more down to 3.0.

The application of Kirsch's Theory to the alternative repair method does have certain limits. Kirsch derived his solution for a drilled hole in an infinite plate. Of course, no plate girder web is as large as the plate in Kirsch's derivation. Therefore, the size of the large circular hole is limited. A discussion of allowable section loss is included in a later section on flame-cut hole criteria.

Slotted Holes Another alternative method to drilling holes in fatigue repair involves drilling two holes at the tips of a crack and grinding out the cracked material between the holes to form a slot. Fig. 4-10 schematically illustrates the slotted hole repair technique (also see Fig. 3-28).

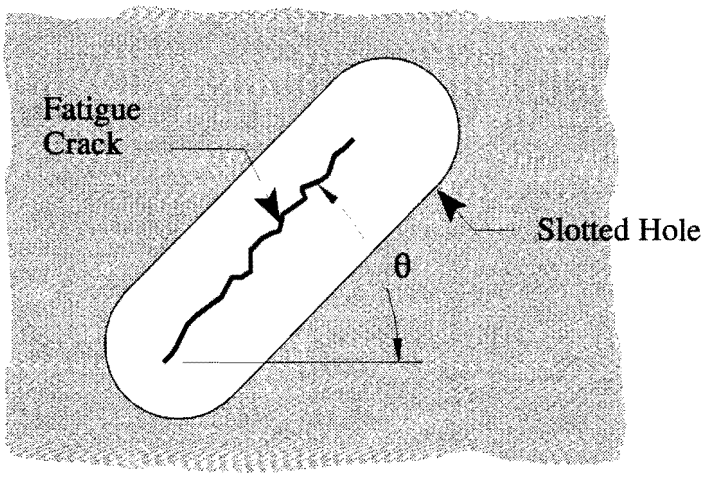

Figure 4-10: Slotted hole repair technique.

Several slotted hole models were developed from the simple plate models used earlier. Each model simulated the removal of cracked material from between two drilled holes at a center-to-center spacing of 38 mm (1-1/2 in.). Fig. 4-11 shows the finite element mesh around a slotted hole with $\theta = 45°$. Values of θ included 90°, 67.5°, 45°, 22.5°, and 0°. Stress concentrations were calculated at each end of the slotted holes.

As should be expected, the highest stress concentration occurred in the model with θ = 90°. In addition, virtually the same stress concentrations occurred in the slotted hole models as occurred in the drilled hole models. Removal of the cracked material did not affect the flow of stress through the model since the applied stress was perpendicular to the slot. However, the slotted hole model with $\theta = 0°$ resulted in the lowest stress concentration and a significant stress reduction compared to the corresponding drilled hole model. In this case, removal of the cracked material between the drilled holes allowed stresses to flow more freely. Fig. 4-12 shows stress contours for the model in Fig. 4-11. Fig. 4-13 compares the maximum stress concentrations for the drilled hole and slotted hole models. As shown in Fig. 4-13, no significant improvement in stress concentration was made above 45°. Therefore, the slotted hole repair technique would not improve fatigue performance over drilled holes for cracks with θ greater than 45°.

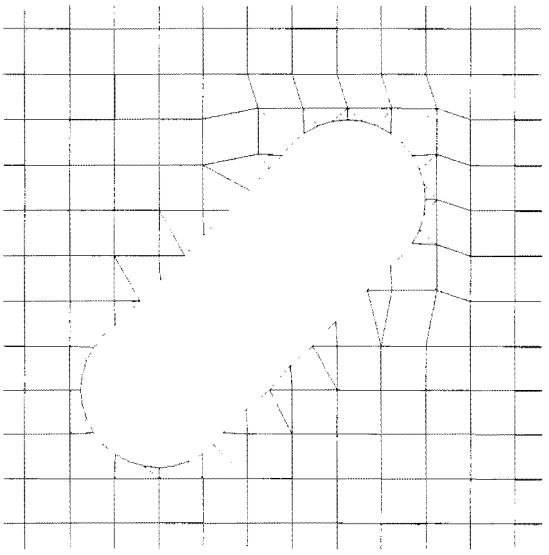

Figure 4-11: Finite element mesh for a slotted hole model: $\theta = 45°$.

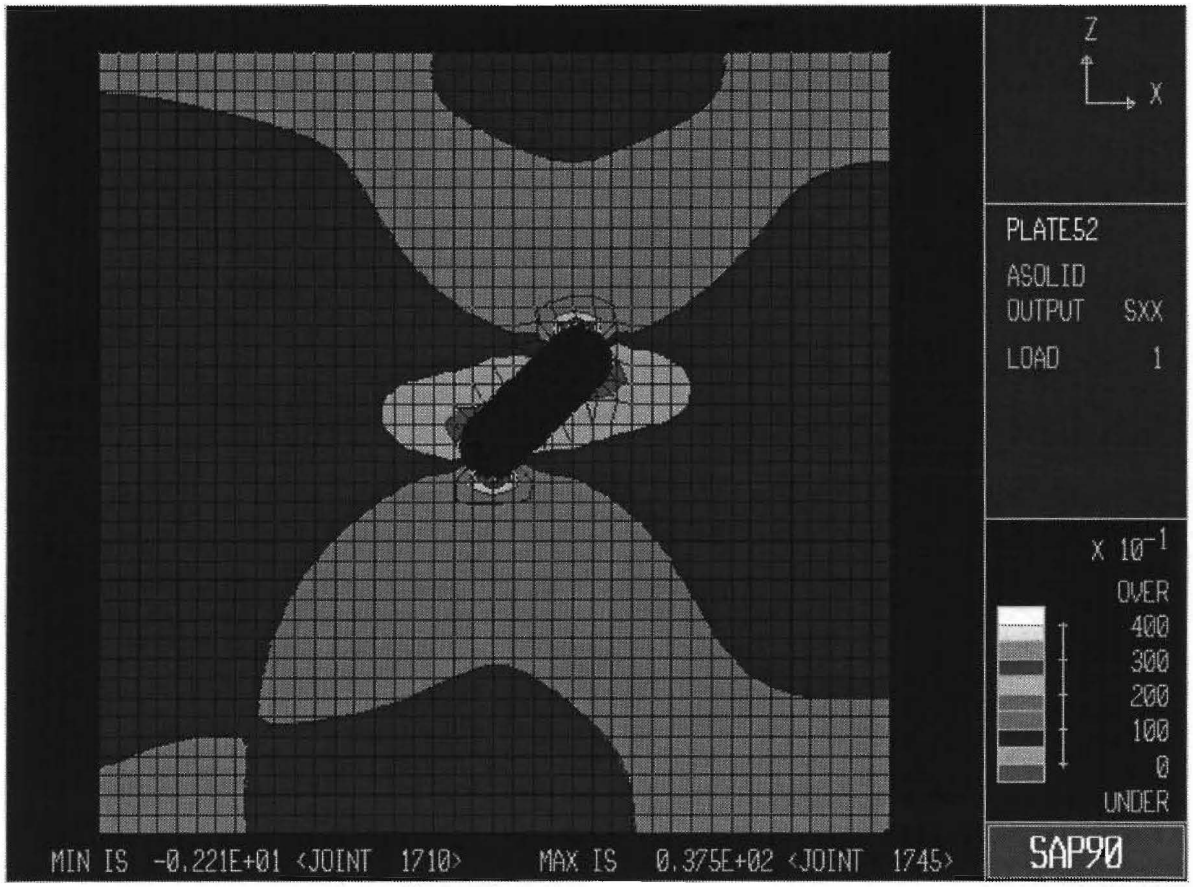

Figure 4-12: FEM stress contour plot for a slotted hole model ($\theta = 45^\circ$).

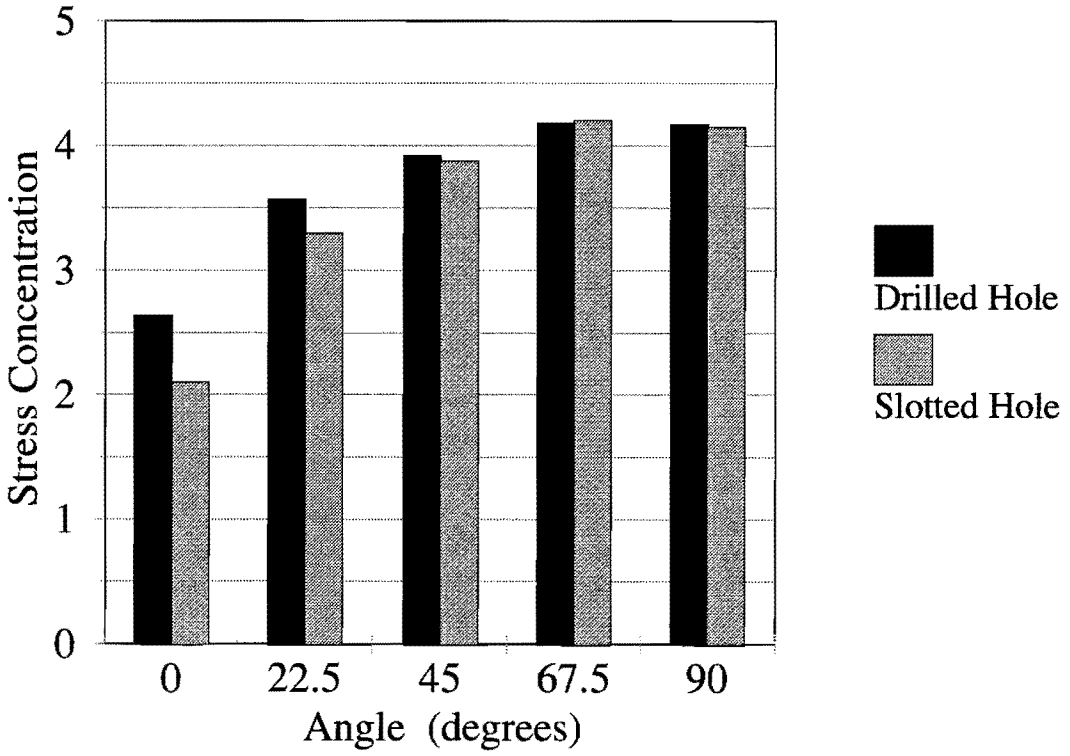

Figure 4-13: Comparison of maximum stress concentrations for drilled hole and slotted hole models.

4.5 GENERAL REPAIR GUIDELINES FOR DRILLED HOLES

Drilled Hole Orientation As indicated earlier, the lowest stress concentrations between two drilled holes occurred at lower values of θ. When using drilled holes to arrest crack growth, θ should be kept to a minimum. The tips of a crack do not necessarily have to lie in the exact centers of the drilled holes, as shown in Fig. 4-14. The holes can be shifted to minimize θ, stress concentration, and section loss. The orientation between drilled holes should be less than 45°, whenever possible. The slotted hole repair alternative may also be used in the repair of cracks with values of θ below 45°.

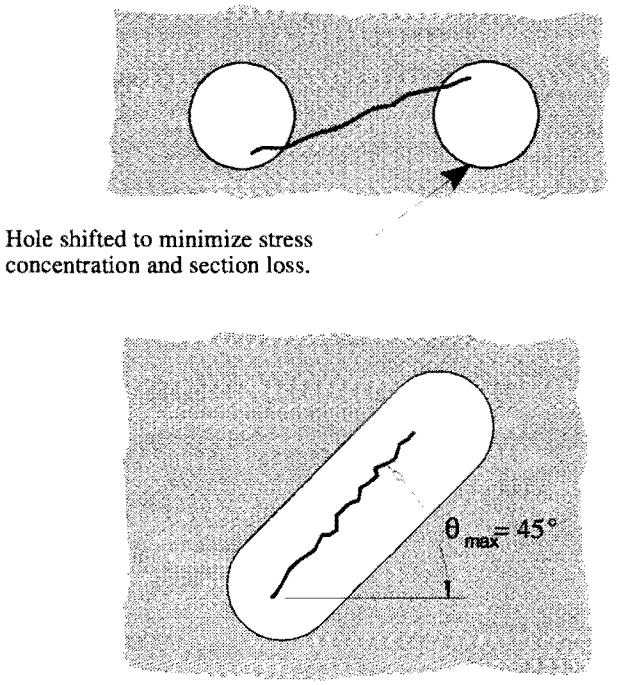

Figure 4-14: Repair guidelines for cracks with lower values of θ.

For cracks requiring drilled holes with θ greater than 45°, larger drilled holes will reduce

the stress concentration and stress intensity, resulting in improved fatigue life. The large circular hole repair technique would also be useful in this case. Criteria for the use of such holes are included in the section on flame-cut holes.

Drilled Hole Spacing Based on the data presented in Table 4-2, when drilling holes to arrest tips of the same crack spacing should be kept to a minimum. This can be accomplished by moving the holes as close together as possible and still containing the crack tips within the holes, as shown in Fig. 4-15. After drilling the holes, dye penetrant testing should be performed to verify that the tips of the cracks are contained in the holes. Containing the crack tips in the holes is of paramount importance since any cracks not contained would propagate in a higher stress field than if the repair had not been performed and render the repair useless, as shown in Fig. 4-16.

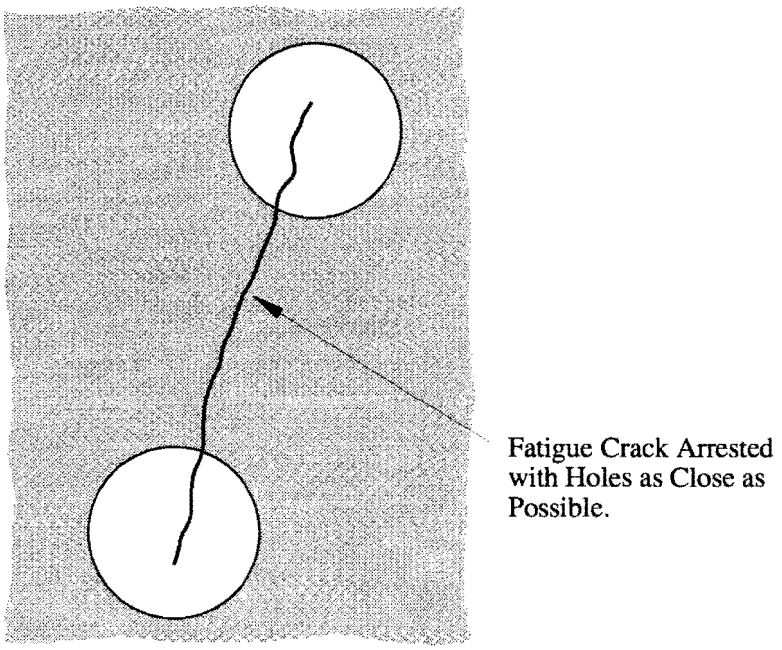

Figure 4-15: Minimizing separation of drilled holes arresting the same crack.

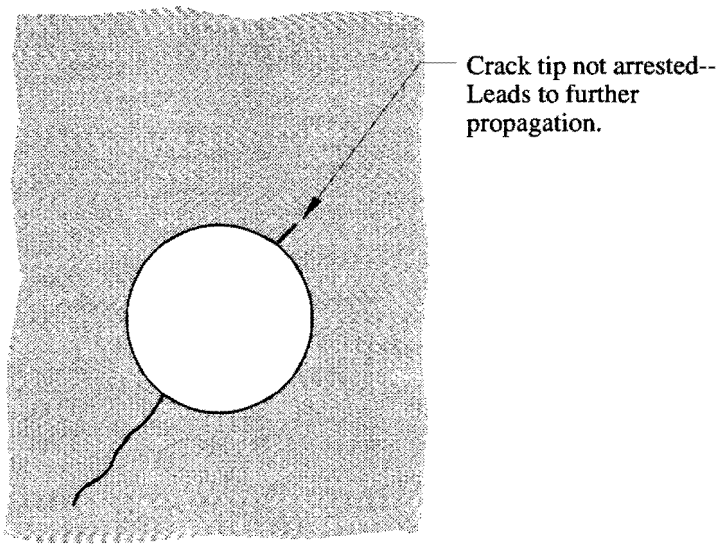

Figure 4-16: Propagation of crack tip not contained by drilled hole.

4.6 FLAME-CUT HOLE MODEL

The plate girder models developed in this study were based on actual girders that were tested as a part of the lab testing phase described in Chapter 3. Three separate test girders underwent various methods of fatigue repair techniques to simulate repairs used in the field. Fig. 3-2 shows a design drawing for Girder 1 and is the basis for the girder model used in this study. In Girder 1, the stiffeners were flame-cut back approximately 190 mm (7-1/2 in.), and the edges were ground smooth. Large holes were then flame-cut directly under each of the three stiffeners and near the longitudinal web-to-flange fillet weld. The edge surfaces of the holes were then ground smooth. The flame-cut holes simulated a repair technique that involves removing an entire region of densely cracked web plate material.

Once the repairs were completed, strain gages were mounted on the girder at key positions around each hole, near the toe of the transverse stiffener, and on the flange of the girder. Figures 5-30, 5-32, and 5-34 show strain gage locations for the flame-cut holes of Girder 1.

A finite element model of Girder 1 was developed based on its section properties and the load conditions applied to it in the laboratory. In the interest of minimizing the number of degrees of freedom, only half the girder section in regions near individual flame-cut holes was modeled. The web of the girder consisted mainly of 5 mm (3/16 in.) thick four-node isoparametric plane stress elements. Three- and four-node plane stress elements were used to model the edges of flame-cut holes. The flange was modeled using beam elements identical in area and moments of inertia to the actual test girder flange. Thicker plane stress elements were used to simulate the stiffness contributed by the web-to-flange fillet weld. The transverse stiffener and stiffener-to-web fillet weld were composed of eight-node solid brick elements. Figures 4-17 and 4-18 show a typical plate girder model and the imposed loading and boundary conditions.

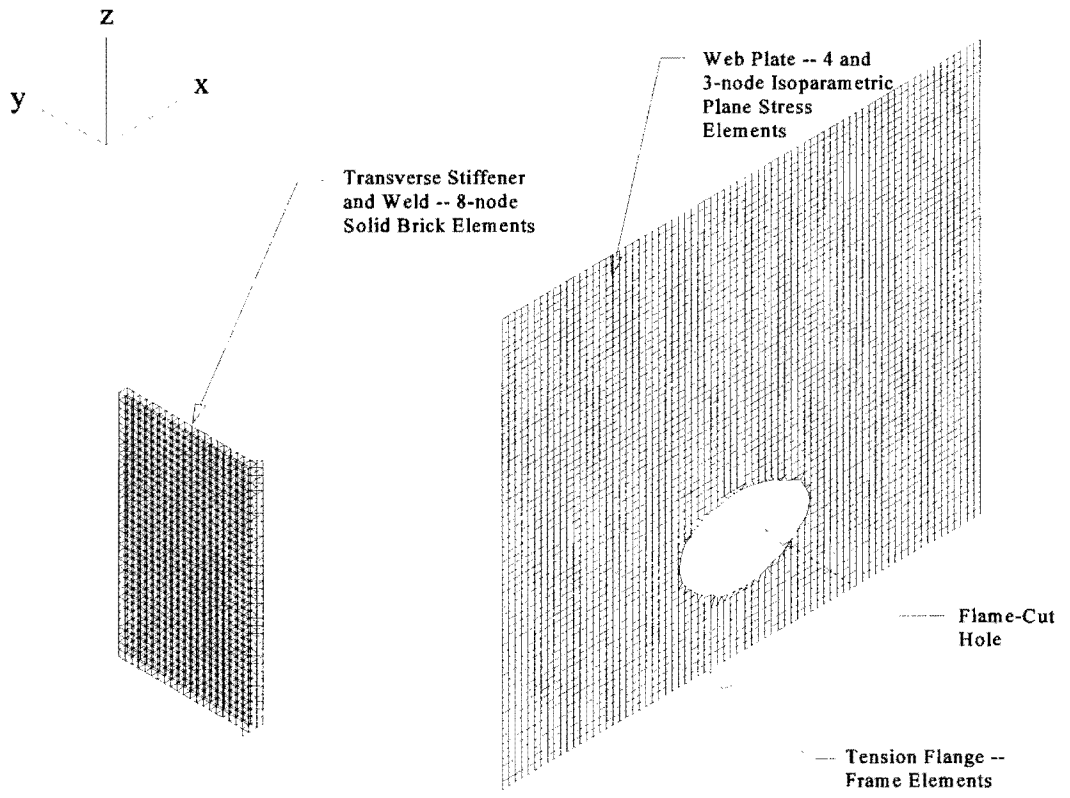

Figure 4-17: Finite element model for web holes.

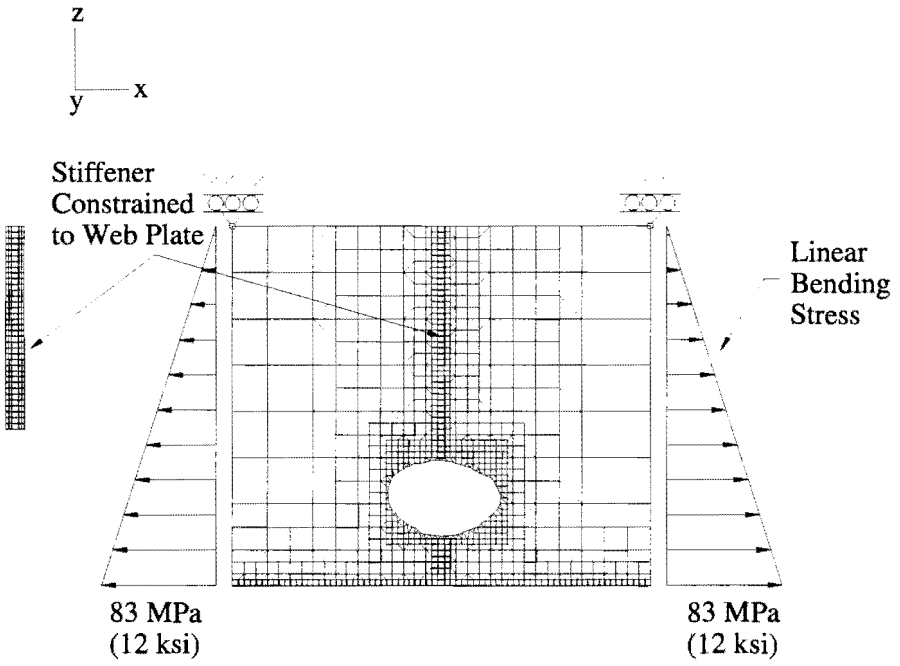

Figure 4-18: Loading and boundary conditions for web holes.

A linear prescribed displacement pattern with a maximum of 0.0946 mm (0.003724 in.) was placed at the ends of the model in the x-direction. The displacement pattern corresponded to a linear bending stress distribution with a maximum stress of 83 MPa (12 ksi) at the extreme fiber of the tension flange. The displacements were calculated using the expression $\delta = \sigma l/E$, where δ equals the prescribed displacement in inches, σ equals the desired magnitude of stress in MPa (ksi), l equals half the length of the model in mm (in.), and E equals the modulus of elasticity of steel (200,000 MPa (29,000 ksi)).

Each of the three flame-cut holes in Test Girder 1 was measured and modeled to scale in three separate finite element models to calibrate the basic girder model against strain gage data. Three separate analyses produced the stress profiles shown in Figs. 4-19 through 4-21. The finite element stress profile in Fig. 4-19 shows much higher stresses than those found through

experimental strain gage data. The strain gages used in the laboratory testing measure 6 mm (1/4 in.) in length. One possible reason for the difference in stress profiles is the fact that a strain gage cannot measure a strain at a discrete point. Instead, it measures an average strain over its 6 mm (1/4 in.) length, thereby possibly causing a point of maximum stress to be missed. Finite element analysis, on the other hand, calculates stresses at points and is able to pinpoint areas of maximum stress more easily.

The other two models (Figs. 4-20 and 4-21), however, produced stress profiles that appear to agree more closely with strain gage readings obtained in the laboratory. Tables 4-3 through 4-5 show numerical comparisons of strain gage readings to point stresses calculated using finite elements. The basic plate girder model was, therefore, determined to be adequate for use in developing repair criteria.

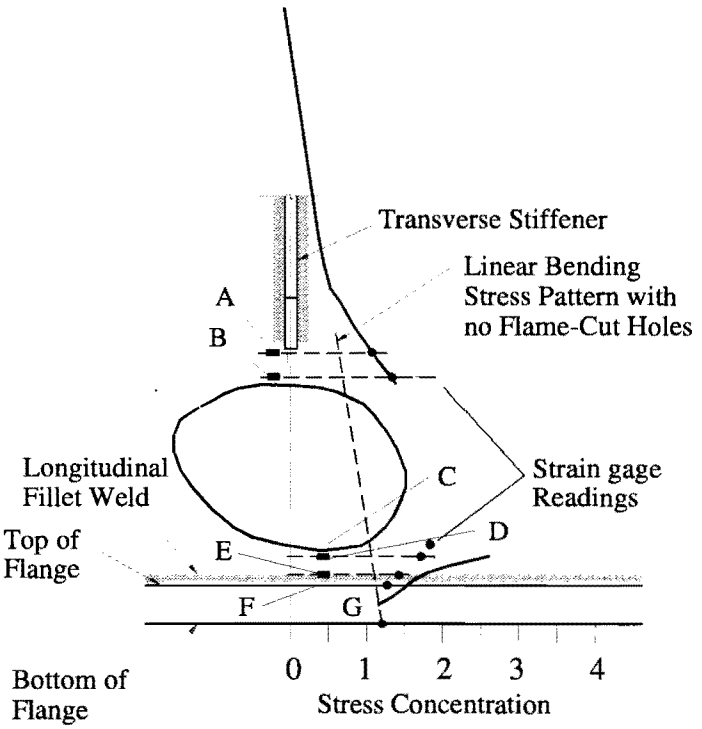

Figure 4-19: Comparison of stress plot to experimental data for Stiffener 1.

Location	Stresses, MPa (ksi)			
	Experimental		FEM	
A	75.2	(10.9)	71.0	(10.3)
B	132	(19.3)	93.8	(13.6)
C	126	(18.3)	180	(26.1)
D	119	(17.3)	172	(25.0)
E	93.8	(13.6)	116	(16.8)
F	92.4	(13.4)	104	(15.1)
G	82.7	(12.0)	80.7	(11.7)

Table 4-3: Comparison of finite element analysis point stresses to strain gage data for Stiffener 1.

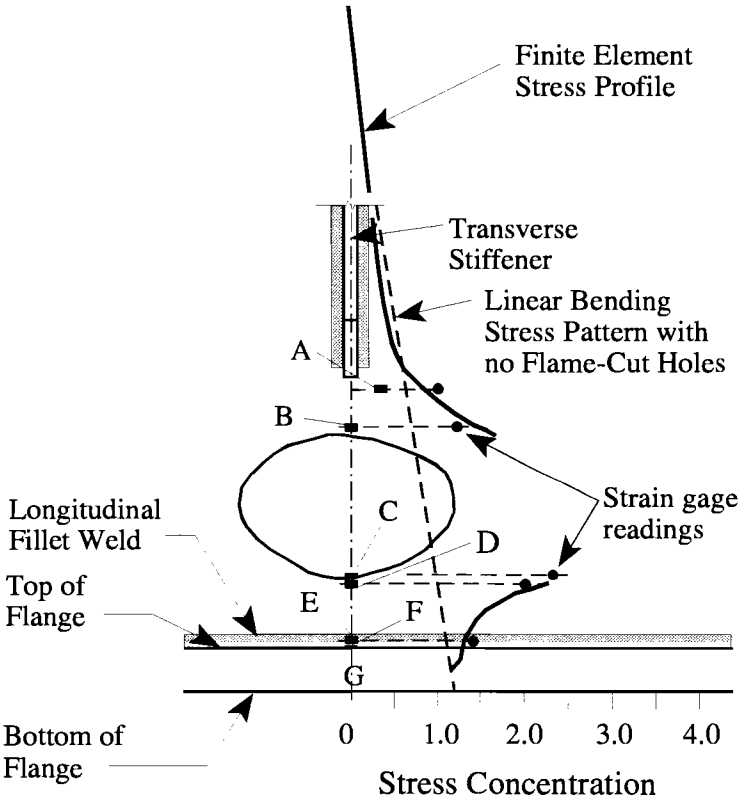

Figure 4-20: Comparison of stress plot to experimental data for Stiffener 2.

Location	Stresses MPa (ksi)			
	Experimental		FEM.	
A	68.9	(10.0)	63.4	(9.2)
B	84.1	(12.2)	94.5	(13.7)
C	160	(23.2)	157	(22.8)
D	139	(20.2)	155	(22.5)
E	92.4	(13.4)	91.7	(13.3)
F	91.0	(13.2)	88.9	(12.9)
G	82.7	(12.0)	80.7	(11.7)

Table 4-4: Comparison of finite element analysis point stresses to strain gage data for Stiffener 2.

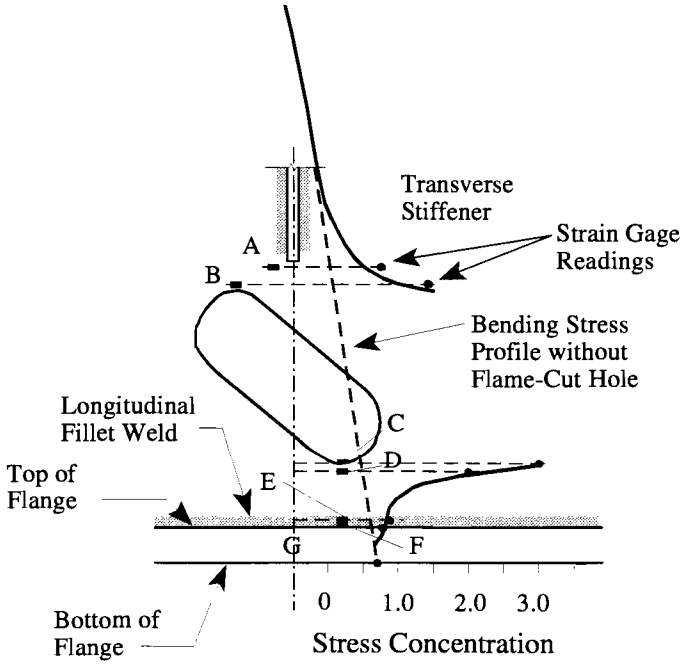

Figure 4-21: Comparison of stress plot to experimental data for Stiffener 3.

Location	Stresses, MPa (ksi)			
	Experimental		FEM	
A	86.2	(12.5)	79.3	(11.5)
B	132	(19.2)	97.9	(14.2)
C	240	(34.8)	243	(35.2)
D	171	(24.8)	179	(26.0)
E	92.4	(13.4)	93.8	(13.6)
F	91.0	(13.2)	90.3	(13.1)
G	82.7	(12.0)	80.7	(11.7)

Table 4-5: Comparison of finite element analysis point stresses to strain gage data for Stiffener 3.

The results of this finite element study confirmed that if the flame-cut hole is properly finished with regard to the surface of the opening, a fatigue strength consistent with AASHTO fatigue Category C is possible. When repairing a detail for fatigue damage, the repair should be in a category that is the same, or better, than the original detail. In other words, a Category C or higher repair should be used to repair a Category C detail. A transverse stiffener and connection plate detail is a Category C detail. The fatigue testing of Girder 1 allowed for an evaluation of flame-cut holes and whether they meet or exceed Category C fatigue life performance

As discussed in Chapter Three, a lack of thorough grinding during the initial repair process left a small surface flaw on the top edge of the flame-cut hole at Stiffener 1, as shown in Fig. 3-38. At approximately 1.8 million cycles, a fatigue crack 10 mm (0.40 in.) long was found propagating upward through the web plate from the surface flaw. Fig. 3-39 shows a photograph of the fatigue crack. A repair of the crack was made by grinding out the cracked material. Care was taken to provide smooth surfaces and transitions, and to avoid introducing additional stress concentrations. Fig. 4-22 shows the repaired hole.

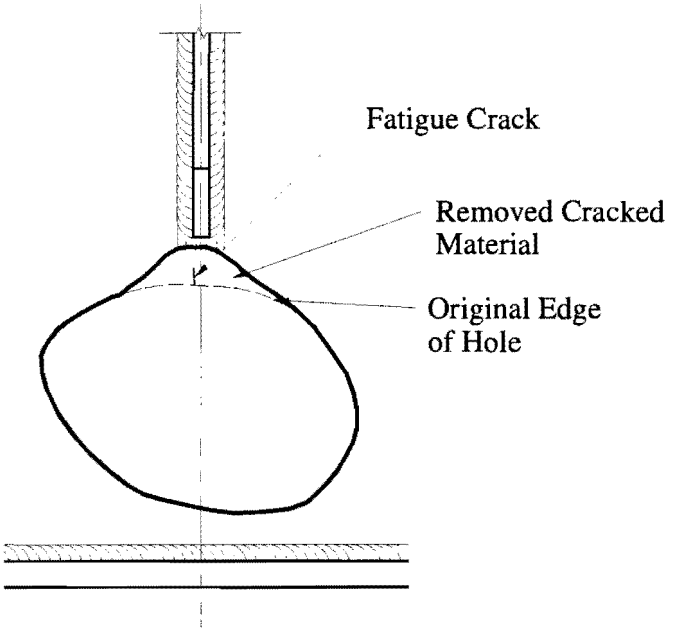

Figure 4-22: Flame-cut hole after repair of fatigue crack

The fact that a crack initiated and propagated from the surface flaw on one of the holes illustrates the importance of providing a smooth surface on the inside edges of both drilled and flame-cut holes. Edges should be ground as smooth as possible and, upon completion of a repair, all edges of every hole should be rechecked with dye penetrant for surface flaws. The smallest flaw could produce a fatigue crack.

Of concern with this type repair is the possibility of stress concentration factor superposition. This is the condition where the stress concentration from one geometric discontinuity overlaps an adjacent stress concentration field. This concern will be addressed in the next section.

4.7 CRITERIA DEVELOPMENT FOR FLAME-CUT HOLES

In order to investigate the effect of a large flame-cut hole on nearby connection details, afinite element study was conducted using a plate girder model with an elliptical hole, as shown

in Fig. 4-23. The hole measured 100 mm (4 in.) on its major axis and 75 mm (3 in.) on its minor axis. A series of analyses was conducted, holding the dimensions of the ellipse constant and varying the distance from the end of the stiffener to the top edge of the elliptical hole. The parameters studied were:

- minimum distance to stiffener termination;
- maximum hole size; and
- minimum distance to weld toe.

The results of this study are given in the following discussion.

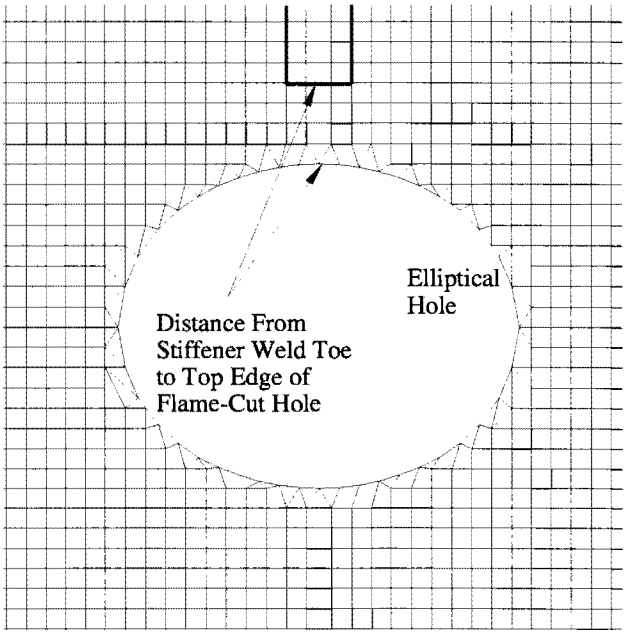

Figure 4-23: Elliptical hole in plate girder model.

Minimum Distance from Top Edge of Hole to Bottom of Transverse Stiffener - The distance was varied by modifying the length of the stiffener. Beginning at 0 mm (0 in.), the

distance was increased at 6 mm (1/4 in.) increments until the transverse stiffener no longer affected the stress concentration at the top of the hole. Table 4-6 shows stress values at both the transverse stiffener toe and the top edge of the elliptical hole for each analysis. The spacing required for the stiffener to have no effect on the stress concentration around the hole was found to be 44 mm (1-3/4 in.).

Distance From Toe of Stiffener to Top Edge of Hole		Stress			
		At Toe of Stiffener		At Top Edge of Hole	
MPa	ksi	MPa	ksi	MPa	ksi
0	(0)	115	(16.6)	112	(16.6)
1.7	(0.25)	91.4	(13.3)	109	(15.8)
3.4	(0.5)	76.5	(11.1)	116	(16.8)
5.2	(0.75)	66.0	(9.58)	117	(17.0)
6.9	(1.0)	58.6	(8.50)	118	(17.1)
8.6	(1.25)	53.9	(7.82)	118	(17.1)
10	(1.5)	48.2	(6.99)	118	(17.1)
12	(1.75)	44.4	(6.44)	118	(17.1)

Table 4-6: Stresses at toe of stiffener and top edge of hole versus toe-to-toe hole spacing.

Maximum Height of Hole - In developing criteria for the maximum height of flame-cut holes, it was assumed that the holes tested in the laboratory were representative of typical field repairs. It was also assumed that since its fatigue performance in the laboratory was satisfactory, a flame-cut hole is a viable fatigue repair technique. The flame-cut holes tested in the laboratory could then be used to develop some general rules of thumb for the maximum height of a hole. The maximum height of the largest hole in Girder 1 was 114 mm (4-1/2 in.). By dividing the height of the hole by the depth of the girder, a factor can be developed. The factor can then be multiplied by the depths of other girders to calculate maximum hole sizes for each girder.

Dividing 114 mm (4-1/2 in.) by 760 mm (30 in.), the depth of Girder 1, yields a factor of 0.15. Therefore, a general expression for the maximum height of a flame-cut hole in a girder of depth, d, is $0.15d$. The use of the expression does have limits. It was developed based on experimental data for a relatively shallow girder. Extremely deep girders would require extremely large maximum hole depths and unacceptable section losses. In the repair of the Midland County bridges, no flame-cut hole exceeded a height of 150 mm (6 in.). Therefore, as a general rule of thumb, the absolute maximum height of a hole should not exceed 150 mm (6 in.).

Distance From Bottom Edge of Hole to Top of Longitudinal Fillet Weld - The three flame-cut holes in Girder 1 can also be used to develop a criterion for the minimum distance from the bottom edge of the hole to the top of the longitudinal fillet weld. Of the three holes, the hole at Stiffener 1 had the shortest distance to the top of the fillet weld, 15 mm (0.6 in.). Because no cracks developed in the bottom of the hole, anything greater than 15 mm (0.6 in.) was assumed to be an acceptable minimum. Rounding to the nearest 6 mm (1/4 in.), the criterion is increased to 19 mm (3/4 in.). Therefore, the minimum distance from the bottom edge of a flame-cut hole to the top of longitudinal fillet weld should be no less than 19 mm (3/4 in.).

4.8 COMPARISON OF MULTIPLE DRILLED HOLES TO FLAME-CUT HOLES

Multiple drilled holes were modeled in a plate girder model and analyzed to determine whether or not drilled holes produce higher stress concentrations in a girder web plate than a flame-cut hole encompassing the same area. Fig. 4-24 illustrates how a flame-cut hole may be used rather than multiple drilled holes. Cracks running from the drilled holes to the transverse stiffener were also simulated in the multiple drilled hole model. The number and placement of drilled holes was determined by anticipating a crack pattern that could be repaired by the flame-cut hole in the model shown in Fig. 4-18. The holes were then placed at each crack tip to simulate a true comparison between the flame-cut hole and multiple drilled holes techniques.

The analysis revealed that multiple drilled holes experience higher stress concentrations than a single flame-cut hole, provided the holes are properly finished. The drilled hole model experienced a maximum stress concentration of 3.5 at the extreme edges of the uppermost holes. In addition, a stress concentration of 2.5 occurred in the web plate at a crack that simulated propagation around the toe of a stiffener-to-web fillet weld. The flame-cut hole model, on the other hand, experienced a maximum stress concentration of only 2.2 at its bottom edge. Figs. 4-25 and 4-26 show stress plots for both models. Results of the finite element analyses comparing maximum stress concentrations between two different techniques repairing the same crack pattern seem to indicate that flame-cut holes are a preferable option when repairing a densely cracked region. It should be noted, however, that the flame-cut hole method was chosen over the multiple drilled hole method on the assumption that the use of the flame-cut hole criteria discussed earlier can be met. The use of multiple drilled holes is a proven method in arresting crack growth and is still a viable option if a flame-cut hole cannot be used.

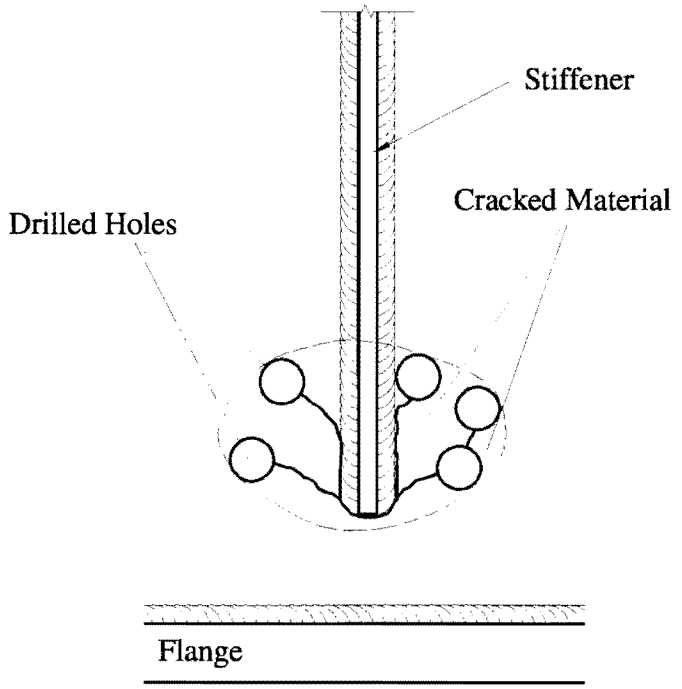

Figure 4-24: Comparison of section loss between drilled and flame-cut holes.

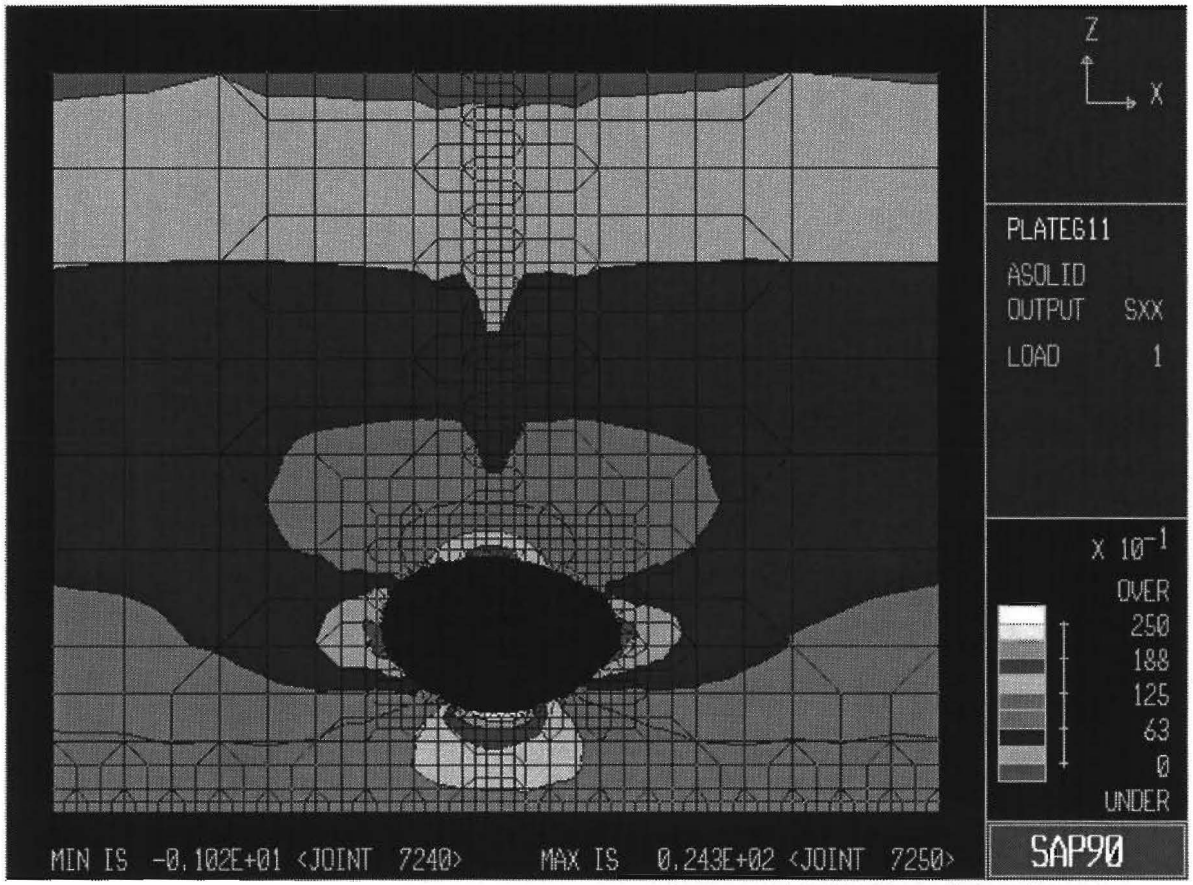

Figure 4-25: FEM stress contours for flame-cut hole model.

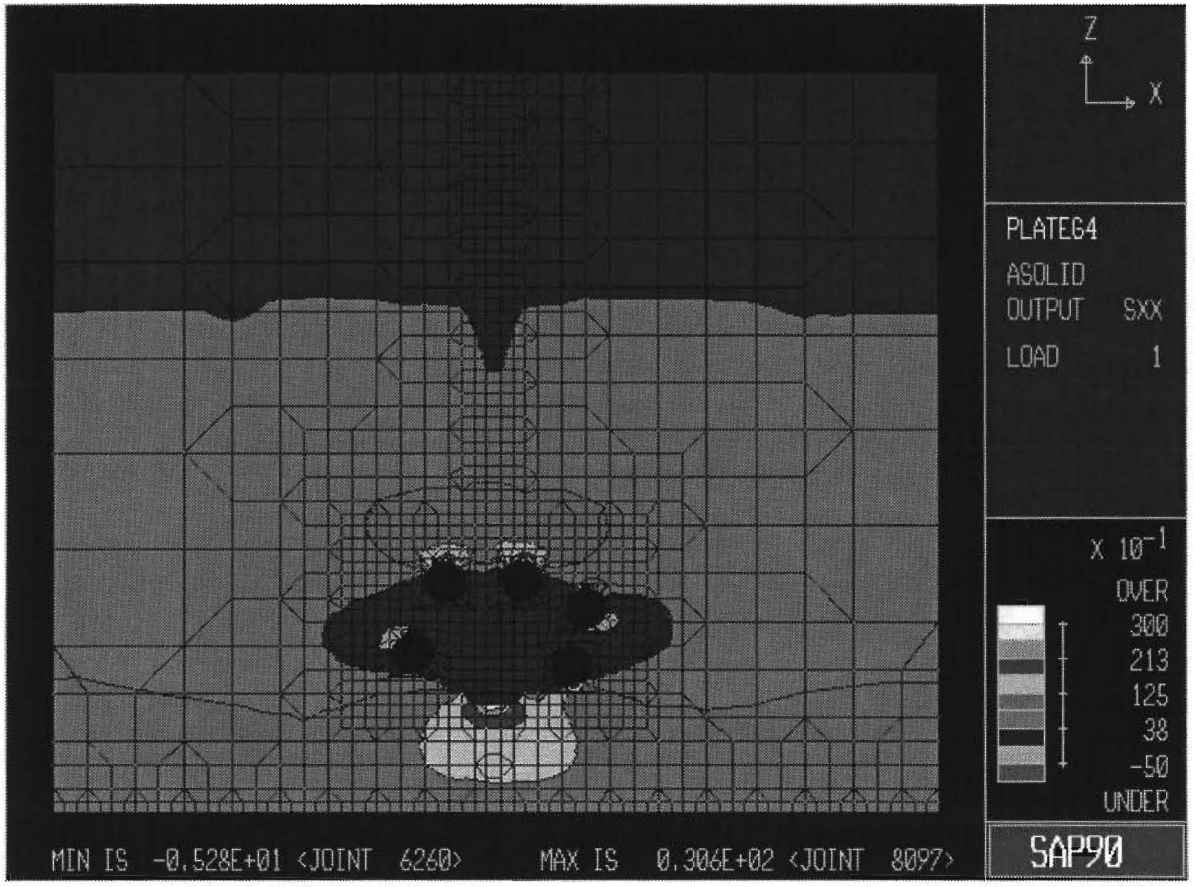

Figure 4-26: FEM stress contours for multiple drilled hole model.

4.9 WEB-TO-FLANGE CRACK STUDY

An additional phase of this study investigated what effect, if any, web-to-flange fatigue cracks produced by out-of-plane distortion have on the stress distribution in the plate girder web. As previously discussed, drilled hole at the tips of web-to-flange fatigue cracks have been shown to be effective in arresting fatigue crack growth along the web-to-flange fillet welds, even if the source of the out-of-plane distortion is not removed (Fisher et al. 1990). Drilling holes does, however, produce stress concentrations in the web plate and web-to-flange fillet weld material and adds to repair expenses. Assuming that the source of out-of-plane distortion is removed, the remaining bending stresses, which are in-plane to the web plate, would not, theoretically, cause the crack to propagate further. It could be argued that the drilled holes are, therefore, unnecessary. The effect of a web-to-flange crack on web stress distribution would determine whether or not drilling holes at crack tips is really necessary. It is important to note that when the source of out-of-plane distortion is not removed, drilled holes must be used to arrest the crack growth in conjunction with other retrofitting procedures.

A finite element model of a partial plate girder section was developed. The web plate of the girder consisted of a plane stress element, similar to previous plate girder models. The flange and longitudinal web-to-flange fillet weld, however, were modeled using eight-node solid brick elements. Figure 4-27 shows the finite element mesh for the basic web-to-flange model. Like previous plate girder models, a linear displacement pattern corresponding to an in-plane bending stress of 83 MPa (12 ksi) in the extreme fiber of the flange was imposed.

The first model simulated a simple crack between the web and the top of the longitudinal web-to-flange fillet weld. The crack was created in the plate girder model by placing additional nodes over existing nodes in a line 150 mm (6 in.) long. The line was centered longitudinally in the girder and placed between the plane stress web plate elements and the solid web-to-flange weld elements. As with previous models, eliminating nodal connectivity by connecting adjacent elements to two sets of nodes with identical locations produced the desired effect.

The stress contours in Fig. 4-28 show no stress concentrations in the x-direction, the direction of the applied bending stress. Examination of the deflected shape of the model indicated no crack separation. Such results suggest that a web-to-flange crack in a constant moment region should not, theoretically, experience any propagation from in-plane bending of the web plate.

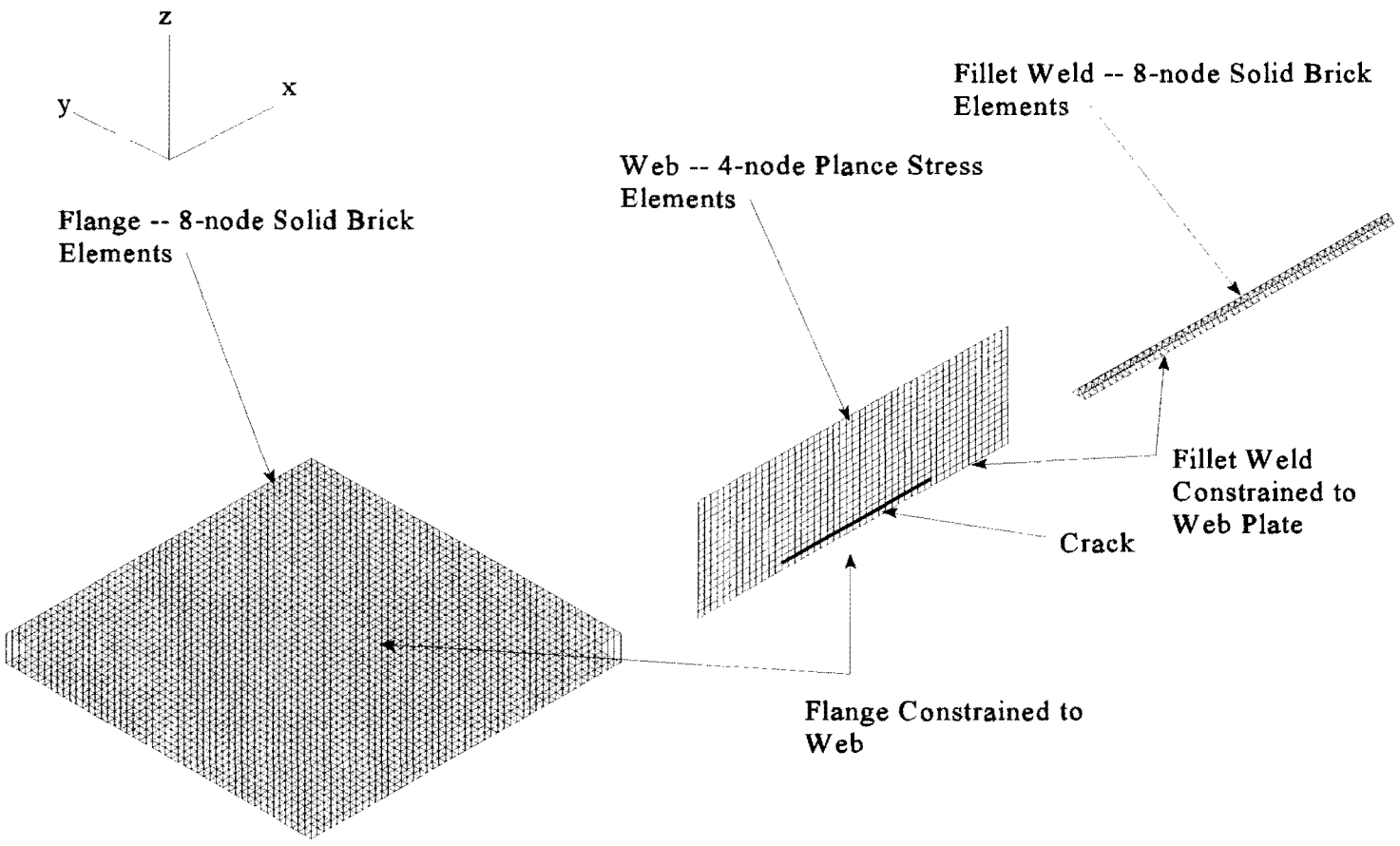

Figure 4-27: FEM mesh for a partial plate girder section with a crack at the web-to-flange connection.

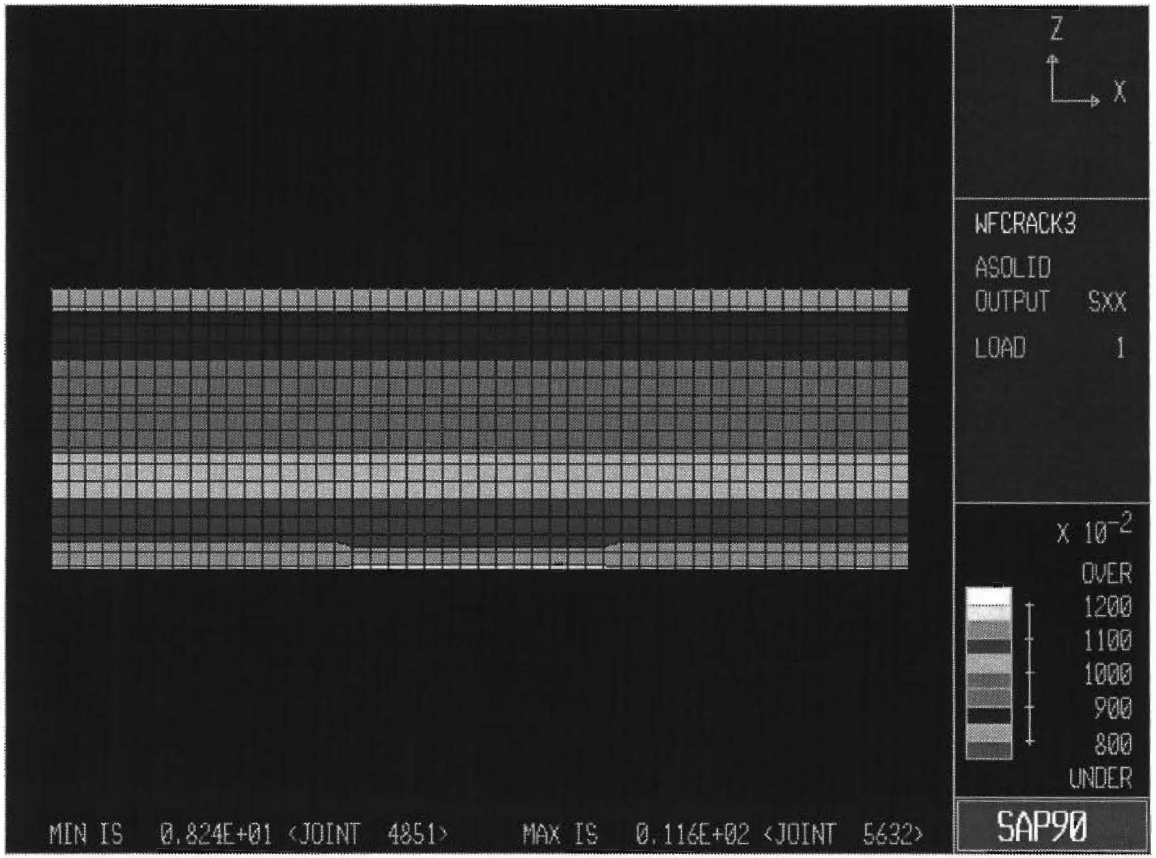

Figure 4-28: FEM stress contours in the x-direction for a partial plate girder section with a crack at the web-to-flange connection.

4.10 MODEL WITH WEB-TO-FLANGE CRACK ARRESTED BY TWO HOLES

A model simulating a web-to-flange fatigue crack repaired by drilling holes was developed using the same types of elements, loading, and boundary conditions used in the simple crack model. The same 150 mm (6 in.) crack is "repaired" by placing 22 mm (7/8 in.) diameter holes at each end of the crack. The holes pass through both the web plate and longitudinal fillet weld.

The analysis of the drilled hole model yielded a maximum stress concentration in the x-direction of 2.8 in the web plate, 2.2 in the fillet weld, and 1.3 in the flange. Stress concentrations were found by dividing the maximum stresses at the web plate, fillet weld, and flange by the nominal stresses at each point of maximum stress. Stress contours for the web, fillet weld, and tension flange are shown in Figs. 4-28 through 4-30. Although stress concentrations in the x-direction are increased significantly by introducing drilled holes, arresting the crack tips prevents stresses in the z-direction from causing the crack to propagate.

As indicated earlier, drilling holes at the tips of web-to-flange out-of-plane distortion cracks is a time-tested and proven method to prevent further crack propagation, even when the source of distortion is not removed. Experimental data suggest that, even after removing the source of out-of-plane distortion, leaving such cracks unrepaired causes them to propagate. As indicated earlier, shear stresses in the web plate of a girder have the potential for causing web-to-flange cracks to grow. Because shear stresses invariably exist in bridge girders, drilling holes to arrest the tips of the cracks should be maintained as the means of repair.

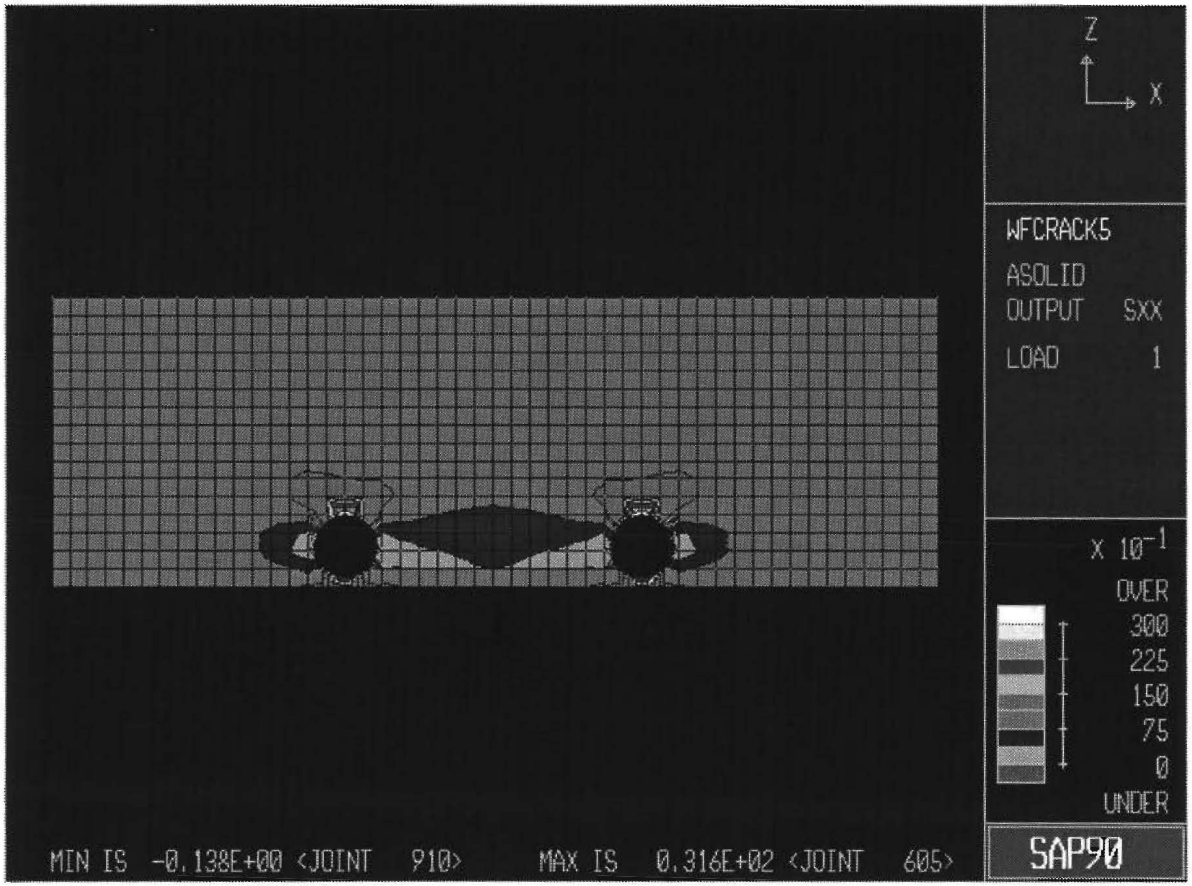

Figure 4-29: FEM stress contours for web plate.

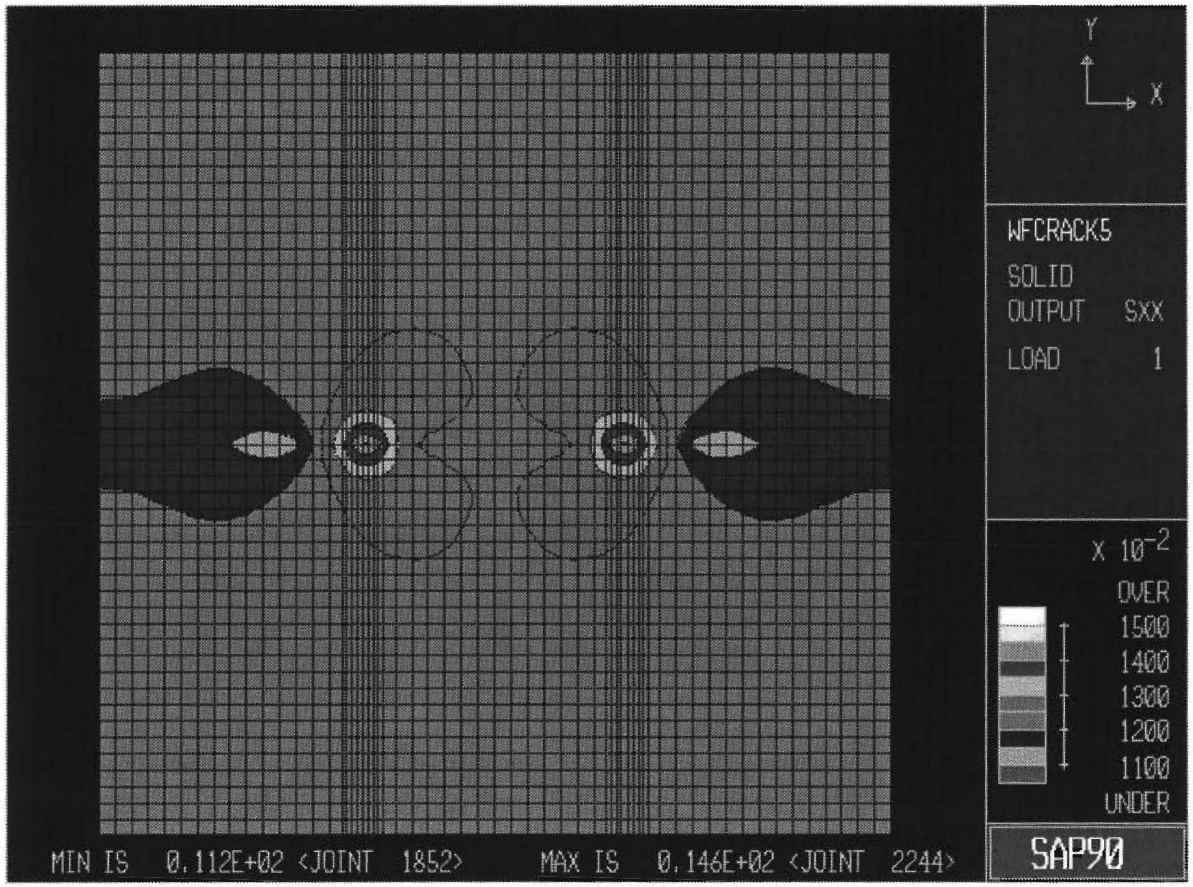

Figure 4-30: FEM stress contours for tension flange.

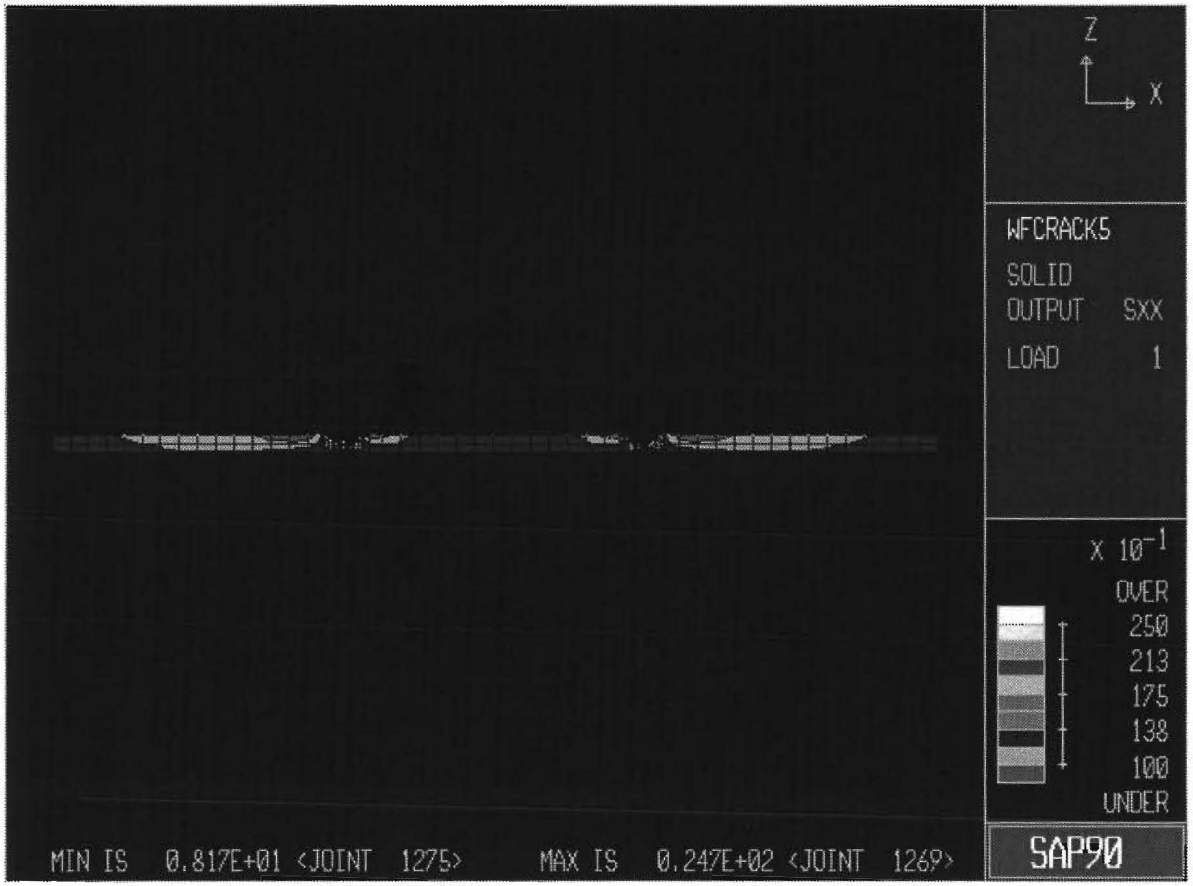

Figure 4-31: FEM stress contours for fillet weld.

Chapter Five
RECOMMENDATIONS AND CONCLUSIONS

The research study described investigated the feasibility of repair procedures for various types of fatigue damage in steel highway bridge girders. Specifically, the fatigue damage is the result of unintended out-of-plane distortion in web plates at cross-frame diaphragms. Through field measurements, laboratory testing, and analytical studies, the following specific repair procedures were evaluated:

- hole drilling at crack tips;
- flame-cut holes;
- gouging and re-welding;
- welded attachment of existing tight-fit connection plate; and
- welded attachment of connection plate with clip.

The following discussion summarizes the findings of this study for each repair method and presents recommendations for their applications.

5.1 DRILLING HOLES AT CRACK TIPS

As suggested in TxDOT Report 1313, it is recommended that holes be drilled at the tips or fronts of all fatigue cracks that are not to be removed from the structure. Even though there may be situations where the drive force behind the crack development has been removed, other stress conditions may continue to propagate the crack. For example, the web-to-flange fatigue crack from web distortion is parallel with the primary web bending stress and would, therefore, not propagate. However, the bending shear stress will cause a principal stress to develop with a component perpendicular to the plane of the crack. An additional secondary, or unintended stress may be present such as out-of-plane web bending from oil canning.

When individual crack tips are to be arrested, a hole diameter between 19 mm (3/4 in.) and 25 mm (1.0 in.) should be used to reduce the crack tip acuity. This range of hole diameters is based on a web plate yield stress of 250 MPa (36 ksi). The criterion used to specify a drilled hole diameter, ϕ, is given as:

$$\phi \geq \frac{S_r^2 L}{35 F_y} \left(\geq \frac{S_r^2 L}{5 F_y} \right) \tag{5-1}$$

where S_r is the maximum expected nominal stress range at the hole, L is the total length of the drilled crack (perpendicular to the stress field), and F_y is the yield strength of the web plate. Strain measurements of in-service bridges have indicated that the stress range seldom exceeds 40 MPa (6.0 ksi). For single crack arresting, larger diameter holes should be avoided to minimize the web cross section loss.

It cannot be overemphasized that the hole finish is as important, if not more so, than the hole diameter. If burrs or rough edges remain after the drilling operation, crack initiation may occur due to the stress risers. All drilled holes should be ground and surfaced to a polished finish. Dye penetrant inspection should be performed upon completion to insure that the hole circumference is free of defects, and that the crack tip has been properly located.

Proper location of the crack tip is essential. If the crack is not properly located and the hole is drilled behind the crack tip, an additional stress concentration is provided by the hole, increasing its propagation rate. It has been suggested that the crack tip be located on the inside circumference of the hole to ensure that the crack intersects the hole, as shown in Fig. 5-1. However, it is recommended that the center of the hole be positioned at the crack tip to reduce the overall length of the finished crack and minimize the web section loss. Normally, the crack tip can be adequately located visually due to the high degree of corrosion emanating from the working crack, or through the use of dye penetrant.

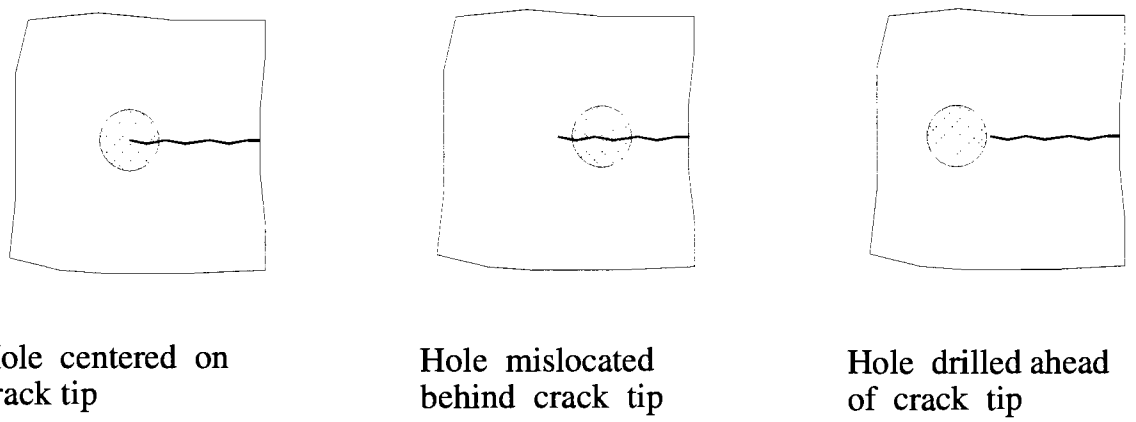

Figure 5-1: Possible drilled hole locations relative to crack tip.

Once the paint in the vicinity of the fatigue damage has been removed and the crack tips have been accurately located by dye penetrant, location of the hole centers should be clearly marked, as in Fig. 5-2. First, 6 mm (1/4 in.) pilot holes should by drilled using a hand drill to aid in properly placing the final hole. Full diameter holes should then be drilled by first positioning the drill bit in the pilot hole, as shown in Fig. 5-3. This photograph also shows the use of a structural angle clamped to the flange. The outstanding leg provides an adequate surface for the base of the magnetic drill.

Once all holes are drilled to their final diameter, both sides of the web plate should be ground smooth using a rotary grinder to remove any burrs from the drilling operation. Each hole should then be ground smooth using a die or rotary burr grinder, one of which is shown in Fig. 2-20. Once all the grinding is complete, a final dye penetrant inspection should be performed to insure that all cracks have been arrested.

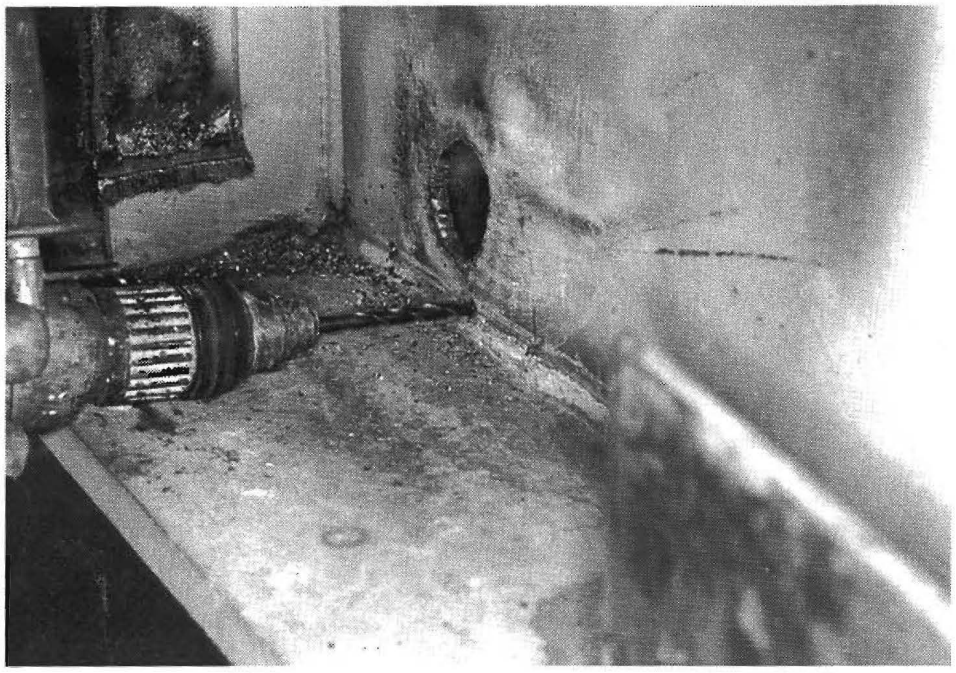

Figure 5-2: Marked hole centers at crack tips.

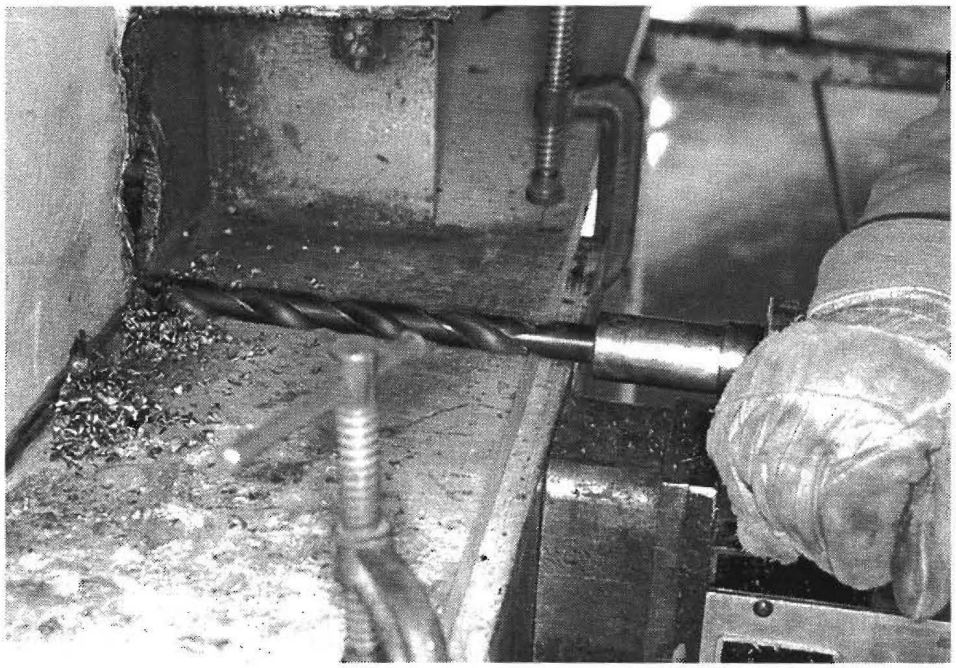

Figure 5-3: Hole drilled to final diameter, note 6 mm (1/4 in.) pilot holes.

If two adjacent holes overlap or leave a narrow ligament, the holes should be combined into one oblong shaped hole, as shown in Fig. 5-4. Again, all surfaces should be ground to a smooth finish.

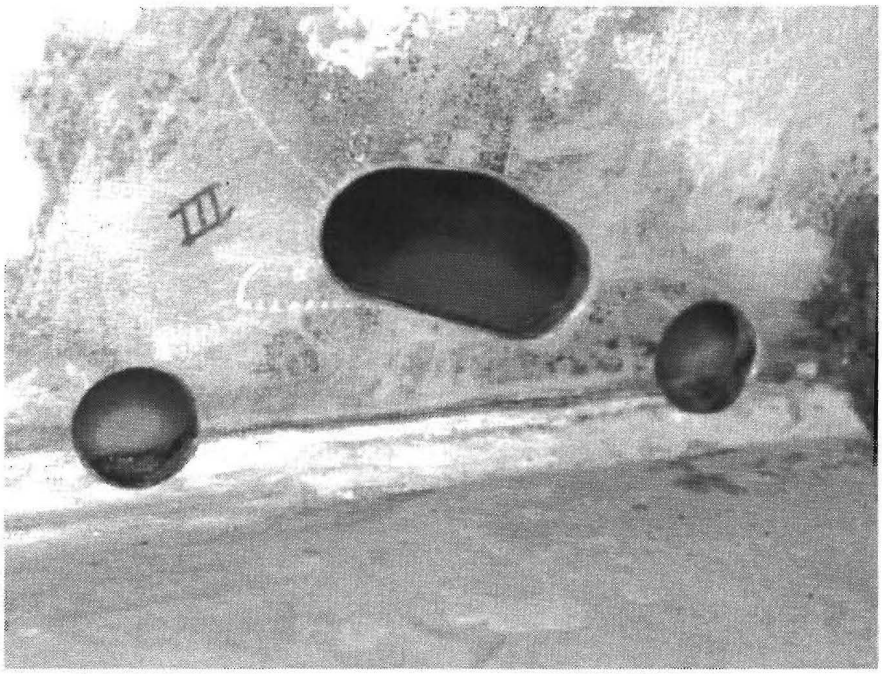

Figure 5-4: View of slotted holes.

Adjacent holes should be aligned to minimize the area of steel taken out of the cross section of the web plate. This may require drilling the holes off center from the crack tip, as shown schematically in Fig. 5-5.

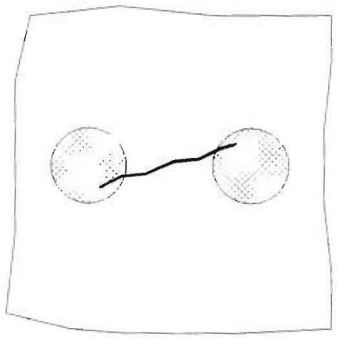

Figure 5-5: Alignment of holes to minimize web section loss.

All longitudinal web-to-flange cracks should be retrofitted with drilled holes at the crack tips, regardless of the repair method used for the web plate fatigue cracks. The holes need not be any greater than 22 mm (7/8 in.) in diameter.

With the exception of the ends, the web-to-flange weld need not be repaired. In fact, its presence acts as a shield for the tension flange from crack growth coming from the web plate damaged area. A crack propagating toward the web-to-flange crack will not grow across the free surface and, thus, it is self-arresting.

The crack interface of web-to-flange welds should be examined for possible crack growth into the flange. Typical, the fatigue crack surface is smooth, thus eliminating any possibility of crack initiation perpendicular to its plane from the in-plane bending stress. However, the crack line on either side of the web plate should be inspected for irregularities that might serve as a crack initiation site. For example, as an extreme case, the fillet weld shown in Fig. 5-6 was welded manually. (Note, detail shown in Fig. 5-6 is not from a bridge located in Texas.)

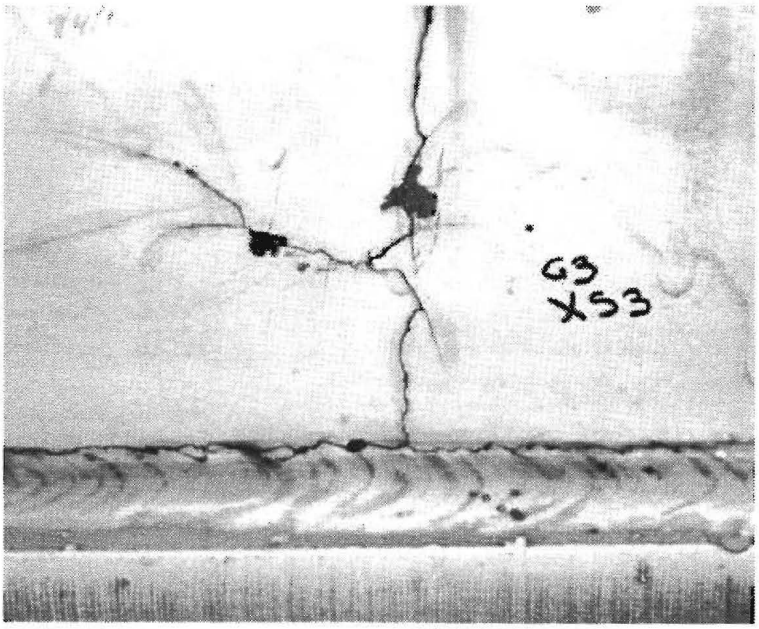

Figure 5-6: View of irregular web-to-flange fillet weld toe.

If an uneven crack surface forms along the toe of the web-to-flange fillet weld, the entire crack should be removed from the structure when adjacent to a tension flange. A crack could develop perpendicular to this surface and propagate into the flange. In addition to drilling holes at the crack tips, a slot should be made with the edge of a rotary grinder along the toe of the fillet weld (see Fig. 5-7) such that the entire crack surface is removed from both the flange and the web plate (the flange being more critical of the two). Procedures for retrofitting the fatigue cracks along the web-to-flange fillet weld should include the following steps:

- Accurately locate, drill, and grind holes at both ends of the web-to-flange crack.
- Inspect both holes with dye penetrant to insure that the crack tips have been removed.
- Remove the portion of the web plate and web-to-flange containing the crack with the edge of a rotary grinder.
- Inspect lower ground surface for cracks and exposed weld flaws. Remove by hole drilling and/or burr grinding as necessary.
- Prior to painting, caulk gap. Do not over-caulk to avoid limiting future inspection of the region.

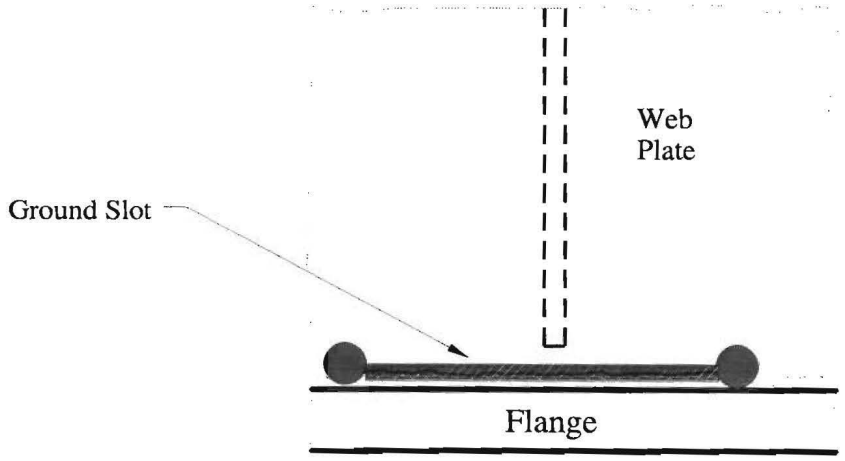

Figure 5-7: Removal of web-to-flange fillet weld crack.

Provided that the length of the slot (including the holes) is no greater than 250 mm (10 in.), no additional work is required. However, if the length exceeds 250 mm (10 in.), a bolted splice between the flange and web plate should be used.

Large circular holes have be used when the crack length is relatively short so that the entire crack can be remove by the hole. Figure 5-8 shows a crack that originated in the weld toe at the end of the connection plate. Note that the end of the connection plate needs to be cut back.

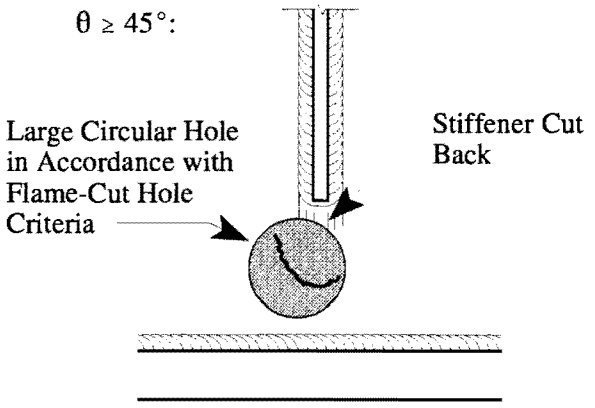

Figure 5-8: Large hole repair technique for web crack.

Hole drilling can be performed under normal traffic conditions. There is no need to limit vehicular loads during this repair procedure.

5.2 FLAME-CUT HOLES

Flame-cut holes can be used to remove multiple fatigue cracks emanating from the termination of the connection plate. Typically, the cut-short connection plate detail will have

more extensive fatigue cracking than the tight-fit detail since the former detail is more flexible and allows for greater distortion-induced stresses. A multiple hole pattern can result in higher stress concentrations than a well-contoured flame-cut web hole. Therefore, the flame-cut hole is a viable alternative to hole drilling.

One drawback to the flame-cut hole is the need to remove the end of the connection plate. If a diaphragm is to remain attached, the connection plate will require an extension, such as the clip shown in Fig. 3-34, to provide a rigid attachment (also see Sec. 5.4).

The information gathered from laboratory testing and finite element analyses has led to the following list of recommended repair guidelines for the use of flame-cut holes :

1. The distance from the toe of the transverse stiffener to the top of the hole should be at least 45 mm (1-3/4 in.).

2. The height of a flame-cut hole should not exceed the lesser of $0.15d$ or 150 mm (6 in.), where d is the depth of the girder to be repaired.

3. The minimum distance from the bottom of the flame-cut hole to the top of the longitudinal fillet weld should not be less than 20 mm (3/4 in.).

Figure 5-9 shows the guidelines schematically. It should be noted that the use of large circular holes, discussed earlier as an alternative to multiple drilled holes, should be governed by the recommended repair guidelines for flame-cut holes as well.

The flame-cut hole perimeter must be properly located. While the area of the hole should be minimized to reduce the web section loss, not removing the crack tip(s) will lead to continued crack propagation. Figure 5-10 shows the marked outline for a flame-cut hole. Note the proximity of the outline to the fatigue crack tip at the lower-left side. After flame-cutting and grinding, dye penetrant inspection indicated a crack at that location. A small rotary grinder was necessary to remove the crack tip, as well as at other locations (see Fig. 5-10).

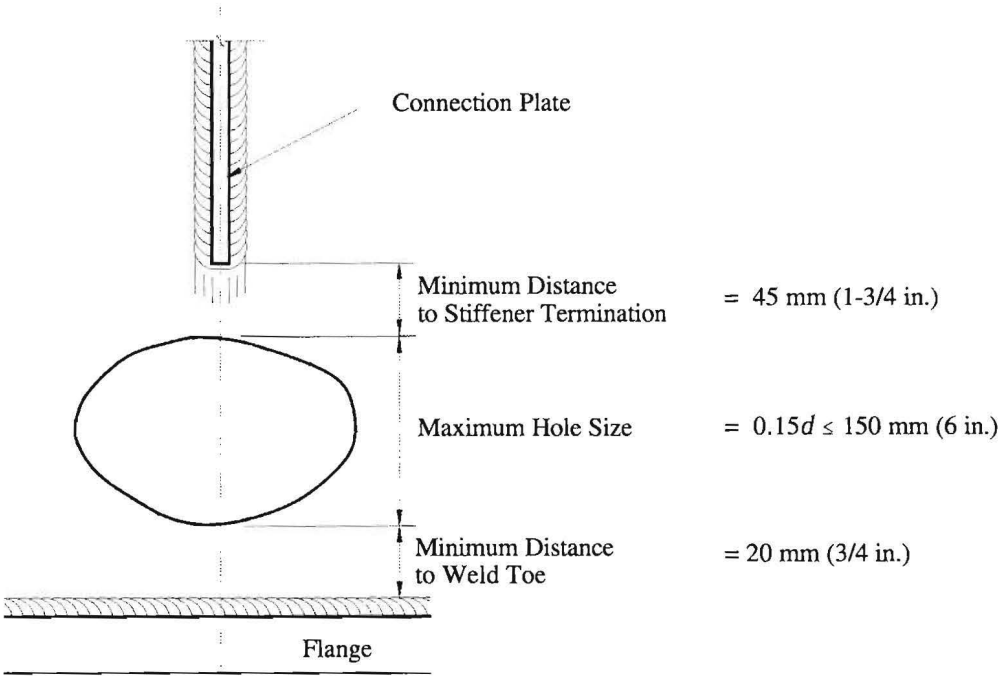

Figure 5-9: Guidelines for the use of flame-cut holes.

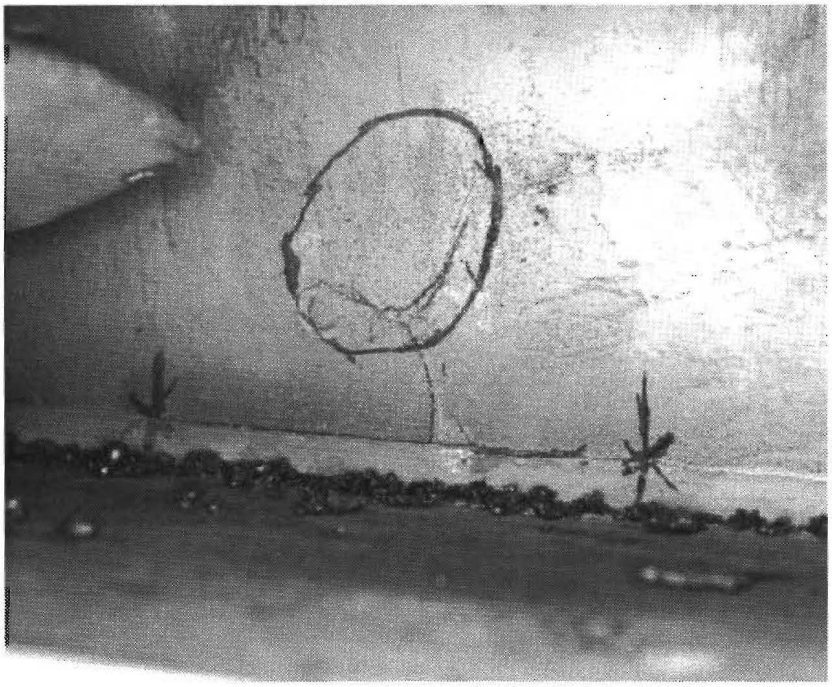

Figure 5-10: View of outlined hole for flame-cutting.

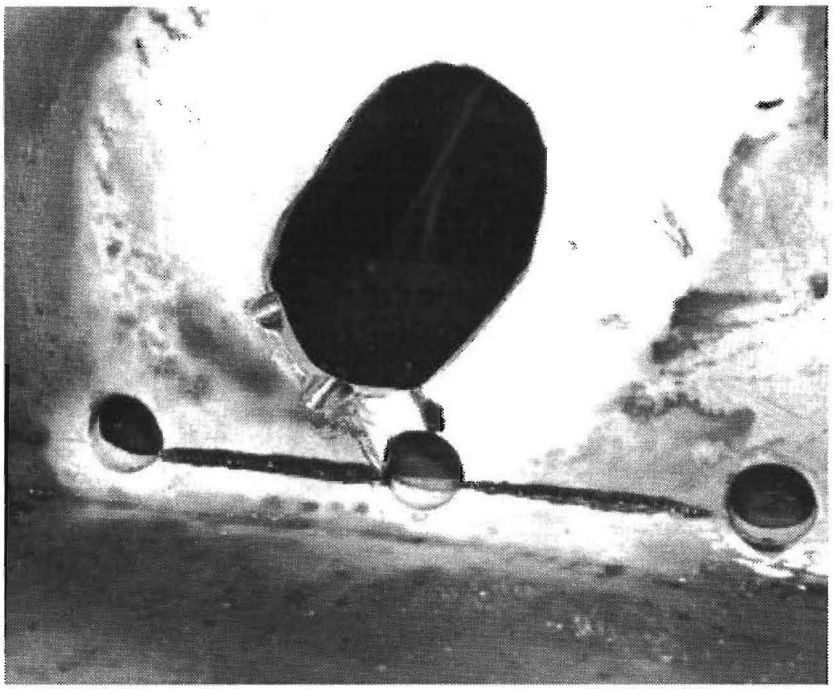

Figure 5-11: Removal of missed crack tips by grinding.

Ideally, the fatigue strength of the flame-cut hole should be AASHTO Category C. This matches the fatigue strength of the original detail and would, therefore, not increase the overall susceptibility of the structure to fatigue damage. As with drilled holes, proper finishing of the flame-cut surface is required for the Category C classification. Flame-cut holes require a higher degree of finishing due to the rough surface that remains from the actual cutting operation, as compared to that from drilling. Figure 5-12 shows a view of a grinder used to finish a flame-cut hole on the Midland County bridge.

Care should also be taken to avoid a small radius of curvature of the hole nearest to the web-to-flange weld. This will result in a higher localized stress concentration at a critical location. Figure 5-13 provides an example of an undesirable curvature of the flame-cut hole. As previously mentioned, the presence of a retrofitted fatigue crack in the web-to-flange weld will act as insurance against crack propagation into the flange.

Figure 5-12: View of die grinder used to finish holes.

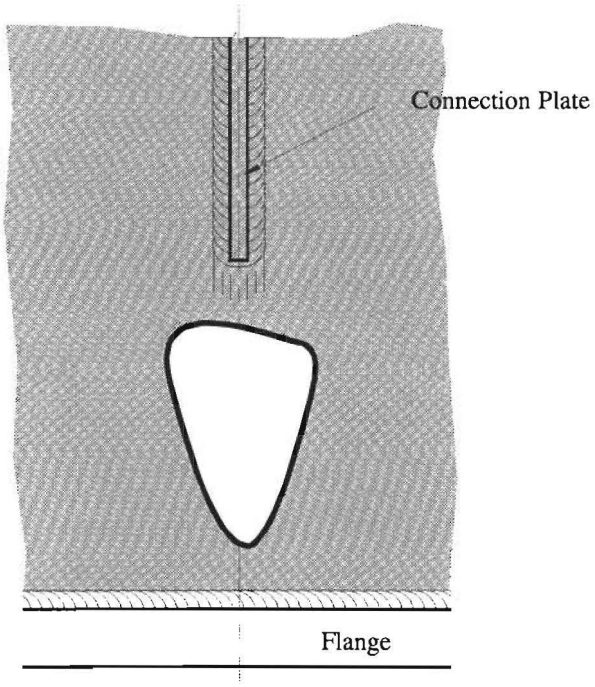

Figure 5-13: Example of undesirable curvature near web-to-flange weld.

5.4 GOUGING AND RE-WELDING

The results of this study have shown that gouging and re-welding is a viable option in the repair of web gap fatigue cracking. The finished repair results in a web plate void of stress concentrations that occur with either drilled or flame-cut holes. However, this repair requires the greatest degree of operator skill and can, therefore, be the costliest repair and have the highest potential for problems. The repair procedure used on the Midland County bridge is outlined below.

- Blast clean the cracked region.
- Cut and remove end of connection plate at least 25 mm (1.0 in.) beyond damaged region.
- Transfer crack mapping on each side of web plate to the other side, reversing image.
- Beginning on one side of the web plate, properly identify and mark all crack tips (both near and far side).
- Back gouge each crack to a depth just over one-half the web plate thickness, beginning 12 mm (0.5 in.) beyond the crack tip back towards the origin of the cracking.
- Re-weld gouge taking care to prevent slag entrapment. Overfill the gouge by 3 mm (1/8 in.) to insure full thickness of web plate.
- Grind surface smooth and flush to the original surface.
- Inspect repaired area with dye penetrant (ultrasonic or radiographic inspection preferred).
- Repeat procedure on far side of the web plate.

It must be emphasized that the crack formation on one side of the web plate is often independent of the other side. The cracking may not go through the thickness of the web plate. Consequently, it is necessary to map both sets of crack lines on both web surfaces. Gouging a

crack may begin on the opposite side of the plate through what appears to be sound metal until the root of the crack is found.

As an alternative to repairing both sets of cracks from both sides of the web plate, the operator can carefully observe the crack during gouging and determine if and when the root has been removed. If the root still remains after one-half the web thickness depth has be reached, gouging and re-welding must be preformed from the other side as well.

As was observed in the laboratory repairs, the heat from gouging and re-welding can cause an advancement of the crack. When welding on the second side of the web plate, the operator must carefully observe the crack to insure that he has removed the crack root. Grinding the root of the gouge is a viable option for insuring a clean gouge and complete removal of the crack. A rotary disc grinder can be used when the crack line is fairly straight.

As with the other repair procedures, the web-to-flange crack should remain but be retrofitted with drilled holes at the crack tips. Again, this crack will act as a shield against possible crack initiation from the repaired region. If drilling is performed after the gouging and re-welding, the crack tips should be located again, since the heat and subsequent shrinkage from the gouging and re-welding can advance the crack.

5.4 WELDED ATTACHMENT OF EXISTING TIGHT-FIT CONNECTION PLATE

When a rigid attachment to the flange is required at an existing tight-fit connection detail, a welded retrofit can be used provided that the weld quality can be guaranteed. This will require not only skilled and qualified welders, but a knowledge of the steel type used in the original fabrication of the bridge as well. Welding of older bridges should not be preformed unless the weldability of the steel can be documented.

Prior to fillet welding the end of the connection plate, the area must be blast cleaned to

remove paint and debris. What will become the root of the fillet weld must be visually inspected for cleanliness. The tolerance on a tight-fit stiffener detail is 0 to +2 mm (1/16 in.). This gap is large enough to allow paint to flow between the plate surfaces. If the cleanliness of the root is suspect, the end of the connection plate can be ground with a small diameter rotary grinder from both sides of the plate. Grinding the full width of the connection plate may be difficult though due to access problems near the web plate. The weld detail then becomes a small double-vee groove weld.

When performing the welding, proper control and techniques must be used to insure a quality weld. Special attention must be given to the profile and toe of the fillet weld. A slightly concave profile is desired since it reduces the stress concentration in the flange. Care should be taken to avoid undersizing the throat of the fillet weld though. The weld must not undercut the flange plate.

After welding, additional retrofit fit techniques can be used if the welding and weldment quality is suspect. The fillet weld profile can be improved by grinding with a die, or burr grinder, where the direction of the grinder rotation is with the direction of stress flow in the flange. Grinding can also be used to remove the fillet weld toe on the flange. This will remove the minute shrinkage discontinuity that exists and is the initiation site for fatigue crack growth for a detail of this type. Section loss of the flange plate due to grinding must be minimized. Peening of the weld is an option to grinding.

5.5 WELDED ATTACHMENT OF CONNECTION PLATE WITH CLIP

When a cut-short connection plate is to be retrofitted for a rigid attachment, or the repair of the web-gap cracking has lead to the removal of a portion of the connection plate, an extension will be required for its rigid attachment (see Fig. 3-34). The clip plate must first be clamped to the existing connection plate with the end butted tight against the flange. The fillet weld between the clip plate and flange must be made first to insure avoiding an excessive lack-of-fusion plane.

Specifications for cleaning and weld quality are the same as those for the tight-fit retrofit.

The thickness of the clip plate must be adequate to provide sufficient stiffness against the out-of-plane diaphragm forces. It is suggested that the thickness equal that required to maintain the same cross sectional area in the clip plate as the original connection plate. Since the clip plate must be narrower than the connection plate to allow room for the fillet welds, a thicker clip plate will always result. When excessively large gaps result from the web-gap repair, the thickness of the clip plate should be increased to increase its stiffness.

5.6 RECOMMENDATIONS FOR ADDITIONAL RESEARCH

This research study report provided a limited investigation into the quality of field weld repairs. CVN testing was conducted on the repair weldments used in the laboratory testing phase of the study. Additional destructive testing of the gouging and re-welding repair procedure should be conducted to evaluate the quality of the complex heat affected zones. The multiple welding in a small region can result in a degradation of steel's material properties. The testing should include CVN testing in the surrounding region of the repair and micro-examination of the steel (hardness and phase structure).

The criterion developed for drilled holes at crack tips assumes that the hole lies in a flat plate. It does not take into account the presence of other geometrical conditions, such as welds and attached plates, that can result in a superposition of stress concentrations. A drilled hole to arrest a crack in a vertical fillet weld toe will have the stress concentration of the connection plate (AASHTO Category C), as well as that from the hole. Laboratory testing and finite element analysis should be performed for this condition.

REFERENCES

American Association of State Highway and Transportation Officials. *Guide Specification for Fracture Critical Non-Redundant Steel Bridge Members*, Washington, D.C. 1986.

American Association of State Highway and Transportation Officials. *Standard Specifications for Highway Bridges*, Fifteenth Edition, Washington, D.C. 1992

American Association of State Highway and Transportation Officials. *LRFD Bridge Design Specifications*, Washington, D.C. 1994

Diaz, M. and Andrews. *Detailed Structural Condition Report for Bridge 06-165-0005-15-201 (IH 20 WestBound) and 06-165-0005-15-202 (IH EastBound)*, ARE, Inc., Engineering Consultants. 1990.

Fisher, J.W., J. Jian, D.C. Wagner, and B.T. Yen. *Distortion Induced Fatigue Cracking in Steel Bridges*, NCHRP Report 336, National Cooperative Highway Research Program, Washington, D.C. 1990.

Keating, P.B. and A.R. Crozier. *Repair of Fatigue Damage to Midland County Bridges*, Research Report 1313-1F, Texas Transportation Institute, College Station, Texas. 1992.

Keating, P.B. and J.W. Fisher. *Evaluation of Fatigue Tests and Design Criteria for Welded Details*, NCHRP Report 286, National Cooperative Highway Research Program, Washington, D.C. 1986.

Kirsch, G. *Z. Ver. duet. Ing.*, Vol. 42. 1898.

Wilson, Scott D. *Development of Criteria for Fatigue Repairs in Bridge Girders Damage by Out-of-Plane Distortion*, Thesis, submitted to the Civil Engineering Department in partial fulfillment of the M.S. Degree, Texas A&M University, College Station, Texas. 1994.

APPENDIX A

Girder 2
Pre-Cracking Test Log

Stiffener #	Date	Time	Approx. Load Rate	Load	# of Cycles	Com-ments
2-1	8/3/93	2:30 pm - 5:00 pm	5 Hz	11 k (48.9 kN) Comp.	-	Cracks in web-to-flange.
"	8/4/93	8:00 am - 12 noon	5 Hz	11 k (48.9 kN) Comp.	90,800	Cracks in web plate.
"	"	1:00 pm - 5:00 pm	5 Hz	11 k (48.9 kN) Comp.	72,000	
"	8/5/93	8:00 am - 12 noon	5 Hz	2 k (8.9 kN) Tens.	72,000	Cracks at toe after 30-min.
			Total Compression		162,800	
			Total Tension		72,000	
2-2	8/5/93	1:30 pm - 5:00 pm	9 Hz	8 k (35.6 kN) Comp.		
"	8/6/93	8:00 am - 9:30 am	9 Hz	8 k (35.6 kN) Comp.	140,000	Cracks in web-to-flange.
"	"	9:30 am - 1:30 pm	7 Hz	10.5 k (46.7 kN) Comp.	70,000	
"	"	1:30 pm - 2:30 pm	5 Hz	12 k (53.4 kN) Comp.	25,000	
"	"	2:30 pm - 5:00 pm	5 Hz	2 k (8.9 kN) Tens.	45,000	Cracks at toe.

Stiffener #	Date	Time	Approx. Load Rate	Load	# of Cycles	Com-ments
"	8/9/93	8:00 am - 11:40 am	5 Hz	11 k (48.9 kN) Comp.	62,000	Cracks in web plate.
			Total Compression		297,000	
			Total Tension		45,000	
2-3	8/9/93	12:45 pm - 5:00 pm	5 Hz	11 k (48.9 kN) Comp.	73,000	Cracks in web-to-flange.
"	8/10/93	8:00 am - 11:30 am	5 Hz	11 k (48.9 kN) Comp.	53,000	Cracks in web plate.
"	"	11:30 am - 2:30 pm	5 Hz	2 k (8.9 kN) Tens.	33,000	Cracks at toe.
			Total Compression		126,000	
			Total Tension		33,000	

APPENDIX B

Static Load Test Data

Girder Number: 1
Test Type: Static
Test Number: 1
Date: 8/23/93

Channel	1	2	3	4	5	6	7	8	9	7	8	9
Gage Number	Gage 1A	Gage 1B	Gage 1C	Gage 1-2A	Gage 1-2B	Gage 1-2C	Gage 1-3A	Gage 1-3B	Gage 1-3C	Gage 1-1A	Gage 1-1B	Gage 1-1C
P (kips)	Strain (microstrains)											
10	56	65	60	62	106	64	103	132	66	89	91	66
20	114	134	120	128	216	128	203	264	132	186	180	132
30	166	198	174	184	314	188	290	388	190	287	267	196
40	220	258	228	240	408	245	368	507	250	380	348	256
50	266	316	280	290	498	300	441	622	306	467	425	312
60	316	370	328	340	586	355	508	735	360	555	498	368
70	360	424	376	386	670	404	572	839	409	641	570	420

Channel	1	2	3	4	5	6	7	8	9	7	8	9
Gage Number	Gage 1A	Gage 1B	Gage 1C	Gage 1-2A	Gage 1-2B	Gage 1-2C	Gage 1-3A	Gage 1-3B	Gage 1-3C	Gage 1-1A	Gage 1-1B	Gage 1-1C
P (kips)	Stress (ksi)											
10	1.624	1.885	1.74	1.798	3.074	1.856	2.987	3.828	1.914	2.581	2.639	1.914
20	3.306	3.886	3.48	3.712	6.264	3.712	5.887	7.656	3.828	5.394	5.22	3.828
30	4.814	5.742	5.046	5.336	9.106	5.452	8.41	11.252	5.51	8.323	7.743	5.684
40	6.38	7.482	6.612	6.96	11.832	7.105	10.672	14.703	7.25	11.02	10.092	7.424
50	7.714	9.164	8.12	8.41	14.442	8.7	12.789	18.038	8.874	13.543	12.325	9.048
60	9.164	10.73	9.512	9.86	16.994	10.295	14.732	21.315	10.44	16.095	14.442	10.672
70	10.44	12.296	10.904	11.194	19.43	11.716	16.588	24.331	11.861	18.589	16.53	12.18

Table B-1: Strain gage readings and calculated stresses from Static Test 1.

Girder Number 1
Test Type: Static
Test Number: 2
Date: 8/27/93

Channel	1	2	3	4	5	6	7	1	2	3	4	5	6	7	8
Gage Number	Gage 1A	Gage 1B	Gage 1C	Gage 1-1A	Gage 1-1B	Gage 1-1C	Gage 1-1D	Gage 1-2A	Gage 1-2B	Gage 1-2C	Gage 1-2D	Gage 1-3A	Gage 1-3B	Gage 1-3C	Gage 1-3D
P (kips)	Strain (microstrains)														
10	52	57	57	86	82	60	65	59	97	58	64	99	120	60	66
20	112	118	120	184	174	128	136	124	205	122	135	200	252	128	138
30	167	180	185	278	262	195	206	184	308	184	204	300	376	192	205
40	225	240	247	373	350	260	277	248	410	250	273	399	503	256	274
50	279	300	310	472	437	326	347	310	511	308	340	494	627	320	342
60	336	362	371	578	526	390	415	372	616	374	408	588	755	384	407
70	391	420	432	686	613	456	484	434	718	436	476	680	881	446	477

Channel	1	2	3	4	5	6	7	1	2	3	4	5	6	7	8
Gage Number	Gage 1A	Gage 1B	Gage 1C	Gage 1-1A	Gage 1-1B	Gage 1-1C	Gage 1-1D	Gage 1-2A	Gage 1-2B	Gage 1-2C	Gage 1-2D	Gage 1-3A	Gage 1-3B	Gage 1-3C	Gage 1-3D
P (kips)	Stress (ksi)														
10	1.508	1.653	1.653	2.494	2.378	1.74	1.885	1.711	2.813	1.682	1.856	2.871	3.48	1.74	1.914
20	3.248	3.422	3.48	5.336	5.046	3.712	3.944	3.596	5.945	3.538	3.915	5.8	7.308	3.712	4.002
30	4.843	5.22	5.365	8.062	7.598	5.655	5.974	5.336	8.932	5.336	5.916	8.7	10.904	5.568	5.945
40	6.525	6.96	7.163	10.817	10.15	7.54	8.033	7.192	11.89	7.25	7.917	11.571	14.587	7.424	7.946
50	8.091	8.7	8.99	13.688	12.673	9.454	10.063	8.99	14.819	8.932	9.86	14.326	18.183	9.28	9.918
60	9.744	10.498	10.759	16.762	15.254	11.31	12.035	10.788	17.864	10.846	11.832	17.052	21.895	11.136	11.803
70	11.339	12.18	12.528	19.894	17.777	13.224	14.036	12.586	20.822	12.644	13.804	19.72	25.549	12.934	13.833

Table B-2: Strain gage readings and calculated stresses from Static Test 2.

Girder Number: 1
Test Type: Static
Test Number: 3
Date: 9/2/93

Channel	1	2	3	4	5	6	7	8	9
Gage Number	Gage 1-1E	Gage 1-1F	Gage 1-1C	Gage 1-2E	Gage 1-2F	Gage 1-2C	Gage 1-3E	Gage 1-3F	Gage 1-3C
P (kips)	Strain (microstrains)								
10	58	88	62	50	114	60	50	170	60
20	118	183	129	102	234	124	110	354	128
30	180	284	200	154	360	190	175	544	196
40	234	375	264	206	475	255	242	720	260
50	287	465	326	256	590	315	304	892	320
60	339	560	392	308	709	378	374	1067	384
70	387	650	455	358	826	438	445	1240	448

Channel	1	2	3	4	5	6	7	8	9
Gage Number	Gage 1-1E	Gage 1-1F	Gage 1-1C	Gage 1-2E	Gage 1-2F	Gage 1-2C	Gage 1-3E	Gage 1-3F	Gage 1-3C
P (kips)	Stress (ksi)								
10	1.682	2.552	1.798	1.45	3.306	1.74	1.45	4.93	1.74
20	3.422	5.307	3.741	2.958	6.786	3.596	3.19	10.266	3.712
30	5.22	8.236	5.8	4.466	10.44	5.51	5.075	15.776	5.684
40	6.786	10.875	7.656	5.974	13.775	7.395	7.018	20.88	7.54
50	8.323	13.485	9.454	7.424	17.11	9.135	8.816	25.868	9.28
60	9.831	16.24	11.368	8.932	20.561	10.962	10.846	30.943	11.136
70	11.223	18.85	13.195	10.382	23.954	12.702	12.905	35.96	12.992

Table B-3: Strain gage readings and calculated stresses from Static Test 3.

Girder Number: 1
Test Type: Static
Test Number: 4
Date: 9/6/93

Channel	1	2	3	4	5	6	7
Gage Number	Gage 1A	Gage 1B	Gage 1C	Gage 1-1E	Gage 1-1F	Gage 1-1C	Gage 1-1D
P (kips)	Strain (microstrains)						
10	53	58	58	68	90	61	66
20	110	119	122	138	186	128	138
30	167	179	185	204	280	194	207
40	226	241	249	276	377	263	279
50	279	300	311	342	468	328	348
60	335	360	371	402	560	392	416
70	392	420	432	460	653	456	486

Channel	1	2	3	4	5	6	7
Gage Number	Gage 1A	Gage 1B	Gage 1C	Gage 1-1E	Gage 1-1F	Gage 1-1C	Gage 1-1D
P (kips)	Stress (ksi)						
10	1.537	1.682	1.682	1.972	2.61	1.769	1.914
20	3.19	3.451	3.538	4.002	5.394	3.712	4.002
30	4.843	5.191	5.365	5.916	8.12	5.626	6.003
40	6.554	6.989	7.221	8.004	10.933	7.627	8.091
50	8.091	8.7	9.019	9.918	13.572	9.512	10.092
60	9.715	10.44	10.759	11.658	16.24	11.368	12.064
70	11.368	12.18	12.528	13.34	18.937	13.224	14.094

Table B-4: Strain gage readings and calculated stresses from Static Test 4.

Girder Number: 2
Test Type: Static
Test Number: 5
Date: 9/16/93

Channel	1	2	3
Gage Number	Gage 2A	Gage 2B	Gage 2C
P (kips)	Strain (microstrains)		
10	53	62	54
20	109	124	109
30	164	188	165
40	224	253	226
50	289	321	288
60	370	398	358
70	425	474	429

Channel	1	2	3
Gage Number	Gage 2A	Gage 2B	Gage 2C
P (kips)	Stress (ksi)		
10	1.537	1.798	1.566
20	3.161	3.596	3.161
30	4.756	5.452	4.785
40	6.496	7.337	6.554
50	8.381	9.309	8.352
60	10.73	11.542	10.382
70	12.325	13.746	12.441

Girder Number: 3
Test Type: Static
Test Number: 6
Date: 10/15/93

Channel	1	2	3
Gage Number	Gage 3A	Gage 3C	Gage 3B
P (kips)	Strain (microstrains)		
10	54	52	66
20	109	109	130
30	164	166	192
40	219	222	255
50	274	280	316
60	328	340	376
70	386	400	440

Channel	1	2	3
Gage Number	Gage 3A	Gage 3C	Gage 3B
P (kips)	Stress (ksi)		
10	1.566	1.508	1.914
20	3.161	3.161	3.77
30	4.756	4.814	5.568
40	6.351	6.438	7.395
50	7.946	8.12	9.164
60	9.512	9.86	10.904
70	11.194	11.6	12.76

Table B-5: Strain gage readings and calculated stresses from Static Test 5 and 6.

APPENDIX C

Test Log
Girder 1

Date	Time	Cycle Count (Total Count)	Comments
8-24-93	08:00	762	Start up
"	09:15	9490	OK
"	10:30	18,950	OK
"	12:25	32,000	OK
"	13:07	36,813	Stop for 500 kip
"	13:27	"	Start up
"	13:36	38,494	Stop for 500 kip
"	13:56	"	Start up
"	15:42	51,400	OK
"	17:00	59,960	OK & Stop
8-25-93	08:05	0 (59,950)	OK & Stop
"	09:45	12,300	OK
"	11:35	25,000	OK
"	12:05	29,300	OK
"	13:05	36,200	OK
"	14:40	47,000	OK
"	16:30	60,000	OK
8-26-93	00:39	17,256	(counter not reset) End of count. Test stopped. Reset counter.
"	00:42	0	OK
"	07:45	50,103 (210,063)	Over temp. Big pump off.

Date	Time	Cycle Count (Total Count)	Comments
"	07:55	0	Start. Crack along bottom weld in high stress region.
"	10:27	16,020	Stop for 500 kip
"	10:35	0	Start up
"	12:19	12,875	Stop for 500 kip
"	12:51	"	Start up
"	14:11	21,500	Crack indicated earlier bad weld toe, crevice between weld and web plate. Could become crack due to wooden stiffener interaction. Everything else OK.
"	14:41	25,126 (235,189)	Stop to put strain gages on.
"	17:00	0	Reset to zero, start.
"	22:30	39,200	OK (Serviced pump to half.)
8-27-93	06:48	98,675 (333,864)	Stop and reset. (Separation of toe of long. fillet weld, like other separation, at end closest to the office on the side of the web having stiffeners.) Marked in chalk.
"	06:51	0	Start up
"	12:14	37,950	OK

Date	Time	Cycle Count (Total Count)	Comments
"	13:09	44,082	OK, Stopped for static test.
"	13:43	"	Start up
"	14:02	44,802	Start again
"	16:37	61,580 (395,444)	Reset counter
"	"	0	OK
"	17:02	3263	OK
8-28-93	01:31	63,600 (459,044)	OK
"	01:32	0	Reset counter
"	06:00	30,960	OK
"	12:35	78,080 (537,124)	Reset counter
"	"	0	OK
"	18:05	39,100	OK
"	22:30	69,800 (606,924)	Reset, OK
"	"	0	OK
8-29-93	05:45	52,696	OK
"	08:46	73,668	OK
"	08:47	0	OK
"	19:00	72,475 & 0 (679,399)	OK
8-30-93	02:05	50,847 & 0 (730,246)	OK
"	06:42	32,833	OK

Date	Time	Cycle Count (Total Count)	Comments
"	08:06	42,484 & 0 (772,530)	OK, Stop for 500 kip
"	13:02	35,024	OK
"	17:42	68,162 (840,692)	OK, Reset
"	17:43	0	OK
8-31-93	01:29	55,111 (895,803)	OK, Reset
"	01:30	0	Start
"	06:46	37,514	OK
"	08:00	46,500	OK
"	12:54	81,026 (976,829)	OK, Reset
"	12:55	0	Start
"	16:24	21,897	OK
"	22:00	61,500 (1,038,329)	OK, Reset
"	"	0	OK
9-1-93	06:50	63,055 (1,101,384)	OK, Reset
"	06:51	0	Start
"	11:45	30,111	Stop, 500 kip
"	13:02	38,156 (1,139,540)	Stop to work on pump.
9-2-93	08:25	0	Restart after new heat exchanger.
"	13:16	30,404	Stop for Static Load Test #3.

Date	Time	Cycle Count (Total Count)	Comments
"	13:51	"	Start
"	16:43	50,774	OK
"	17:09	53,814 (1,193,354)	OK
"	22:57	41,210 (1,234,564)	Stop
"	22:58	0	Start
9-3-93	05:52	48,972 & 0 (1,283,536)	OK
"	06:48	6588	OK
"	14:11	58,486	OK
"	16:11	72,405 (1,355,941)	Stop, Reset, 500 kip.
"	16:27	0	Start
9-4-93	00:50	59,128 (1,415,069)	Stop, Reset, OK
"	00:51	0	Start
"	09:45	63,158 (1,478,227)	Stop, Reset, OK
"	09:46	0	Start
"	21:38	84,027 (1,562,254)	Stop, Reset, OK
"	21:39	0	Start
9-5-93	09:54	86,658 (1,648,912)	Stop, Reset, OK
"	09:55	0	Start
"	19:35	68,186 (1,717,098)	Stop, Reset, OK

Date	Time	Cycle Count (Total Count)	Comments
"	19:36	0	Start
9-6-93	06:50	81,035 (1,798,133)	Stop, Reset, OK
"	06:51	0	Start
"	13:10	44,974 (1,843,107)	Stop, crack in hole at 1-1. 9 mm (0.35") up web on one side, 11 mm (0.45") long on stiffener side.
9-7-93	13:50	0	Restart after grinding out crack.
"	21:53	57,150 (1,900,257)	Stop, Reset, OK
"	21:54	0	Start
9-8-93	06:49	63,595 (1,963,802)	Stop, Reset, OK
"	06:50	0	Start
"	13:12	45,350	OK
"	16:53	71,200 (2,035,002)	Reset, OK
"	16:54	0	Start, Reset, OK
"	20:31	26,293 & 0 (2,061,295)	Reset
"	23:55	23,953	OK
9-9-93	06:48	73,171 (2,134,466)	Stop, Reset, OK
"	06:49	0	Start
"	15:48	63,898	OK
"	18:20	81,600 (2,216,066)	Reset, OK

Date	Time	Cycle Count (Total Count)	Comments
"	18:21	0	OK
"	23:28	37,000	OK
9-10-93	06:27	86,679 (2,302,747)	Reset, OK
"	13:55	53,259	OK
"	18:30	85,729 & 0 (2,388,476)	OK
"	19:15	5454	Long. weld separation from web near wooden stiffener at bottom of end closest to door.
9-11-93	06:30	85,624 & 0 (2,474,100)	OK
"	12:23	41,837 & 0 (2,515,937)	OK
"	22:30	73,734 & 0 (2,589,671)	Reset, OK
9-12-93	11:10	88,518 (2,678,189)	Stop, Crack in web plate at end of girder in high bending stress region.

APPENDIX D

Test Log
Girder 2

Date	Time	Cycle Count (Total Count)	Comments
9-20-93	08:04	0	Start
"	13:06	34,469	OK
"	15:12	49,175	OK
"	17:02	62,472 (62,472)	Stop for day.
9-21-93	07:52	0	Up load to Δ 77 kips each, gives correct ϵ of 407 με avg. across flange.
"	13:44	41,371	OK
"	16:13	59,046	OK
"	17:03	64,862 (127,334)	Stop for day.
9-22-93	07:45	0	Start
"	13:17	39,320	OK
"	17:00	65,630 (192,964)	OK, Reset
"	17:01	0	OK
"	20:20	23,588 (216,552)	OK, Reset
"	20:21	0	Start
9-23-93	06:47	74,151 (290,703)	OK, Reset
"	06:48	0	Start
"	13:05	44,684	OK
"	17:18	74,075 (364,778)	OK, Reset

Date	Time	Cycle Count (Total Count)	Comments
"	17:19	0	OK
"	20:37	24,127 (388,905)	OK, Reset
"	20:38	0	OK
9-24-93	06:49	72,237 (461,142)	OK, Reset
"	06:50	0	OK
"	13:01	43,940	OK
"	16:30	68,100 (529,142)	OK, Reset
"	16:31	0	OK
"	22:10	40,782 (569,924)	OK, Reset
"	22:11	0	OK
9-25-93	10:03	84,350 (654,274)	OK, Reset
"	10:04	0	OK
"	22:20	87,182 (741,456)	OK, Reset
"	22:21	0	OK
9-26-93	10:19	84,993 (826,549)	OK, Reset
"	10:20	0	OK
"	21:24	78,551 (905,100)	OK, Reset
"	21:25	0	OK
9-27-93	06:52	67,195 (972,295)	OK, Reset

Date	Time	Cycle Count (Total Count)	Comments
"	06:53	0	OK
"	12:59	43,230	OK, Crack in one of green columns at toe of weld.
"	13:35	49,005	Stop to repair crack.
"	15:45	"	Start
"	17:13	59,804 & 0 (1,032,099)	OK, Reset
"	22:26	36,917 (1,069,016)	OK, Reset
"	22:27	0	OK
9-28-93	06:52	59,713 (1,128,729)	OK, Reset
"	06:53	0	OK
"	13:01	43,463	OK
"	16:55	70,800 (1,199,529)	OK, Reset
"	16:56	0	OK
"	18:35	12,120 & 0	OK
"	21:15	19,062	OK
9-29-93	06:54	87,522 (1,287,051)	OK, Reset
"	06:53	0	OK
"	13:40	47,893	Stop to grind rough cut holes.
"	14:04	"	Start
"	20:26	92,987 (1,380,038)	Stop, column cracking at repaired area again.

Date	Time	Cycle Count (Total Count)	Comments
9-30-93	10:30	0	Repaired column, start.
"	13:31	21,847	Stop, fix strain gage.
"	13:45	"	Start
"	16:55	43,700 (1,423,738)	Reset, OK
"	16:56	0	OK
"	22:28	39,631 (1,460,369)	Reset, OK
"	22:29	0	OK
10-1-93	06:50	59,350 (1,519,719)	Reset, OK
"	06:51	0	OK
"	13:08	44,365	OK
"	16:56	71,571 & 0 (1,635,925)	OK
"	20:05	22,661 & 0 (1,658,586)	OK
10-2-93	08:50	90,310 & 0 (1,748,896)	OK
"	17:50	59,800 & 0 (1,808,696)	Reset, OK
"	21:00	25,900 & 0 (1,834,596)	Reset, OK
10-3-93	06:45	70,000 & 0 (1,904,596)	Reset, OK
"	22:30	100,000 (2,004,596)	Reset, OK
"	22:31	0	OK

Date	Time	Cycle Count (Total Count)	Comments
10-4-93	06:56	60,006 (2,064,602)	Reset, OK
"	06:57	0	OK
"	13:15	44,723	OK
"	17:06	71,981 & 0 (2,136,583)	OK
"	20:31	25,505 (2,162,088)	Reset, OK
"	20:32	0	OK
10-5-93	06:54	72,451 (2,234,539)	Reset, OK
"	06:55	0	OK
"	07:15	2000 (2,236,539)	Reset, stopped, low oil.
"	08:10	0	Restart, OK
"	13:01	34,484	OK
"	17:00	62,800 (2,299,339)	Reset, OK
"	17:01	0	OK
"	22:38	39,768 (2,339,107)	Reset, OK
"	22:39	0	OK
10-6-93	06:54	58,572 (2,397,679)	Reset, OK
"	06:55	0	OK
"	13:09	44,125	OK
"	17:03	71,425 (2,469,104)	Reset, OK

Date	Time	Cycle Count (Total Count)	Comments
"	17:04	0	OK
"	22:21	37,937 (2,507,041)	Reset, OK
"	22:22	0	OK
10-7-93	06:48	59,792 (2,566,833)	Reset, OK
"	06:49	0	OK
"	12:49	42,413 & 0	Check out actuators.
"	17:00	20,500 (2,587,333)	Reset, OK
"	17:01	0	OK
"	22:49	43,140 (2,630,473)	Reset, OK, One of cables now vibrating.
"	22:50	0	OK
10-8-93	06:51	58,916 (2,689,389)	Reset, OK
"	06:52	0	OK
"	13:07	46,071 (2,735,460)	OK
"	14:20	54,955	Stop to tighten frame.
"	14:57	"	Start
"	16:45	68,500 (2,858,915)	Reset, OK
"	20:45	29,660 & 0 (2,888,575)	OK
10-9-93	10:37	100,000 & 0 (2,988,575)	OK
"	21:32	80,436 (3,069,011)	Reset, OK

Date	Time	Cycle Count (Total Count)	Comments
"	21:33	0	OK
10-10-93	08:10	77,850 (3,146,861)	Reset, OK
"	08:11	0	OK
"	16:25	60,700 (3,207,561)	Reset, OK
"	16:26	0	OK
"	18:54	18,916 (3,226,477)	Reset, OK
"	18:55	0	OK
10-11-93	07:15	91,000 (3,317,477)	OK
"	08:20	7600 (3,325,077)	Stopped, end of test.

APPENDIX E

Test Log
Girder 3

Date	Time	Cycle Count (Total Count)	Comments
10-15-93	08:40	0	Start
"	17:00	52,500 (52,500)	Reset, OK
"	17:01	0	OK
"	21:55	36,557 (89,057)	Reset, OK
"	21:56	0	OK
10-16-93	08:14	76,414 (165,471)	Reset, OK
"	08:15	0	OK
"	11:30	23,200 (188,671)	Reset, OK
"	11:31	0	OK
"	20:50	69,600 (258,271)	Reset, OK
"	20:51	0	OK
10-17-93	08:05	83,700 (341,971)	Reset, OK
"	08:06	0	OK
"	15:25	54,300 (396,271)	Reset, OK
"	15:26	0	OK
"	22:38	53,897 (450,168)	Reset, OK
"	22:39	0	OK
10-18-93	06:49	60,738 (510,906)	Reset, OK
"	06:50	0	OK

Date	Time	Cycle Count (Total Count)	Comments
"	13:12	47,122	OK
"	17:00	74,600 (585,506)	Reset, OK
"	23:01	45,330 (630,836)	Reset, OK
"	23:02	0	OK
10-19-93	06:45	57,234 (688,070)	Reset, OK
"	06:46	0	OK
"	13:00	45,550 (733,620)	Stop, header beam failure.
11-2-93	08:52	0	Start, new header beam.
"	16:57	59,640 (793,260)	Reset, OK
"	22:21	39,747 (833,007)	Reset, OK
"	22:22	0	OK
11-3-93	06:50	62,609 (895,616)	Reset, OK
"	06:51	0	OK
"	13:33	49,497	OK
"	17:00	75,040 (970,656)	Reset, OK
"	21:44	34,997 (1,005,653)	Reset, OK
"	21:45	0	OK
11-4-93	06:53	67,588 (1,073,211)	Reset, OK
"	06:54	0	OK

Date	Time	Cycle Count (Total Count)	Comments
"	13:28	48,733	OK
"	17:00	74,650 (1,147,861)	Reset, OK
"	17:01	0	OK
"	22:25	40,331 (1,188,192)	Reset, OK
"	22:26	0	OK
11-5-93	06:50	62,280 (1,250,472)	Reset, OK
"	06:51	0	OK
"	15:03	60,696	OK
"	16:55	74,150 (1,324,622)	Reset, OK
"	16:56	0	OK
"	23:31	49,230 (1,373,852)	Reset, OK
"	23:32	0	OK
11-6-93	06:50	54,437 (1,428,289)	Reset, OK
"	06:51	0	OK
"	17:15	77,170 (1,505,459)	Reset, OK
"	17:16	0	OK
11-7-93	05:50	93,780 (1,599,239)	Reset, OK
"	05:51	0	OK
"	20:51	100,000 (1,699,239)	Reset, OK
"	20:52	0	OK

Date	Time	Cycle Count (Total Count)	Comments
11-8-93	06:47	73,652 (1,772,891)	Reset, OK
"	06:48	0	OK
"	16:40	73,301 (1,846,192)	Reset, OK
"	16:41	0	OK
11-9-93	01:05	62,470 (1,908,662)	Reset, OK
"	01:06	0	OK
"	06:49	42,628 (1,951,290)	Reset, OK
"	06:50	0	OK
"	10:00	12,075 (1,963,365)	Stopped, 500 kip actuator.
"	17:20	0	Start
"	21:20	28,800 (1,992,165)	Reset, OK
"	21:21	0	OK
11-10-93	05:35	60,900 (2,053,065)	Reset, OK
"	05:36	0	OK
"	06:52	9954	OK
"	07:30	14,036 (2,067,101)	Stopped, 500 kip actuator.
"	18:00	0	Start
11-11-93	06:51	95,805 (2,162,906)	Reset, OK
"	06:52	0	OK
"	12:12	39,802	OK

Date	Time	Cycle Count (Total Count)	Comments
"	17:05	75,700 (2,238,606)	OK
"	17:06	0	Reset, OK
"	21:08	30,649 (2,269,255)	Reset, OK
"	21:09	0	OK
11-12-93	06:53	72,591 (2,341,846)	Reset, OK
"	06:54	0	OK
"	12:44	43,560	OK
"	17:08	75,900 (2,417,746)	Reset, OK
"	17:09	0	OK
"	21:09	28,800 (2,446,546)	Reset, OK
"	21:10	0	OK
11-13-93	06:51	72,175 (2,518,721)	Reset, OK
"	06:52	0	OK
"	16:50	74,400 (2,593,121)	Reset, OK
"	16:51	0	OK
11-14-93	06:14	98,950 (2,692,071)	Reset, OK
"	06:15	0	OK
"	18:40	92,350 (2,784,421)	Reset, OK
"	18:41	0	OK
11-15-93	06:49	90,518 (2,874,939)	Reset, OK

Date	Time	Cycle Count (Total Count)	Comments
"	06:50	0	OK
"	16:01	68,146 (2,943,085)	Reset, Cracks in web plate at end, one all the way through the web about 75 mm (3") long at 45° starting in longitudinal weld.
"	16:02	0	OK
"	23:06	52,249	OK
11-16-93	07:13	56,915 (3,000,000)	End of test.